EFFECTS OF MIR-376 FAMILY MIRNAS ON CHRNA5 DEPLETED MCF7 CELL LINE MODEL AND CO-CULTURE COMPETITION STUDIES

A THESIS SUBMITTED TO

THE GRADUATE SCHOOL OF ENGINEERING AND SCIENCE

OF BILKENT UNIVERSITY

IN PARTIAL FULFILLMENT OF THE REQUIREMENTS FOR

THE DEGREE OF

MASTER OF SCIENCE

IN

MOLECULAR BIOLOGY AND GENETICS

By

Rafed Said Tiryaki

July, 2019

Effects of miR-376 Family miRNAs on CHRNA5 Depleted MCF7 Cell Line Model and Co-culture Competition Studies
By Rafed Said Tiryaki
July, 2019

We certify that we have read this thesis and that in our opinion it is fully adequate in scope and in quality, as a thesis for the degree of Master of Science.

Özlen KONU KARAKAYALI

(Advisor)

Ayşe Elif ERSON BENSAN

Bahar DEĞİRMENCİ UZUN

Approved for the Graduate School of Engineering and Science:

Ezhan KARAŞAN

Director of the Graduate School of Engineering and Science

Abstract

Effects of miR-376 Family miRNAs on CHRNA5 Depleted MCF7 Cell Line Model and Co-culture Competition Studies

Rafed Said Tiryaki

MSc. in Molecular Biology and Genetics

Supervisor: Özlen KONU KARAKAYALI

July, 2019

Cholinergic receptor nicotinic alpha 5 (CHRNA5) is a ligand-gated ion channel and one of the subunits of nicotinic acetylcholine receptors. Role of CHRNA5 in tumorigenesis has been initially shown in the lung tissue in which higher CHRNA5 expression has been significantly correlated with worse prognosis in lung cancer. In addition, our laboratory members recently shown that CHRNA5 depletion in breast cancer cell line MCF7 is antiproliferative (TUBITAK 111T316). In present study, effects of CHRNA5 depletion on miRNA expression profile were investigated and a significant decrease in the expressions of two members of the miR-376 family miRNAs, miR-376a-3p and miR-376c-3p, were identified. To test the effects of these two miRNAs, mimics were used in combination with CHRNA5 depletion on MCF7 cell line model. To investigate the synergism and/or antagonism of miR-376a mimic with CHRNA5 siRNA treatment a microarray study was performed and the signaling pathways involved were identified. Expressions of genes of interest were tested with RT-qPCR for both miRNAs. In addition, the effects of rescue on the cell phenotype and viability were also studied by using phalloidin staining and MTT experiments, respectively. Next a co-culture-based competition assay was developed using MCF7 cell lines expressing different fluorescent molecules to assess competition by both flow cytometer and fluorescent imaging. In summary, the results revealed that combinational treatments of si-CHRNA5 together with the miRNA mimics of two members from miR-376 family revealed enhancement of the antitumor effects. This study has been supported by TUBITAK (grant no. 114S367).

Keywords: Breast cancer, cholinergic signaling, CHRNA5, siRNA, microRNAs, co-culture, cell competition

Özet

CHRNA5 İfadesi Düşürülmüş MCF7 Meme Kanseri Hücre Hattı Modelinde miR-376 Familya mikroRNA'larının Etkileri ve Ko-kültür Rekabet Çalışmaları

Rafed Said Tiryaki

Moleküler Biyoloji ve Genetik Bölümü Yüksek Lisans

Tez Danışmanı: Özlen KONU KARAKAYALI

Temmuz, 2019

Kolinerjik reseptör nikotinik alfa 5 (CHRNA5) ligand kapılı iyon kanalları olan nikotinik asetilkolin reseptörlerinin alt birimlerinden biridir. CHRNA5'in tümörgenezde rolü, daha önce akciğer dokusunda gösterilmiştir. Yüksek CHRNA5 ekspresyonunun, akciğer kanserinde daha kötü prognoza ile korelasyonu gösterilmiştir. Buna ek olarak, laboratuvar üyelerimiz yakın zamanda meme kanseri hücre hattı MCF7'deki CHRNA5 ifadesinin deplesyonunun antiproliferatif etkilerini olduğunu göstermiştir (TÜBİTAK 111T316). Bu MS tezinin baz alındığı çalışmada ise, CHRNA5 deplesyonunun mikroRNA ekspresyon profili üzerindeki etkileri araştırılmış ve miR-376 familyası mikroRNA'larının iki üyesinin ifadelerinde (miR-376a-3p ve miR-376c-3p) anlamlı bir azalma tanımlanmıştır. Bu iki mikroRNA'nın etkilerini test etmek için ekspresyon seviyeleri, CHRNA5 tüketilmiş MCF7 hücrelerinde, mikroRNA mimik sistemleri kullanılarak kurtarılmıştır. CHRNA5 siRNA ile miR-376a mimik uygulamasının arasındaki sinerjizmi ve/veya antagonizmini araştırmak için bir mikrodizilim çalışması yapılarak dahil olan sinyal yolları tanımlanmıştır. İlgili genlerin ifadeleri, her iki mikroRNA için RT-qPCR ile test edildikten sonra gen ifade kurtarımının, hücre fenotipi ve hücre canlılığı üzerindeki etkileri, sırasıyla faloidin

boyaması ve MTT deneyleri kullanılarak kontrol edilmiştir. Daha sonra, farklı flüoresan molekülleri eksprese eden MCF7 hücre hatları kullanılarak bir ko-kültür bazlı rekabet protokolü geliştirilmiş olup akış sitometresi ve flüoresan görüntüleme metotları ile hücreler arası rekabet değerlendirilmiştir. Sonuçlar, si-CHRNA5'in ve miR-376 ailesinden iki üyenin mikroRNA mimikleri birlikte kombinasyonel etkilerinin antitümör etkilerinin artışını desteklediği görülmüştür.

Anahtar Kelimeler: Meme kanseri, kolinerjik sinyal yolakları, CHRNA5, siRNA, mikroRNA, ko-kültür, hücresel rekabet

to my precious family and friends,

Acknowledgements

First and foremost, I want to express my gratitude my supervisor Assoc. Prof. Ozlen Konu, for her guidance throughout all my undergraduate years and graduate studies as well as for giving me a chance to work on her laboratory and during this project.

I also would like to thank my jury members, Prof. Dr. Ayşe Elif Erson Bensan and Asst. Prof. Bahar Değirmenci Uzun, for giving their time for reviewing my thesis and their helpful discussions. I would like to thank all my past and current instructors in the Bilkent Molecular Biology and Genetics Department as well.

I would like to thank Prof. Dr. İhsan Gürsel and his group members for helping me with flow cytometry analyses and letting me use the tools in their lab whenever I needed.

Konu lab members, who are the greatest people I had in my life, I thank them all for all their support and friendship. I would like to thank, Sahika Cingir Köker, Seniye Targen and Bircan Çoban, my mentors and colleagues in the Konu lab, from whom I learned all my scientific knowledge and great lessons in life. I also want to acknowledge other members of the Konu Lab during my study; Fatma Betül Dincaslan, Damla Güneş, Büşra Korkmaz, Murat Yaman, Tuğberk Kaya and Alperen Taciroğlu for their great friendship as well as fruitful discussions. Lastly, I want to thank previous members of the Konu Lab, Başak Özgürsoy, Mehtap Yılmaz Tezcan, Ermira Jahja and Huma Shehwana whom started and gave the foundations to the project.

Aside from all above, I would like to thank my lab-mate and friend Ayşe Gökçe Keskus specifically. Her friendship and help in almost all parts of my work were very valuable, especially during hard times and will be something I will remember for the rest of my life.

I want to give my most precious thanks to my two closest friends, Özlem Bulut and Zeynep Boyacıoğlu. When I was in my darkest hours and hardest times it was those two always picking me up and making me well again.

In addition, I would like to thank my dearest friends; Gizem Kılıç, Onur Karasu, Saygın Bilican, Dilara Boğa and Oben Karasaka. Their friendship is one of the things I value most in my life.

On another note, I want to thank parents, my mother Nazmiye Tiryaki and my father Mehmet Recep Tiryaki for always believing me and never stop supporting me. As well as my sister Meriç Şeyma Tiryaki, my brother Esat Tiryaki and my sister-in-law Ruveyda Paçacı Tiryaki for always being there for me and being close friends for me aside from being siblings.

Last but not least, I would like to thank all members of the Bilkent Molecular Biology and Genetics family for providing us with a convenient lab environment to support out work.

This project was supported by a research grant (to OK) funded by The Scientific and Technological Research Council of Turkey (TUBITAK) (114S367) and COST (BM1406). I was supported by Bilkent University and TUBITAK 114S367 for my graduate studies.

Table of Contents

Abstract iii

Özet v

Acknowledgements viii

List of Figures xiii

List of Tables xviii

Abbreviations xix

1 Introduction 1

1.1 Breast Cancer 1

1.2 Calcium Signaling and Nicotinic Acetylcholine Receptors 2

1.3 MicroRNAs 5

1.3.1 miR-376 Family miRNAs (miR-376a and miR-376c) 8

1.3.2 Other miRNAs Used in the Study 9

1.4 miRNA Targeting and Prediction 9

1.5 Expression Analysis 10

1.6 Co-Culture Competition Experiments 12

1.7 Aims and Rationale 15

2 Materials and Methods 17

2.1 Materials 17

2.1.1 Laboratory Reagents and Kits 17

2.1.2 Cell Culture Products and Reagents 18
2.1.3 Reagents Used in Transfections 18
2.1.4 Primers 19
2.1.5 Laboratory Equipment Used in The Study 19
2.1.6 Solutions and Media Preparations 20
2.2 *In Vitro* Methods 21
2.2.1 Cell Culture Methods 21
2.2.2 Gene Expression Analyses 23
2.2.3 MTT Experiments 25
2.2.4 Phalloidin Staining 26
2.2.5 Fluorescence Microscopy Images and Competition Assay 26
2.3 *In Silico* Methods 28
2.3.1 miRNet Network Generation 28
2.3.2 Acquisition of miRNA Target List 29
2.3.3 Enrichment Analyses 29
2.3.4 Functional Classifications from PantherDB tool 29
2.3.5 Affymetrix mRNA Microarrays 29
2.3.6 Ingenuity Pathway Analysis 30
3 Results 31
3.1 miR-376a 33

3.1.1 Preliminary *in silico* Analyses 33
3.1.2 miRNA rescue and RT-qPCR confirmations 35
3.1.3 Transcriptome Analysis Results 36
3.1.4 Target Predictions and Confirmations 39
3.2 miR-376c 41
3.2.1 Preliminary *in silico* Analyses 41
3.2.2 miRNA rescue and RT-qPCR Confirmations 44
3.2.3 Target Predictions and Confirmations 44
3.3 Phalloidin Results 46
3.4 MTT Results 47
3.5 Co-Culture Competition Experiments 47
4 Discussion and Conclusions 58
4.1 CHRNA5 and miR-376 miRNAs as co-effectors 60
4.2 Co-culture Competition Model for the Observation of Combination Treatments 64
4.3 Conclusions and Future Perspectives 66
References 69
Appendix 83

List of Figures

Figure 2.1: Outline for the co-culture competition experiments. 28

Figure 3.1: RT-qPCR confirmations of the downregulation of mir-376a (A) and miR-376c (B) in the scramble or siRNA-1 treated MCF7 cells (n=5), **: p-value ≤ 0.01. 32

Figure 3.2: Target network of the miR-376a with miRNet tool; blue square represents miRNA and circles show gene targets and green circles represents genes from cell cycle, apoptosis and cancer related pathways. 34

Figure 3.3: Results of the enrichments done on the online Enrichr tool for the miR-376a predicted targets from the mirDIP tool as bar graphs of combined scores of Z-scores ranks and p-values. Graphs were color coded as; purple for KEGG pathways, red for Reactome pathways, green for Panther Pathways and blue for GO Biological Processes. 35

Figure 3.4: Functional classifications of miR-376a predicted targets from the mirDIP for the biological processes with the online PantherDB tool. 35

Figure 3.5: RT-qPCR confirmations of the CHRNA5 downregulation with si-CHRNA5(A) and miR-376a rescue with miRNA mimic (B) **: p-value ≤ 0.01 and ****: p-value ≤ 0.0001, when compared to scrambled control group. 36

Figure 3.6: Scatter plot representations of log fold changes (logFC) in mimic-376a (A) and si-CHRNA5+mimic-376a (B) against si-CHRNA5 logFC: mimic-376a only sample shown a mild negative correlation with si-CHRNA5 (A) but si-CHRNA5+mimic-376a sample shown a significant positive correlation(B). Effect ranges of mimic-376a shown with blue line, [-2.38, 1.40], si-CHRNA5 shown with red line, [-3.05, 4.04], and si-CHRNA5+mimic-376a, [-3.51, 4.08], shown with green line. 37

Figure 3.7: Top affected ‘Canonical Pathways’ (left) and ‘Diseases and Bio Functions’ (right) from the IPA core analyses of the miR-376a array data comparisons, orange color shows activation from the z-score and blue color shows inactivation on the pathway or function..... 38
Figure 3.8: RT-qPCR results of the direct targets of miR-376a, STON2 and BMPR2, on si-CHRNA5 and miR-376a mimic given samples. *: p-value ≤ 0.05 and **: p-value ≤ 0.01, #: p-value ≤ 0.1 from Tukey’s multiple comparison test..... 39
Figure 3.9: RT-qPCR results of the p53 pathway genes , MDM2, FOS and CDKN1A (p21), on si-CHRNA5 and miR-376a mimic given samples. *: p-value ≤ 0.05, **: p-value ≤ 0.01, ****: p-value ≤ 0.001 from Tukey’s multiple comparison test. 40
Figure 3.10: RT-qPCR results of the cell cycle genes , CDC6, WDHD1, BIRC5 and ANLN, on si-CHRNA5 and miR-376a mimic given samples. *: p-value ≤ 0.05 and **: p-value ≤ 0.01 #: p-value ≤ 0.1 from Tukey’s multiple comparison test..... 41
Figure 3.11: Target network of the miR-376c with miRNet tool where blue square shows miRNA and circles show gene targets, genes from cell cycle, apoptosis and cancer related pathways are labeled with green. 42
Figure 3.12: Results of the enrichments done on the online Enrichr tool for the miR-376c predicted targets from the mirDIP tool as bar graphs of combined scores of Z-scores ranks and p-values. Graphs were color coded as; purple for KEGG pathways, red for Reactome pathways, green for Panther Pathways and blue for GO Biological Processes. 43
Figure 3.13: Functional classifications of miR-376c predicted targets from the mirDIP for the biological processes with the online PantherDB tool. 43

Figure 3.14: RT-qPCR confirmations of the CHRNA5 downregulation with si-CHRNA5(A) and miR-376c rescue with miRNA mimic (B) **: p-value ≤ 0.01 when compared to scrambled control group. 44
Figure 3.15: RT-qPCR results of the selected genes (A) WDHD1, (B) FOS, (C) CDKN1A (p21) and (D) CLDN on si-CHRNA5 and miR-376c mimic given samples. #: p-value ≤ 0.1 from Tukey's multiple comparison test. 45
Figure 3.16: Phalloidin staining images of the miRNA mimic treated cells with or without si-CHRNA5, green shows actin filaments whereas blue shows DAPI staining of nuclei. 46
Figure 3.17: MTT results showing the relative cell viability of the treatments with miR-376a (A) and miR-376c (B) mimics in the presence or absence of si-CHRNA5, *: p-value ≤ 0.05, **: p-value ≤ 0.01 and ****: p-value ≤ 0.0001, when compared to scrambled control group. 47
Figure 3.18: Single colony selection from the polyclonal cells; GFP (top row) and BFP (bottom row) counts from the untransfected control cells(first column), polyclonal cell populations (second column) and selected single colony populations(third and fourth columns). 48
Figure 3.19: RT-qPCR results for CHRNA5 for the comparison of the different transfection trials. 49
Figure 3.20: Diagram of experiment plans for tree different batches of competition assays. 50
Figure 3.21: Co-culture competition results of the first experiment for mimics of miR-495, miR-376a and miR-409: A) microscope images and B) respective cell percentages of

green tagged si-CHRNA5 and blue tagged scramble cells on co-culture second transfections done with scramble or miRNA mimics as labeled above. ***: p-value < 0.001, ****: p-value < 0.0001 51
Figure 3.22: Co-culture competition experiment results for the second batch for miR-495 with A) microscope images and B) their corresponding cell percentages of green tagged miR-495 mimic and blue tagged scramble treated cells in the absence (left) or presence (right) of si-CHRNA5. *: p-value < 0.05, **: p-value < 0.01 52
Figure 3.23: Co-culture competition experiment results for the second batch for miR-376a with A) microscope images and B) their corresponding cell percentages of green tagged miR-376a mimic and blue tagged scramble treated cells in the absence (left) or presence (right) of si-CHRNA5. *: p-value < 0.05 53
Figure 3.24: Co-culture competition experiment results for the second batch for miR-409 with A) microscope images and B) their corresponding cell percentages of green tagged miR-409 mimic and blue tagged scramble treated cells in the absence (left) or presence (right) of si-CHRNA5. ***: p-value < 0.001 54
Figure 3.25: Co-culture competition results of the third experiment part 1 for mimics of miR-376c and miR-654: A) microscope images and B) respective cell percentages of green tagged si-CHRNA5 and blue tagged scramble cells on co-culture second transfections done with scramble or miRNA mimics as labeled above. *: p-value < 0.05 55
Figure 3.26: Co-culture competition experiment results for the third experiment part 2 for miR-376c: A) microscope images and B) their corresponding cell percentages of green

tagged miR-376c mimic and blue tagged scramble treated cells in the absence (left) or presence (right) of si-CHRNA5. *: p-value < 0.05, ***: p-value < 0.001 56
Figure 3.27: Co-culture competition experiment results for the third experiment part 2 for miR-654: A) microscope images and B) their corresponding cell percentages of green tagged miR-654 mimic and blue tagged scramble treated cells in the absence (left) or presence (right) of si-CHRNA5. *: p-value < 0.05 ***: p-value < 0.001 57

List of Tables

Table 2.1: Products used for experimental procedures. 17

Table 2.2: Products used during cell culture practices. 18

Table 2.3: Nucleic acids and reagents used for the transfections. 18

Table 2.4: List and sequences of the primers used for RT-qPCR gene expression studies. 19

Table 2.5:Name of the equipment used with their corresponding experiments and manufacturer companies. 20

Table 2.6: Recipes for the used solutions during experimental procedures. 20

Table 2.7: Recipe for the Complete DMEM used in the cell culture practices. 20

Table 2.8: Conditions for the transfections in the different sized plates. 23

Table 2.9: Realtime qPCR steps for miRNA quantification..... 25

Table 2.10: Realtime qPCR steps for mRNA quantification 25

Table 3.1: Changes in miRNA expression from the microarray study of the scrambled or si-CHRNA5 treated samples. 31

Abbreviations

ANLN: Anillin Actin Binding Protein

BFP: Blue Fluorescent Protein

BIRC5: Baculoviral IAP Repeat Containing 5

BMPR2: Bone Morphogenic Protein Receptor Type 2

CDC6: Cell Division Cycle 6

CDKN1A: Cyclin Dependent Kinase Inhibitor 1A

cDNA: complementary DNA

CHRNA5: Cholinergic Receptor Nicotinic Alpha 5

CLDN1: Claudin 1

CXCR4: C-X-C Motif Chemokine Receptor 4

DAPI: 4′,6-diamidino-2-phenylindole

DMEM: Dulbecco's Modified Eagle Media

ER: Estrogen Receptor

FOS: Fos Proto-Oncogene, AP-1 Transcription Factor Subunit

GFP: Green Fluorescent Protein

HMGB1: High Mobility Group Box 1

IGF1: Insulin Like Growth Factor 1

IPA: Ingenuity Pathway Analysis

LFC: Log2 Fold Change

MDM2: MDM2 Proto-Oncogene

miRNA: microRNA

miR-376a: hsa-miR-376a-3p

miR-376c: hsa-miR-376c-3p

miR-495: hsa-miR-495-3p

miR-409: hsa-miR-409-3p

miR-654: hsa-miR-654-3p

MTT: 3-(4,5-dimethylthiazol-2-yl)-2,5-diphenyltetrazolium bromide

nAChR: Nicotinic Acetylcholine Receptor

NFAT: Nuclear Factor of Activated T Cells 2

NNK: 4-(methylnitrosamino)-1-(3-pyridyl)-1-butanone

NNN: N'-nitrosoronornicotine

p53: Tumor Protein P53

PBS: Phosphate-buffered saline

PFA: Paraformaldehyde

PR: Progesterone Receptor

RIN: RNA Integrity Number

RISC: RNA-induced Silencing Complex

RT-qPCR: Reverse Transcription Quantitative Polymerase Chain Reaction

siRNA: Small Interfering RNA

STON2: Stonin 2

TPT1: Tumor Protein, Translationally-Controlled 1

WDHD1: WD Repeat And HMG-Box DNA Binding Protein 1

1 Introduction

1.1 Breast Cancer

Cancer is a disease of abnormal cell growth. When normal cells undergo certain changes, they may turn into more aggressive cells which divide and invade other parts of the organism in an uncontrolled manner. There are certain hallmarks of cancer that are accepted by researchers such as, sustained cell growth, evasion of apoptosis, angiogenesis and tissue invasion or metastasis [1]. Most common cancer types worldwide are lung, breast and colorectal cancers on all population, as documented by World Health Organization. When only female patients are checked, breast cancer is the most common cancer type (25.1%) with the highest mortality rate (14.7%) [2].

Under normal circumstances, mammary tissue is a secretive tissue consisting of alveolar and tubular structures including different types of cells, like luminal, basal and adipose cells [3]. However, when cells undergo tumorigenesis this orderly structure is disturbed and results in uncontrolled masses of cells in the tissue. Later on, they may even start to metastasize into other tissues [3]. Breast cancers show general characteristics of the cancers, such as aberrant cell division and angiogenesis, but within themselves they show a heterogeneity depending on the cells causing formation of the tumors [4]. Because each breast cancer subtype shows different characteristics, targeting and finding optimal treatment options for individual breast cancer subtypes is required [5].

There are different categorization methods for breast cancers depending on their histological structures and molecular profiles. Histologically breast cancers are divided into two main subtypes, *in situ* carcinoma and invasive carcinoma; and under these, there

are also number of subtypes, by which tumors are classified depending on the different features such as lesion size, cellular arrangement patterns as well as nuclear grading and mitotic index [4, 6]. On the other hand, researcher use yet another classification method depending on the molecular portraits of the cancers, which depends on the expression profiles of group of genes with functional coherence and these expression signatures are based on several different microarray studies [7, 8]. This second classification method includes five main subtypes, i.e., luminal A, luminal B, basal, HER2 overexpressing and normal breast-like breast tumors. This approach to classification holds a better determinant for prognosis, predisposition to metastasize and response to therapies as well as molecular characteristics [3].

Using 2-dimensional cancer cell lines to study cancer cell biology is one of the *in vitro* models, in which these cells hold the main features of their respective cancer types. In the case of breast cancer many different cell lines are established for the study of heterogenous population of breast tumors [9]. In this masters' study, MCF7 breast cancer cell line was used for all experiments and analyses. MCF7 cell line well represents the breast cancer luminal A subtype where it is estrogen, progesterone receptor positive (ER+ and PR+ respectively) as well as it expresses p53 protein in the wild-type form [9]. MCF7 cell line was obtained from pleural effusions sourced from invasive ductal carcinoma [10].

1.2 Calcium Signaling and Nicotinic Acetylcholine Receptors

Calcium ions (Ca^{++}) are the key secondary messengers used by cells and may affect number of different physiological processes including contraction in the muscles, regulation of proliferation or cell survival as well as adjustments in the gene expression profile [11, 12]. For the maintenance of the cellular homeostasis intercellular Ca^{++}

concentration is tightly regulated by calcium pumps, channels and calcium binding proteins in the cell [11]. Recently, it has been shown that remodeling of Ca^{++} homeostasis occurs during tumorigenesis; as this may affect proliferation, cell survival, migration and invasion in a direct or indirect manner [13, 14]. Several groups studied the aberrant Ca^{++} signaling on the number of different cancer types including breast [15], cervical [16], esophageal [17], glioblastoma [18] and melanoma [19] and show contribution of Ca^{++} signaling to the cancer development through different aspects as explained below.

One of the effector factors of the Ca^{++} homeostasis are the nicotinic acetylcholine receptors, nAChRs, which are ligand-gated ion channels that cause the flow of cations inside cells upon agonist binding [20]. As their main ligand, nAChRs bind to acetylcholine however, they also have high affinity for nicotine and derivatives such as N'-nitrosoronornicotine (NNN) and 4-(methylnitrosamino)-1-(3-pyridyl)-1-butanone (NNK) [20]. nAChRs are classically divided in to two main subtypes, muscle or neuronal receptors. Muscular nAChRs are expressed mainly in the neuromuscular junctions, whereas neuronal subtypes are more effective in the neuron excitation and synaptic transmissions [21]. Thus, nAChRs may have important roles on ion balance and signaling in neural and muscular and other types of tissues. On the other hand, nAChRs also have roles in the various epithelial tissues like ion balance and autocrine or paracrine signaling regulation [22-24].

Structure-wise, nAChRs consists of five subunits that are arranged to form a transmembrane pore. Each subunit has similar a structure and consists of a long N-terminal domain, four transmembrane parts, and a small extracellular C-terminal domain. Long N-terminal domain varies among subunits and includes ACh-binding domain, where

transmembrane segments contribute to the formation of pore structure [25, 26]. Pentameric structures form from different subunits through homomeric or heteromeric combinations [23, 25]. Expression of different subunits have been shown in non-neuronal tissues and cells as well, including lung tissue [27, 28], epithelial cells [29-31], lymphocytes and immune system [32, 33], keratinocytes [34, 35] and breast tissues [36, 37]. In addition, there were also number of studies showing aberrant expressions of nAChR subunits in different types of cancers (i.e. cervical [38], colon [39], lung [21, 40, 41], breast [36, 37, 42] cancers, leukemia [43], mesothelioma [44], medulloblastoma [45] and neuroblastoma [46]).

Cholinergic receptor nicotinic alpha 5 subunit (α5 or CHRNA5) is one of the subunits of nAChRs. It is encoded from the same gene cluster which houses α3 and β4 subunits that is located in the long (q) arm of chromosome 15. Functionally, CHRNA5 does not contribute to ligand binding from its N-terminus. However, inclusion of CHRNA5 to the structure increases the Ca^{++} permeability as well as affinity to the ligands [24]. In various studies CHRNA5 had been associated with number of pathological conditions such as schizophrenia [47], acute myocardial infraction [48], chronic obstructive pulmonary disease (COPD) [49], attention deficit hyperactivity disorder (ADHD) [50], nicotine addiction [51] and various cancer types including lung [51] and gastric cancers [52]. In our laboratory we were the first ones to show the relevance of the CHRNA5 to the breast cancer (Theses of Huma Shehwana (2017), Ermira Jahja (2017), Sıla Özdemir (2014), Azer Açıkgöz (2013), and Şahika Cingir Koker (2019)). In these studies, silencing of CHRNA5 was performed using three different siRNA molecules causing cell cycle arrest, a decrease in DNA damage response and hence increased chemosensitivity [53]. In

addition to these, knockdown of CHRNA5 leads to alterations in the miRNA expression profile of MCF7 cell line (Theses of Sahika Cingir Koker, 2019 and Basak Ozgursoy, 2017).

1.3 MicroRNAs

MicroRNAs (miRNAs) are small non-coding RNA molecules which consists of 18-22 nucleotides and act as negative regulators of their target genes. Binding to their target messenger RNA molecules perfectly or partially, miRNAs may cause the degradation through RNA-inducing silencing complex (RISC) or decrease translational activity, respectively [54, 55]. One miRNA molecule through its conserved seed sequence possibly can target multiple mRNAs. Because of this, miRNAs may have drastic effects on the cells, on both molecular and physiological levels [56]. On different studies it has been shown that miRNAs affect several processes, i.e., proliferation [57-59], differentiation [60], apoptosis [61], epithelial to mesenchymal transition [62], drug resistance [63, 64] and invasion [58, 65].

In addition to the regulatory roles of the miRNAs on cellular functions, in several studies aberrant expression of specific miRNAs or changes in miRNA expression profile are found associated with different pathological conditions [66]; including cardiovascular system diseases (i.e., heart failure [67-69], cardiac hypertrophy [70]), systemic lupus erythematosus [71], Down Syndrome [72], Alzheimer's Disease [73] and inflammation [74]. In addition, when cancer is considered miRNAs again are one of the hot topics that is studied in various cancer types [75]. A significant number of miRNAs have been shown to have disturbed expression profiles in different cancers i.e. glioblastoma multiforme (decreased miR-181 and increased miR-21 and miR-221) [76], chronic lymphocytic

lymphoma (decreased miR-15 and miR-16) [77, 78], colorectal neoplasia (decreased miR-143 and miR-145) [79], hepatocellular carcinoma (increased miR-18 and miR-224 with decreased miR-199, miR-195, miR-200, miR-125) [80], lung cancer (decreased let-7 and increased miR-17-92) [81-84] and lymphomas (increased miR-155 and miR-17-92) [85-87]. miRNAs may act differently in various cancers as they may have oncogenic or tumor suppressor roles [75]. Oncogenic miRNAs (or oncomirs) have increased expression in tumors and may either negatively regulate tumor suppressor genes or genes control cell differentiation and apoptosis. An example for oncogenic miRNAs would be miR-17-92 cluster located at chromosome 13q31 locus and suspected to target tumor suppressors PTEN and RB2 genes in lung cancer [83]. On the other hand, tumor suppressor miRNAs, whose expressions are decreased in tumors, prevent the tumor progression by targeting oncogenes or are themselves able to stimulate apoptosis. One of the best characterized miRNAs is let-7, which acts as tumor suppressor by directly targeting well known RAS oncogene in lung cancer [81].

In the case of breast cancer however, numerous miRNAs have been shown to be relevant, i.e., decreased expression of miR-125b, miR-145, miR-21 and miR-155 had been found in breast tumors [88]; miR-210 was induced by hypoxia [89] while miR-30a, miR-30c and miR-182 were found to be associated with response to treatment in ER+ breast tumors [64]. miR-26a was shown to be a determinant factor in treatment outcomes [90] and lastly miR-335 and miR126 were found to be tumor suppressor miRNAs in breast cancers through suppression of metastasis and inhibition of growth, respectively [91]. In addition to these roles, miRNAs have also been studied as new biomarkers to be explored for breast cancer [92-94]. However, one of the most striking findings about miRNAs in

breast cancer has come from two separate profiling studies on patient breast tumor samples and cancer cell lines [95, 96].

In the first study, the authors profiled mRNA and miRNAs of 93 primary breast tumor samples. When they applied unsupervised clustering to miRNA profiles, they observed a clear separation between ER+ and ER- samples. In addition, they observed differential miRNA expression patterns in between five molecular breast tumor subtypes, where miRNAs from same families showed high correlation and seven miRNA families were differentially expressed between luminal A and luminal B subtypes. They also checked the association of miRNAs with clinical factors and found out 31 miRNAs, corresponding to 20 miRNA families, showed difference between ER status and tumor grade [95]. In the second and more recent study however, researchers preformed the profiling of 51 human breast cancer cell lines for mRNAs and miRNAs. Depending on the mRNA profiles they found 2 groups resembling luminal and basal subtypes. Later on, in miRNA profiles they observed 2 groups as well, which were similar to classification from the mRNA profiling. From most variable 87 miRNAs they also found out two groups of miRNAs high in either group [96].

Expressions of miRNAs can be modified using mimic or inhibitor/antimiR systems, which increase or decrease expressions, respectively. Along with miRNA expression control mechanisms, roles of miRNAs as therapeutics for cancer and other diseases have been shown in different settings, i.e., tumor suppressor effects of miR-34 and oncogenic effects of miR-122 [97] as well as inhibition of oncogenic miR-155 was shown in a lymphoma model in mouse [98]. Along with roles of single miRNAs, expression systems also allow to the discovery of the combinational effects of miRNAs with other mRNA regulator

molecules, as in other miRNAs [56] or siRNA molecules [99] as synergism or antagonism. Although, there are limited number of studies in the literature using a combination of the siRNA and miRNA expression technologies, these two types of interference modes, in combination, may alter each other's effects [65, 100]. In this master's study, the combinational effects of two members of miR-376 miRNA family (miR-376a-3p and miR-376c-3p) with an si-CHRNA5 molecule in the MCF7 cell line have been studied.

1.3.1 miR-376 Family miRNAs (miR-376a and miR-376c)

miR-376a-3p (MIMAT0000729), AUCAUAGAGGAAAAUCCACGU, and miR-376c-3p (MIMAT0000720), AACAUAGAGGAAAUUCCACGU, are closely related miRNAs from the same family [101, 102]. In miRNA annotation, same number with different letter suffixes means similar miRNAs with slightly different sequences, in this case between miR-376a-3p and miR-376c-3p there are changes at the 2^{nd} and 14^{th} nucleotides [103]. The expression changes of miR-376a-3p and miR-376c-3p were seen in the number of cancers [104] as well as can be seen from the miRNA-cancer association database (miRCancer) [105]. The examples for miR-376a-3p includes downregulation in breast cancer [106], glioblastoma [107], hepatocellular carcinoma [108], non-small cell lung cancer [109] and upregulation in ovarian cancer [110], pancreatic ductal adenocarcinoma [111], whereas for miR-376c-3p the modulations include downregulation in cervical cancer [112], gastric adenocarcinoma [113], non-small cell lung cancer [114], osteosarcoma [115, 116], oral squamous cancer [117]. Lastly, in metastatic melanoma [118] and chondrosarcoma [119] both microRNAs were downregulated. Overall downregulation in all these cancer types might indicate that both miR-376a-3p and miR-

376c-3p could have tumor suppressor roles and their re-introduction to the cell using mimics might provide a therapeutic relevance.

1.3.2 Other miRNAs Used in the Study

In addition to two miRNAs from miR-376 family, three additional miRNAs were included in the last part of the thesis in co-culture competition experiments, miR-495-3p (MIMAT0002817), miR-409-3p (MIMAT0001639) and miR-654-3p (MIMAT0004814) [101, 102]. miR-495-3p which is downregulated in breast cancer [120-122], gastric cancer [123, 124], non-small cell lung cancer [125] and glioma [126-128] has been focused on its transcriptomic and anti-cancer effects in more detail by Sahika Cingir Koker in her thesis (Sahika Cingir, PhD Thesis, Bilkent University 2019). miR-409-3p has been shown to be downregulated in breast cancer [129], lung adenocarcinoma [130] and bladder cancer [131] while miR-654-3p was downregulated in papillary thyroid cancer [132] but upregulated in mantle cell lymphoma [133].

These miRNAs mentioned above, miR-376 family and other miRNAs, are all located on the long (q) arm of the chromosome 14, clustered along with number of other miRNAs modulated by CHRNA5 siRNA molecules [134]. This miRNA cluster has been previously reported to be downregulated in the metastatic prostate cancer cells [135], giant cell tumor of bone [136], metastatic melanoma cells [118] and gastrointestinal stromal tumors [137], however exhibit increased expression in lung adenocarcinoma and has been associated with the metastasis and poor prognosis [138].

1.4 miRNA Targeting and Prediction

Since miRNAs work through inhibiting expression of their target genes, one of the main points for understanding the effects of the miRNAs on cells is the identification of the

miRNA-target interactions. In last decade there are number of miRNA target prediction tools developed and all have four main features, seed match, conservation, free energy and site accessibility. Briefly, seed match looks for the Watson-Crick match between the miRNA and its targeted sequence. Conservation has been used by multiple tools because in general seed sequences of the miRNAs are more conserved. Free energy (Gibbs free energy) is widely used for showing the stability of a biological system which is taken into consideration for miRNA-target interaction; and lastly site accessibility is a measure of how easily miRNAs can bind to their target region [139]. Commonly used miRNA prediction tools can be listed as: miRanda [140-142], TargetScan [143], DIANA [144, 145], miRDB [146]. In this study however, mainly two tools have been used, miRNet and mirDIP. Online miRNet tool can be used for finding the experimentally validated miRNA-target interactions to show in a network as well as for in-built enrichment analysis [147, 148]. On the other hand, mirDIP is an integrative database for the miRNA target predictions, it makes use of the 30 independent target prediction resources, including ones listed above, and generates an “integrated score” while it allows to select which databases to be included [149, 150].

1.5 Expression Analysis

Translation of genomic sequence data to the functional biological information requires the acquisition of the expression data for genes. After 1990s one of the most used expression profiling methods is DNA microarrays [151]. Microarray technology uses fixed DNA probes on a chip surface and hybridization of sample to those probes for the identification of DNA abundance [152]. Different array chips can be designed for various purposes, i.e., expression profiling, resequencing and genotyping of single nucleotide polymorphisms

(SNPs) or point mutations [153]. DNA arrays have allowed scientists to find expression profiles of diverse number of cases including cancer [153]. Microarrays can also be used for the analysis of miRNA expression profiles with specified probes for the purpose [154]. miRNA profiling can be an important approach for the understanding of the miRNA functions and effects, especially when coupled with the mRNA expression profiling [155]. This approach had been used for various research groups for understanding different cases, i.e., for breast cancer [156, 157], interstitial lung diseases [158], hepatitis C virus infection [159] and mesenchymal tumors [160]. In addition to expression profiling with arrays another analysis method for expression is the reverse transcription quantitative polymerase chain reaction (RT-qPCR), where a complementary DNA (cDNA) is generated from RNA samples with reverse transcription and expression is examined with the help of SYBR green assisted real time polymerase chain reaction [161]. This method can be used for detecting the expression of a specific gene by using specific primers as well as for miRNAs [162].

Giving a biological meaning to the high-throughput data coming from microarrays is an important step in the understanding the effects of a treatment of interest [163]. For this purpose, one of the most used approaches is generation of a set of differentially expressed (DE) genes before comparing it with the previously generated gene lists and pathway library databases such as Gene Ontology Consortium (GO) [164], Kyoto Encyclopedia of Genes and Genomes (KEGG) [165], Reactome Pathways [166], Molecular Signatures Database (MSigDb) [167], Gene Signature DataBase (GeneSigDB) [168] and Encyclopedia of DNA Elements (ENCODE) [169]. In this masters' study several databases have been used for enrichment analyses including miRNet in-built enrichment

analysis that is using KEGG [147, 148]; PANTHER classification system for the categorization of genes in respect to their gene functions, ontology and pathways [170, 171]; Enrichr, an online enrichment analysis tool which integrates multiple databases including the ones listed above [172, 173]; and lastly Ingenuity Pathway Analysis (IPA) tool, a commercial software package that uses casual networks curated from the literature for analysis of upstream or downstream effects [174].

1.6 Co-Culture Competition Experiments

Cell competition is the process in which elimination of normally viable but relatively less fit or growth-disadvantaged cells occurs within a group of cells. It was first discovered in *Drosophila melanogaster* embryos, where *Minute*$^{+/-}$ cells were eliminated when they were near wild-type cells in embryo during wing development [175, 176]. Later on, similar mechanisms also shown in the mammalian cells, both *in vivo* and *in vitro* [177, 178]. In addition to development, role of cell competition has also been shown in different circumstances including tissue health, aging and tumorigenesis [179]. Even though removal of less viable cells is required for development, tissue health and aging; it can play a dual role in different phases of tumorigenesis, acting on both tumor suppression and expansion. In early stages of tumor formation, transformed cells can be eliminated by neighboring normal cells by a process called epithelial defense against cancer (EDAC) [180]; however, in later stages cancer cells may become “supercompetitors” which may result in removal of surrounding normal cells for more space or resources [181]. In addition to these, in immortalized cell lines cell competition has also been observed in between sub-clones of the cells [177]. In all these scenarios, cells mainly attempt to eliminate their neighbors for limiting factors in the environment, i.e., available resources,

growth factors or limited space in the tissue or organ. Several well-known molecules and signaling pathways had been associated with the cell competition; including Myc [182-184], BMP pathway [185], Hippo pathway, Wnt and JAK/STAT pathways [186, 187]. Although the results of cell competition are understood to an extent, mechanisms by which cell competition occurs and cells are driven to apoptosis are not fully understood yet. There are two hypotheses have been proposed and acknowledged for different conditions. First, more viable (winners) cells, diffuse a short-range signal that only less-fit cells (losers) respond to and gets eliminated [182, 186]. On the other hand, second hypothesis states, loser removal occurs through direct interaction of membrane-bound receptors with winner cells [188]. Since cell competition is such an important phenomenon, we can also take advantage of it for a prevent tumor progression.

One of the methodologies used for the study of cell to cell interactions is to culture different cells together. There are different types of co-cultures used for various purposes, one way to classify them would be the interaction settings of the cells; direct or indirect cultures. In case of direct cultures cells are seeded by directly mixing or on top of each other where they are on physical interactions with each other. On the other hand, for indirect cultures constructs such as membranes, transwell inserts or Boyden chambers can be used to separate cells to inhibit direct physical interactions between different cell types. Cell to cell communication types change depending on the culture setting. In direct cultures, cells can interact by cell-cell adhesions; through tight, adherent and gap junctions as well as paracrine signaling with soluble factors. However, in indirect cultures, since physical contact is inhibited, they can communicate only through soluble factors [189]. As well as interaction type, classification also could be done based on environment

that cells are cultured. Both direct and indirect culture settings can be achieved through two-dimensional (2D) culture environments, such as flasks and dishes, or three-dimensional (3D) culture environments, in example collagen or agarose gels [190].

In the literature various usages of co-cultures are explained thoroughly; these includes infection studies [191], drug research [192], increased culturing success for specific cell types [193, 194], using mutual interactions between different cells [195], layered cultures on top of feeder cells to grow [190] and lastly using more than two types of cells in the same environment to generate a niche for cells to mimic *in vivo* conditions [190, 196]. In addition to the ones listed above, another usage of the co-cultures is for generation of artificial tissues [197, 198]; which had been applied to number of tissue types such as bone [199, 200], heart [201-203], vascular [204, 205], lung [206], kidney [207], liver [208] and nerve tissues [209]. Co-culture techniques are also used in the cancer studies, mainly for understanding the interplay between tumor cells and surrounding cells or microenvironment [210-212] as well as for dig out the underlying mechanisms of angiogenesis [213, 214].

Aside from the usages mentioned above, although co-cultures could also be used for observation of cell competition, there are limited number of studies that uses co-culture techniques for competition assays. In one of the studies, a competition assay model was suggested by a research group for the observation of changes in the cell proliferation. Where co-culture of transduced GFP (+) cells and untransduced GFP (-) cells was used to show effects of shRNAs on cells' proliferation rates by determining GFP (+) cell ratio with flow cytometry over number of passages [215]. In another study, effects of ascorbic acid on growth of Barrett's esophageal cell lines was checked on co-cultures with

florescent labeled normal squamous esophageal cells, outcome was measured over 14 days of treatment [216]. On a third study, researchers tried to find drugs that are preferably cytotoxic to MUC16 positive ovarian cancer cells on co-culture with their negative counterparts. Where they used a 384-well plated system for drug screens and automated imaging with analysis for the acquisition of results [217]. Lastly, a co-culture system was used for the discovery of the genetic interactions and synthetic lethality from a genome-scale shRNA screen and a query of genes. In which parental cells labeled with red and knockout cells labeled with green fluorescent proteins and are co-cultured together. They are treated with siRNAs for query genes in a span of 7-days with daily automated imaging [218]. In all these studies, the purpose of the treatments on the co-cultures was to change the dynamics in the cell fitness; either by decreasing the proliferation of the target cells or increasing the relative fitness of the surrounding normal cells. To the best of our knowledge, there were no studies comparing the interactions between siRNA and miRNAs using competition co-culture models.

1.7 Aims and Rationale

Previous studies in our lab showed the effects of CHRNA5 silencing in the MCF7 breast cancer cell line as causing cell cycle arrest, decreased DNA damage response and increased chemosensitivity by using three different siRNA molecules [53]. Furthermore, miRNA expression of siRNA treated samples has been checked with a miRNA microarray, which revealed two members of miR-376 miRNA family, miR-376a and miR-376c, was downregulated by the CHRNA5 siRNA (Sahika Cingir, PhD Thesis, Bilkent University 2019). These two miRNAs were shown to be downregulated in number of cancers before which might indicate a tumor suppressor role. Therefore, we hypothesized

CHRNA5 siRNA treatment in combination with miR-376a or miR-376c mimics could further enhance anti-tumor effects of the CHRNA5 depletion. Main aims of this study can be stated as:

a) Increasing the amount of miR-376a or miR-376c with miRNA mimics in MCF7 cells in the presence or absence of CHRNA5 siRNA.
b) To reveal transcriptomic profile of miR-376a mimic treatment in the presence or absence of CHRNA5 siRNA and validate several targets identified by *in silico* methods.
c) Compare the transcriptomic profiles of CHRNA5 siRNA only, miR-376a mimic only, and siRNA and mimic together groups using functional annotation and miRNA-mRNA network tools.
d) Check antiproliferative and phenotypical effects of miR-376a and miR-376c mimics on MCF7 cells in the presence or absence of CHRNA5 siRNA.
e) To develop a co-culture competition assay between MCF7 cells stably expressing GFP or BFP, to analyze cell competition between cells treated with different molecules using microscopic and/or quantitative analyses for the observation of combinational effects of CHRNA5 siRNA and miRNA mimics.

2 Materials and Methods

2.1 Materials

2.1.1 Laboratory Reagents and Kits

Reagents from the general laboratory stocks and the kits used are given in the Table 2.1 with their catalog numbers and company information.

Table 2.1: Products used for experimental procedures.

Product Name	Catalog No	Company (Country)
NaCl	31434	Sigma-Aldrich (Germany)
KCl	12636	Sigma-Aldrich (Germany)
$Na_2HPO_4.2H_2O$	4272	Sigma-Aldrich (Germany)
KH_2PO_4	4243	Sigma-Aldrich (Germany)
PFA	76240	Fluka (USA)
NaOH	6203	Sigma-Aldrich (Germany)
HCl	7102	Sigma-Aldrich (Germany)
Triton X-100	T8787	Sigma-Aldrich (Germany)
BSA	A7906	Sigma-Aldrich (Germany)
Water, molecular biology grade, nuclease free	SH30538.01	HyClone (USA)
EtOH	B2221	Sigma-Aldrich (Germany)
SDS	71725	Sigma-Aldrich (Germany)
Alexa Fluor® 488 Phalloidin	A12379	Life Technologies (USA)
UltraCruz Mounting Medium	sc-249401	Santa Cruz Biotechnology
Vybrant MTT Cell Proliferation Assay Kit	V-13154	Invitrogen (USA)
miRNeasy	217004	Qiagen (Germany)
QIAzol	79306	Qiagen (Germany)
miScript II RT kit	218160	Qiagen (Germany)

RevertAid First Strand cDNA Synthesis Kit	K1622	Fermentas (Canada)
miScript SYBR Green PCR Kit	218073	Qiagen (Germany)
LightCycler 480 SYBR Green I Master	4887352001	Roche Applied Science (Germany)
Sodium Azide	BCBP7328V	Sigma-Aldrich (Germany)

2.1.2 Cell Culture Products and Reagents

Reagents and molecules that are used in the cell culture procedures are listed in the Table 2.2 with their catalog numbers and companies.

Table 2.2: Products used during cell culture practices.

Product Name	Catalog No	Company (Country)
DMEM, Low Glucose	BE12-707F	Lonza (Switzerland)
DMEM w/o phenol red	11880-028	Thermo Scientific (USA)
Fetal Bovine Serum (FBS)	S181H-500	Biowest (France)
Sodium pyruvate	BE13-115E	Lonza (Switzerland)
L-Glutamine	BE17-605E	Lonza (Switzerland)
Penicillin/Streptomycin	DE17-602E	Lonza (Switzerland)
NEAA 100X	BE13-114E	Lonza (Switzerland)
DMSO	A3672,0100	AppliChem (USA)
PBS	BE17-516F	Lonza (Switzerland)
Trypsin	BE-17-161E	Lonza (Switzerland)

2.1.3 Reagents Used in Transfections

The chemicals and the reagents used for the transfection protocols are listed in the Table 2.3 with their catalog numbers and companies.

Table 2.3: Nucleic acids and reagents used for the transfections.

Product Name	Catalog No	Company (Country)
HiPerFect transfection reagent	301704	Qiagen (Germany)
Hs_CHRNA5_5	SI03051111	Qiagen (Germany)
Syn-hsa-miR-376a-3p miScript miRNA Mimic	MSY0000729	Qiagen (Germany)
Syn-hsa-miR-376c-3p miScript miRNA Mimic	MSY0000720	Qiagen (Germany)
AllStars Negative Control siRNA	SI03650318	Qiagen (Germany)

2.1.4 Primers

Primer sequences that are used in the RT-qPCR experiment are listed in the Table 2.4 with their working conditions and sizes of amplicons.

Table 2.4: List and sequences of the primers used for RT-qPCR gene expression studies.

Primer Name	Sequence (5' - 3')	Amplicon Size (bp)
CHRNA5	F: AGATGGAACCCTGATGACTATGGT R: AAACGTCCATCTGCATTATCAAAC	104
TPT1	F: GATCGCGGACGGGTTGT R: TTCAGCGGAGGCATTTCC	100
STON2	F: GGCTGACTCAACTGACAATTCC R: AAACGAGCAGAGGTCACTGG	129
BMPR2	F: AAGCGAGGTTGGCACTATCA R: ACTCTGGTACGGATTCCCCT	173
MDM2	F: CCCGGATTAGTGCGTACGAG R: CATTTGCCTGCTCCTCACCA	166
FOS	F: ATGAGCCTTCCTCTGACTCG R: ACGCACAGATAAGGTCCTCC	177
CDKN1A (p21)	F: GTCACTGTCTTGTACCCTTGTG R: CGGCGTTTGGAGTGGTAGAA	129
CDC6	F: AGTCAGATGTCAAAAGCCAGACT R: TTGGCTCAAGGTCATCCTGTTA	146
WDHD1	F: AGCAGCCAAGGACGAGTAAA R: CTTCGGCTTTGGAATCAGAG	192
BIRC5	F: GTTGCGCTTTCCTTTCTGTC R: TCTCCGCAGTTTCCTCAAAT	141
ANLN	F: TAAAGCAGGTGATTGTTCGG R: GTTCTTCATCAACACAGCAG	180
CLDN1	F: CTGTCATTGGGGGTGCGATA R: CTGGCATTGACTGGGGTCAT	118

2.1.5 Laboratory Equipment Used in The Study

The equipment used in this study for the acquisition of the results is listed below in the Table 2.5 with the experiments they were used and manufacturing companies.

Table 2.5:Name of the equipment used with their corresponding experiments and manufacturer companies.

Name of the instrument	Assay	Company (Country)
LightCycler® 480 Instrument II	Real-time qPCR	Roche (Switzerland)
Axio Imager A1	Phalloidin Staining	Zeiss (Germany)
Synergy Multi-Mode Reader	MTT experiments	BioTek (USA)
NovoCyte 3000 Flow Cytometer	Competition Experiment	ACEA (USA)
Leica DMi8 Inverted Microscope	Competition Experiment	Leica (Germany)
NanoDrop™ One	RNA quantification	Thermo (USA)
2720 Thermal Cycler	cDNA Synthesis	Applied Biosystems (USA)

2.1.6 Solutions and Media Preparations

The solution preparation recipes used for various experiments can be seen in the Table 2.6 and the recipe for the complete media cells were grown and treated is given in the Table 2.7.

Table 2.6: Recipes for the used solutions during experimental procedures.

Solution Name	Preparation	Total Volume
10X PBS	80 g NaCl, 2 g KCl, 15.2 g $Na_2HPO_4.2H_2O$, 2 g KH_2PO_4	1000 ml
1X PBS	100 ml 10X PBS	1000 ml
4% PFA	2 g PFA, 1N NAOH, 1M HCl	50 ml
PBX	0.1% Triton-X in PBS	50 ml
BBX	1% BSA in PBX	50 ml
FACS buffer	0.5 g BSA, 25 mg Na-Azide	50 ml

Table 2.7: Recipe for the Complete DMEM used in the cell culture practices.

Reagent	Volume	Ratio
DMEM, Low Glucose	500 ml	
Fetal Bovine Serum (FBS)	50 ml	10%
Sodium pyruvate	10 ml	2%
L-Glutamine	10 ml	2%
NEAA 100X	5 ml	1%
Penicillin/Streptomycin	5 ml	1%

2.2 *In Vitro* Methods

2.2.1 Cell Culture Methods

2.2.1.1 Thawing Cells

Frozen cell stocks that were stored in the liquid nitrogen tanks taken and placed in the water bath (37°C) until half is thawed (~2-3 minutes), then rest is solved by mixing with complete media (given in the Table 2.7). Mixture with freezing medium and cells, centrifuged at 1500 rpm for 5 minutes to remove DMSO. Cell pellets were solved in the fresh complete media gently and transferred to T25 flasks, maintained in the incubator 37°C %5 CO_2 until next day where cells are checked and passaged to T75 flasks when they reach confluency with standard passaging procedure.

2.2.1.2 Passaging Cells

When cells reached %75-80 confluency in their flasks they were passaged for the continuation of the cell lines. First, old medium was aspirated from the cells then washed over cells with PBS once. Cells detached using 0.25% Trypsin/EDTA for 3-5 minutes at 37°C %5 CO2 in the incubator and mixed with new complete DMEM containing FBS (at least twice amount of trypsin) to neutralize trypsin. Detached cells transferred to new T75 or T25 flasks with 1:3 to 1:5 dilutions depending on the incoming experiment plans. Passage number of the cells were recorded and for all experiments, cells used were up to passage number of 10.

2.2.1.3 Freezing Cells

For the sake of keeping cell lines younger, whenever cells were opened from the frozen stocks after two to three passages frozen stocks were taken from them. For this procedure, cells were detached as in the passaging procedure then centrifuged at 1500

rpm for 5 minutes to get cell pellets. Cell pellets were solved in the freezing medium (90% FBS and 10%DMSO as cryoprotectant); and split to cryovials as each will take around one million cells. Cryovials were frozen step-wise, first stored in the -20°C until solidification occurs (two to three hours), then transferred to -80°C for short-term storage (two to three weeks). Lastly, they were transferred to liquid nitrogen tanks for the long-term storage (months to years).

2.2.1.4 Treatments for Scrambled Oligos, CHRNA5 siRNA and miRNA Mimics

On a day before treatments cells were seeded to new plates. Cells were detached using trypsin and after addition of new media, centrifuged at 1500 rpm for 5 minutes to remove trypsin. Cell pellets were re-suspended in fresh media and counted with the help of hemocytometer and glass cover-slips. Cells then were seeded to 6, 12, 24 or 96-well plates, as in the numbers given in the Table 2.8. Different transfection reagent concentrations were used for experiments; HiPerfect transfection reagent concentration for RNA isolation and MTT experiments were 0.006%; whereas for imaging and competition experiments 0.003% used and on both cases concentrations of 0.0005% (10 nM final concentration) for RNA reagents (scrambled oligos{sc}, siRNA{si} and miRNA mimics{mimic}) were used. All transfection conditions can be seen in the Table 2.8. If double transfections were to be done together (for example, si+mimic or si+sc) both RNA molecules were added to same transfection mixture. On the day of treatment first transfection mixes were prepared then during 10 minutes incubation time of the mix, in which transfection complexes were formed, media of the cells were changed. Transfection complexes added on top of the cells dropwise and plates were swirled 2-3 times to make sure even distribution on the cells. Lastly plates were left in the incubator

for required incubation times (72 or 48 hours). Each treatment was performed in duplicates for RNA isolation, with 5 replicates in MTT experiments and triplicates in co-culture competition experiments.

Table 2.8: Conditions for the transfections in the different sized plates.

Plate	Number of cells (#/well)	HiPerfect reagent (µl/well)	RNA (µl/well)
6-well	200 000	12	1
12-well	100 000	3	0.5
24-well	50 000	1.5	0.25
96-well	2 000	1.2	0.1

2.2.2 Gene Expression Analyses

2.2.2.1 RNA Extraction

After 72 hours of incubation RNA was collected from the cells with miRNeasy, miRNA isolation kit. For this; cell lysates were collected by washing 2 times with PBS then scraping with the QIAzol Lysis Reagent. Lysates were frozen in liquid nitrogen by snap-freezing and stored in the -80 °C until the day of extraction. Isolation was done following the manufacturers protocols, on the last step 30 µl of nuclease-free water was used for elution. RNA concentrations were measured with the NanoDrop™ One using 1.5 µl of the samples. Also, RNA integrity number (RIN) values were determined for the RNA quality of samples that were going to be used in the microarrays with Agilent.

2.2.2.2 cDNA Synthesis

Two different sets of cDNAs were synthesized, for miRNA and mRNA genes, with the help of miScript II RT kit and RevertAid RT Reverse transcription kit respectively. For both RT reactions 800 ng of RNA is used. For miScript reaction required amount of RNA, 2 µl of 5X HiSpec buffer, 1 µl 10X Nucleus mix, 1 µl RT mix and nuclease free water added

until total volume of 10 µl. Reaction took place as 60 minutes at 37°C and 5 minutes deactivation at 95°C in 2720 thermal cycler (Applied Biosystems). On the other hand; for RevertAid RT reaction, 800 ng of template RNA is mixed with 1 µl of Oligo(dT) and added nuclease free water until 12 µl. Then 4 µl of 5X reaction buffer, 1 ul of Ribolock (RNase inhibitor), 2 µl of 10 mM dNTP mix and 1 µl of RT enzyme is mixed in to total of 20 µl volume for each sample. This reaction took place in the 42°C for 60 minutes and 70°C for 5 minutes in 2720 thermal cycler (Applied Biosystems). After both reactions, cDNA samples are diluted 1:20, diluted samples are stored in the -20°C and stocks at -80°C.

2.2.2.3 Real-time Quantitative PCR

Two different protocols were followed for the quantitation of miRNAs and the genes. For miRNA qPCR Qiagen miScript primer assays were used with the Qiagen SYBR green PCR kit. For this 2 µl of diluted cDNA samples were mixed with the reaction mixture consisting of; 1 µl forward primers, 1 µl universal reverse primers, 1 µl nuclease free water and 5 µl SYBR green into total volume of 10 µl then reaction was run as in the steps at Table 2.9. For miRNA quantification RNU6-1 gene was used as the reference gene. In the mRNA gene quantification RT-qPCR experiments on the other hand, Roche SYBR green PCR kit was used in which 2 µl diluted cDNA samples were mixed with the reaction mixture including; 1 µl forward primers, 1 µl reverse primers, 1 µl nuclease free water and 5 µl 2X Roche SYBR green mix into total volume of 10 µl, then reaction was run as in the steps at Table 2.10 and for quantification TPT1 reference gene was used. Both reactions were conducted in the LightCycler® 480 Instrument II and for the analysis and the quantification of both RT-qPCRs results, $\Delta\Delta C_t$ method was used, where relative

expression is calculated and normalized to a reference gene. Statistical analyses and graph representations of the results was done on the GraphPad Prism tool.

Table 2.9: Realtime qPCR steps for miRNA quantification

Step	Temperature (°C)	Time (mm:ss)	Cycles
Pre-incubation	95	15:00	1
Amplification	94	0:15	45
	55	0:30	
	70	0:30	
Melting Curve	95	0:05	1
	55	1:00	
	95	Acquisition per 5 °C	
Cooling	40	0:30	1

Table 2.10: Realtime qPCR steps for mRNA quantification

Step	Temperature (°C)	Time (mm:ss)	Cycles
Pre-incubation	95	5:00	1
Amplification	95	0:10	50
	60	0:20	
	72	0:20	
Melting Curve	95	0:05	1
	55	1:00	
	95	Acquisition per 5 °C	
Cooling	40	0:30	1

2.2.3 MTT Experiments

In the 96-well plates, in which MTT experiments are going to be conducted, complete phenol-free DMEM was used during transfection protocol. After the 72 hours of incubation time, MTT assay protocol had been followed according to manufacturer's instructions. In which; first MTT had been solved in PBS then mixed with the complete phenol-free DMEM. This mixture had been distributed on to cells as 110 µl/well and left to incubator (37°C %5 CO_2) for 4 hours. After first incubation; SDS-HCl solution was added as 100

µl/well and incubated for the 18 hours in the 37°C %5 CO_2 incubator. Next day, results are taken with the help of Synergy Multi-Mode Reader at 570 nm. Normalizations, statistical analyses and graphical representations of the results were done using GraphPad Prism tool.

2.2.4 Phalloidin Staining

For phalloidin staining, first cover slips were sterilized by first autoclave then with UV. Sterile cover slips were placed at the bottom of the 12-well plates before cells were seeded. After transfection protocols and 72 hours incubation cover slips with cells were washed over with PBS and cells were fixated with 4%PFA in PBS for 10 minutes at room temperature. After washing with PBS for 5 minutes 3 times, permeabilization was done using PBS with 0.1% Triton-X (PBX) for 10 minutes. Blocking was done with 1% BSA in PBX (BBX) for 45 minutes and washed using PBX for 5 minutes 3 times. For staining; actin dye phalloidin was diluted in PBX (1:1000) and incubated on slips for 45 minutes inside humidified chambers. Excess dye is washed with PBX for 15 minutes 2 times and before mounting to slides another wash was made in PBS for 10 minutes. Lastly, cover slips are mounted on to cover slides with UltraCruz Mounting Medium including DAPI with a drop and left to dry at room temperature. For storage they are transferred to +4°C. Fluorescent images were taken with Axio Imager A1 (Zeiss) microscope then image normalization and merging was done using ImageJ image analysis tool.

2.2.5 Fluorescence Microscopy Images and Competition Assay

To see the effects of the miRNA mimics individually or in combination on of the siRNA for CHRNA5 on the cell growth and competition of the cells, fluorescent (GFP or BFP) tagged MCF7 cell lines were generated.

2.2.5.1 Single Colony Generations from The Polyclonal Cells

GFP and BFP transfected polyclonal cells were a kind courtesy of Sahika Cingir Koker (Sahika Cingir, PhD Thesis, Bilkent University 2019). These cells opened from the frozen stocks and then seeded on to the 96-well plates with a serial dilution method, where 4000 cells are serially diluted on the first column. Then this column is serially diluted through the columns 1 to 12. These cells are grown for 4 to 6 weeks with conditioned media which was the mixture of old media of the wild-type cells (centrifuged at 5000rpm for 10 minutes to remove any floating cells) and fresh media[219]. Lastly, GFP or BFP positive cell percentages of the grown single colonies are measured with the help of the NovoCyte 3000 flow cytometry and 100% tagged colonies are selected.

2.2.5.2 Co-Culture Competition Experiments

To see the effects of the miRNA mimics on the cell growth and the cell competition; cells were transfected with the specified molecules in a step-wise manner. First transfections had been done on the cells that were seeded on the 24-well plates. After the 72 hours incubation time of the first transfections; cells were transferred into new plates in equal densities and second transfections were done on top of them after attachment. After 48 hours of incubation with the second transfections; fluorescent images were taken with the Leica DMi8 Inverted Microscope. Cells then collected and fixed for the flow counting. Fixation has been done with 4%PFA in PBS and solved in the FACS buffer in which they are stored until the counting at 4°C at dark. Percentages of the GFP or BFP positive cells were counted with the NovoCyte 3000 flow cytometry and statistical analyses with graphical representations were done using GraphPad Prism tool. General experiment flow can be seen in the Figure 2.1.

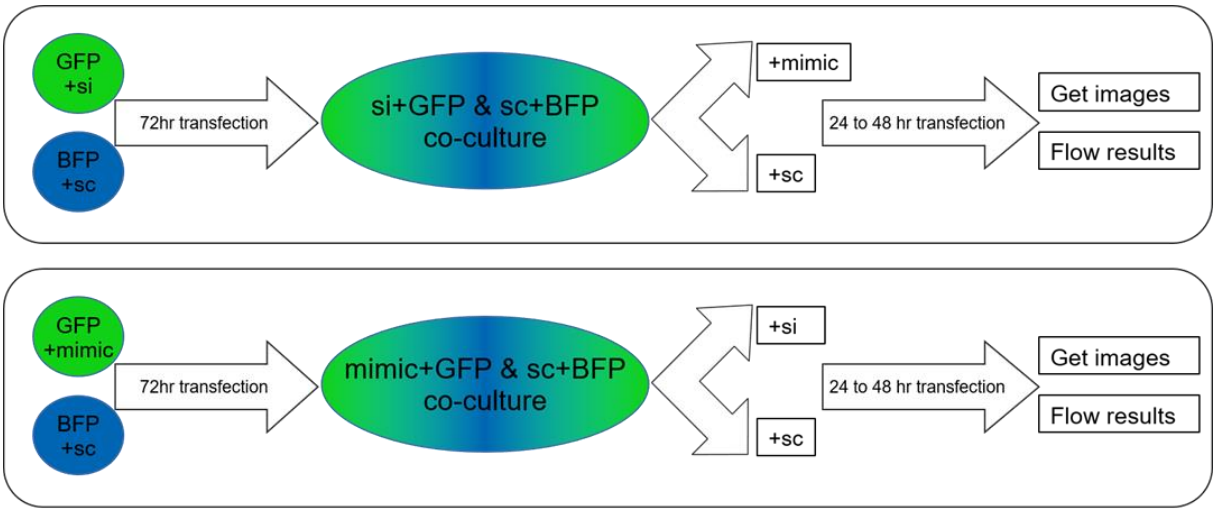

Figure 2.1: Outline for the co-culture competition experiments.

2.3 *In Silico* Methods

2.3.1 miRNet Network Generation

In the miRNet tool website (*www.mirnet.ca*), miRNAs were selected as input method [147, 148]. In the specifications above; Organism: H. sapiens (human), ID type: miRbase ID and Target type: Genes were selected. In the box below mature miRNA names; hsa-miR-376a-3p or hsa-miR-376c-3p, were submitted as input. In the next two steps of '*Interaction Table*' and '*Network Builder*' tabs default settings were used. In the next tab at '*Network Viewer*' preliminary network can be seen. From settings at top, background color and topology of network were adjusted. On the right side under '*Function Explorer*' box, all genes were taken as query and hypergeometric test was used as algorithm for KEGG analysis. Genes from the pathways that are relevant to cell cycle, apoptosis and cancer were highlighted. Lastly, from the '*View Options*' network structure and node size were adjusted and image was downloaded.

2.3.2 Acquisition of miRNA Target List

miRNA target list was downloaded from online mirDIP tool (*ophid.utoronto.ca/mirDIP/*) [149, 150]. Mature miRNA names; hsa-miR-376a-3p or hsa-miR-376c-3p, were given as input to microRNA box then in below for minimum score class '*Very High*' was selected and total list of targets was downloaded.

2.3.3 Enrichment Analyses

The miRNA target lists were used for the enrichment analyses on the online Enrichr tool (*amp.pharm.mssm.edu/Enrichr/*) [172, 173]. Official gene symbols from the gene list was put to input box, then in the results page bar graphs of 'KEGG Pathways', 'Reactome Pathways', 'Panther Pathways' and 'GO Biological Processes' were downloaded after color scheme adjustments.

2.3.4 Functional Classifications from PantherDB tool

The miRNA target list acquired above was used as input for the PantherDB tool (*pantherdb.org*) [170, 171]. For organism '*Homo Sapiens*' was selected then in below for analyses 'Functional classification viewed in graphic charts' and display as a pie chart was selected. In the chart page opened biological processes were selected as ontology and results data was exported from the link above. Data was redrawn as a pie chart in the GraphPad Prism tool with adjustments to color scheme and sizes.

2.3.5 Affymetrix mRNA Microarrays

Samples that were going to be used in the microarray experiments had their RIN total RNA quality measured and all samples had RIN values between 9 and 10. One replicate of each sample, was studied on the Affymetrix Human Genome U133 Plus 2.0 (HGU133_plus2.0) array platforms (AY-KA Ltd.). Raw expression results were taken as

the .CEL files then quality controls and RMA normalizations were done using R Bioconductor package in collaboration with Ayse Gokce Keskus [220, 221]. Log-fold changes (LFC) of genes was calculated by subtracting the expression value of the group (si-CHRNA5+mimic or mimic) from the scramble control group. Then expression values matrix was merged with the expression data from the previous studies (Ermira Jahja PhD Thesis, Bilkent University 2017). Lastly, these values were plotted against si-CHRNA5 expression data using GraphPad Prism tool and correlation scores in between were calculated using the *cor* function in R.

2.3.6 Ingenuity Pathway Analysis

In Ingenuity Pathway Analysis (IPA) tool [174], expression data of genes that were affected most, genes with log2 fold changes (LFC) higher than 0.5 was analyzed. With the '*Core Analysis*' option all data was analyzed for each condition and 'Analysis Comparison' function was used to observe the differences in the affected '*Canonical Pathways'* and '*Diseases and Bio Functions*' side by side. In addition, most significantly affected pathways or molecules were also further investigated.

3 Results

In the previous studies from our lab, Ermira Jahja successfully downregulated CHRNA5 in the MCF7 breast cancer cell line with three different siRNA molecules (Ermira Jahja PhD thesis, Bilkent University 2017). Later on, a microRNA microarray analysis of scrambled and si-CHRNA5 treated MCF7 cells samples was performed and several highly downregulated microRNAs were selected (Table 3.1) for further experiments (Theses of Sahika Cingir Koker,2019 and Basak Ozgursoy, 2017). In the present study, I have focused on change of expression in two of these microRNAs from miR-376 family, namely, miR-376a and miR-376c. I was able to validate the decrease in the expression by CHRNA5 siRNA application in comparison to scrambled control molecule, by RT-qPCR (Figure 3.1).

Table 3.1: Changes in miRNA expression from the microarray study of the scrambled or si-CHRNA5 treated samples.

Probe.Set.ID	Transcript ID	MIMAT ID	logFC	p-value
20503805	miR-495	MIMAT0002817	-4.4868775	0.0000008
20501239	miR-376a	MIMAT0000729	-3.2156815	0.0000109
20504421	miR-654	MIMAT0004814	-3.775904	0.0000187
20502456	miR-409	MIMAT0001639	-3.822047	0.0006924
20501224	miR-376c	MIMAT0000720	-2.3593845	0.0016417

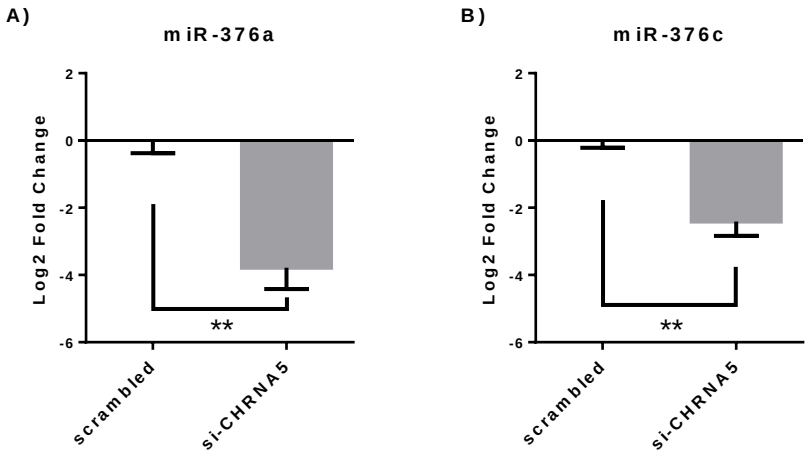

*Figure 3.1: RT-qPCR confirmations of the downregulation of mir-376a (A) and miR-376c (B) in the scramble or siRNA-1 treated MCF7 cells (n=5), **: p-value ≤ 0.01.*

Rescue experiments were also conducted for these two miRNAs using specific miRNA mimics. For miR-376a, the effects of mimic application on transcriptome were investigated with microarrays followed by validation studies using RT-qPCR; and for miR-376c, only RT-qPCR of selected predicted targets was performed. Phalloidin staining was used to investigate the effects of mimics on cytoskeletal organization of cells while cell viability in the presence or absence of siRNA against CHRNA5 was tested using MTT experiments. In addition, I have established a co-culture competition experimental procedure and applied it the microRNAs listed in Table 3.1 to investigate their effects on the cell competition when miRNA mimics were given in combination with si-CHRNA5. In the following sections, the experiments described above and the results obtained from these experiments are provided.

3.1 miR-376a

3.1.1 Preliminary *in silico* Analyses

Online miRNet tool was used to generate a target network as in the Figure 3.2 and from in-built enrichment analysis I found out 112 genes, 11 of which were from the pathways related to cell cycle, apoptosis and cancer (labeled green). Then, another predicted targets list was taken from the online mirDIP tool. Enrichment analyses and functional classifications for biological processes were applied for this list using online Enrichr and PantherDB tools, respectively. In enrichment results, from four selected criteria; in KEGG, cancer related pathways including Ras signaling and PI3K-Akt axis were observed along with cytoskeleton regulation (Figure 3.3, purple). On Reactome and Panther results similar results came out as development and growth factors related pathways as well as cell communication in Reactome (Figure 3.3, red) and cytoskeleton in Panther pathways (Figure 3.3, green). Lastly on GO biological processes; vascular processes, RNA polymerase II regulation and cell migration with proliferation appeared (Figure 3.3, blue). On the functional classifications, I observed localization, adhesion, reproduction and development related processes (Figure 3.4).

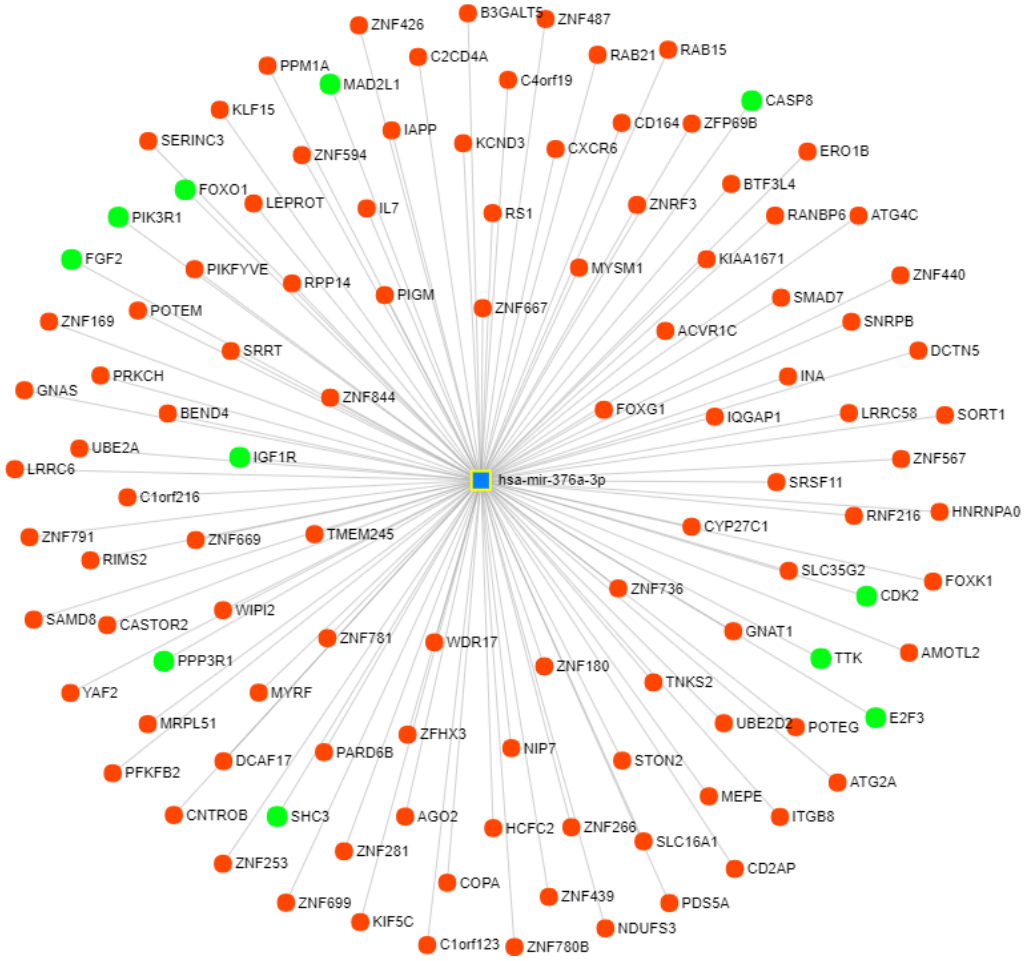

Figure 3.2: Target network of the miR-376a with miRNet tool; blue square represents miRNA and circles show gene targets and green circles represents genes from cell cycle, apoptosis and cancer related pathways.

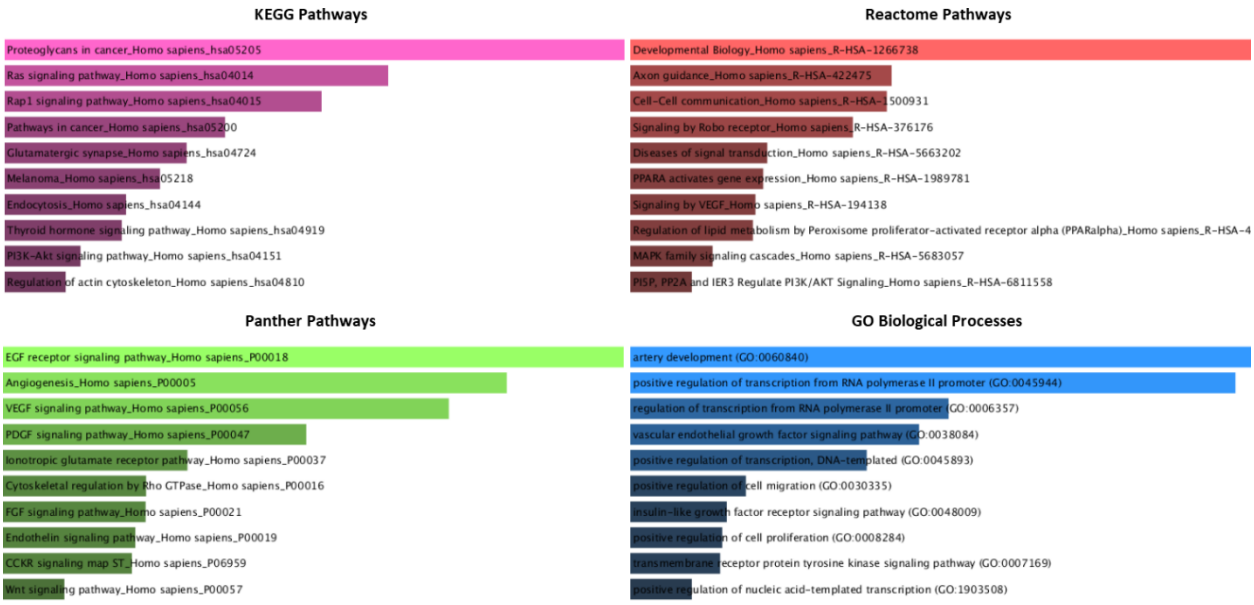

Figure 3.3: Results of the enrichments done on the online Enrichr tool for the miR-376a predicted targets from the mirDIP tool as bar graphs of combined scores of Z-scores ranks and p-values. Graphs were color coded as; purple for KEGG pathways, red for Reactome pathways, green for Panther Pathways and blue for GO Biological Processes.

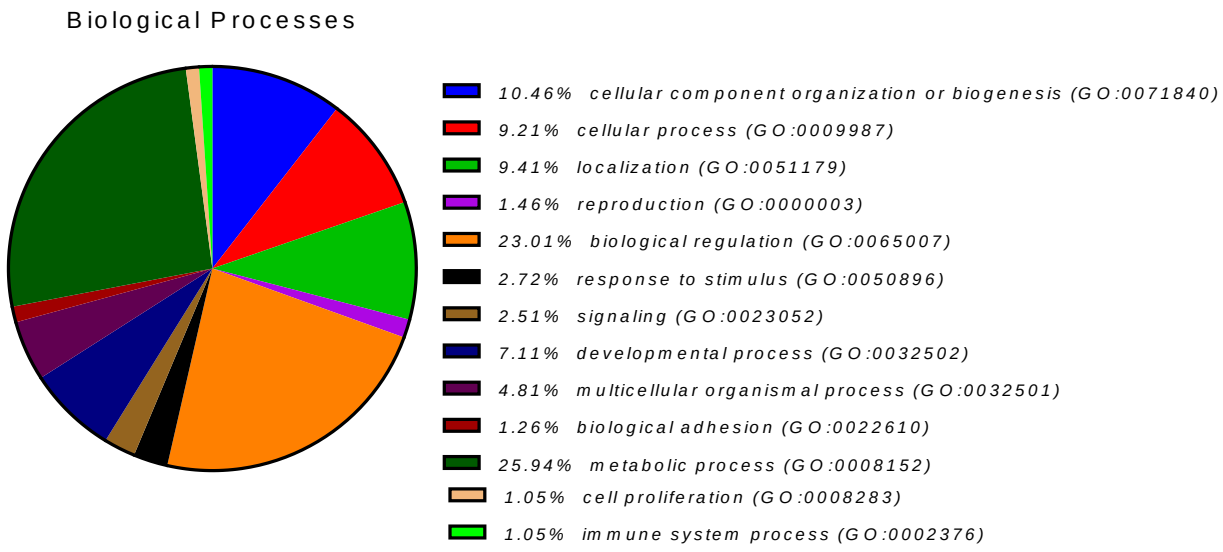

Figure 3.4: Functional classifications of miR-376a predicted targets from the mirDIP for the biological processes with the online PantherDB tool.

3.1.2 miRNA rescue and RT-qPCR confirmations

For the validation of miRNA rescue; MCF7 cells were transfected with si-CHRNA5 and/or miR-376a mimic. RT-qPCR experiments were conducted for both, CHRNA5 and miR-

376a, in which, I observed a significant decrease in the CHRNA5 expression on the si-CHRNA5 treated samples and an increased miR-376a expression on the mimic given samples (Figure 3.5).

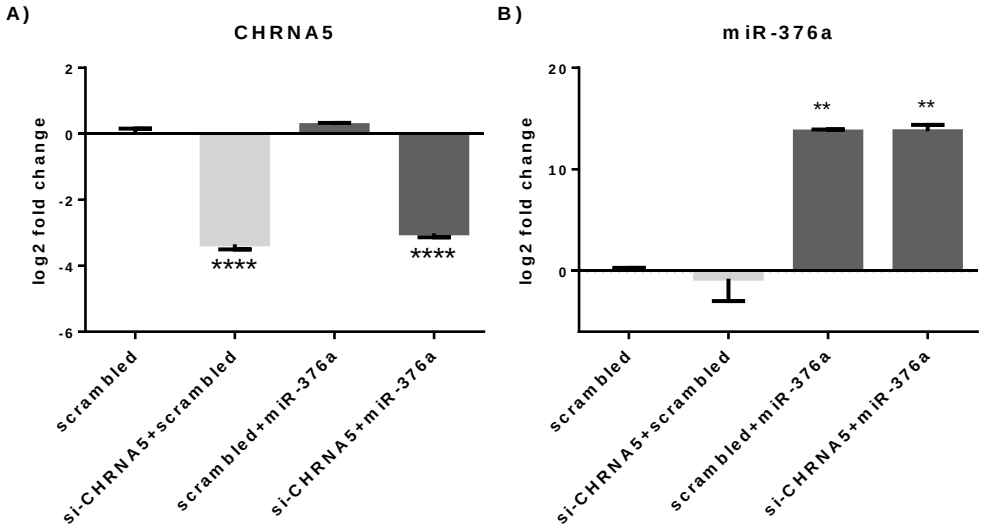

*Figure 3.5: RT-qPCR confirmations of the CHRNA5 downregulation with si-CHRNA5(A) and miR-376a rescue with miRNA mimic (B) **: p-value ≤ 0.01 and ****: p-value ≤ 0.0001, when compared to scrambled control group.*

3.1.3 Transcriptome Analysis Results

Transcriptomic profiling of mimic and/or si-CHRNA5 treated samples were performed with microarrays. Log-fold (logFC) changes were calculated for mimic-376a and si-CHRNA5+mimic-376a samples using *rma* normalized results. In comparative transcriptomic analysis with previous microarray done by Ermira Jahja (PhD Thesis, Bilkent University 2017), there was a mild negative correlation between the expression profiles from mimic-376a and si-CHRNA5 treatments (r= -0.05668286, p=2.2e-16), however the addition of si-CHRNA to mimic increased the correlation score expectedly (r=0.7367566; p=2.2e-16). Also, I observed the effect range of si-CHRNA5 (indicated by red line, [-3.05, 4.04]) and si-CHRNA5+mimic (indicated by green line, [-3.51, 4.08]) were

comparatively larger than the range of mimics (indicated by blue line, [-2.38, 1.40]) (Figure 3.6).

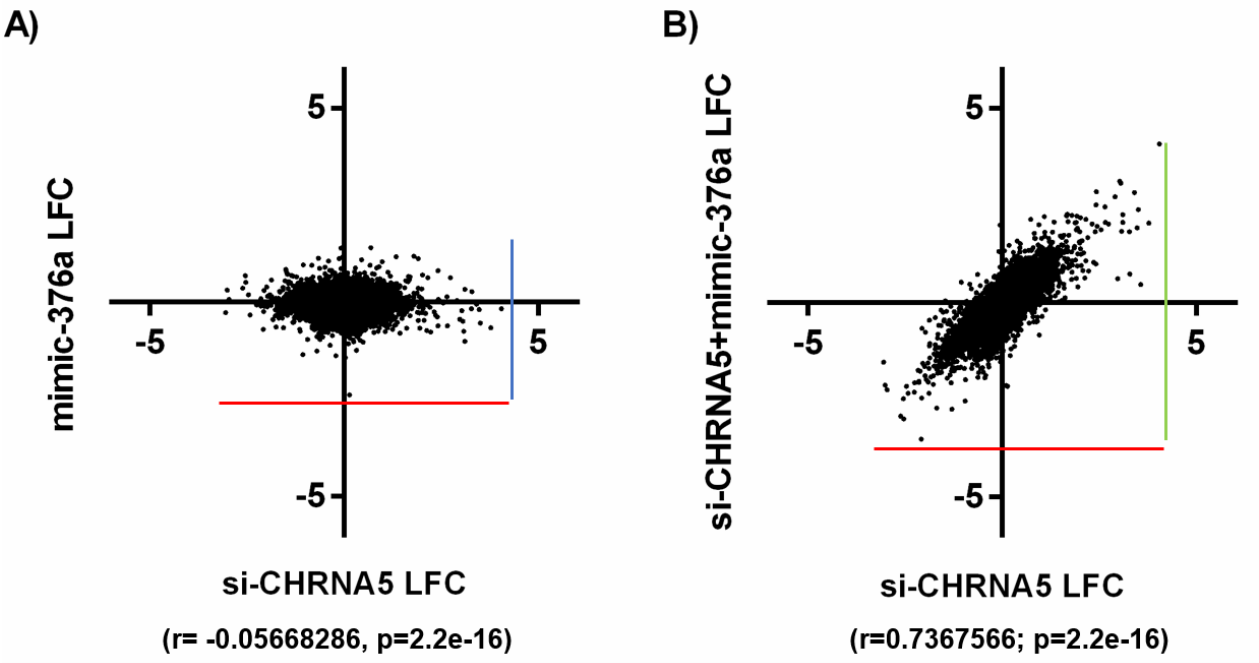

Figure 3.6: Scatter plot representations of log fold changes (logFC) in mimic-376a (A) and si-CHRNA5+mimic-376a (B) against si-CHRNA5 logFC: mimic-376a only sample shown a mild negative correlation with si-CHRNA5 (A) but si-CHRNA5+mimic-376a sample shown a significant positive correlation(B). Effect ranges of mimic-376a shown with blue line, [-2.38, 1.40], si-CHRNA5 shown with red line, [-3.05, 4.04], and si-CHRNA5+mimic-376a, [-3.51, 4.08], shown with green line.

3.1.3.1 Ingenuity Pathway Analysis (IPA) Results

In IPA tool, logFC values obtained from the mimic-376a and si-CHRNA5+mimic-376a experiments were used for a core analysis and heatmaps of top affected *'Canonical Pathways'* and *'Diseases and Bio Functions'* were generated (Figure 3.7). On the top twenty canonical pathways, seven were only affected by the si-CHRNA5 and after that, other thirteen pathways were affected by both si-CHRNA5 and mimic-376a exposure. Interestingly eleven of them showed a pattern, si-CHRNA5 caused activation and mimic addition leads to inactivation. This group of pathways included role of NFAT in regulation of the immune receptors, HMGB1 signaling, Tec kinase signaling, CXCR4 signaling, IGF1

signaling, sphingosine-1-phosphate signaling, $G_{\alpha q}$ signaling and sumoylation pathway (Figure 3.7, left side). On the diseases and bio functions however, from top twenty, we found four functions that were synergistically inhibited by both si-CHRNA5 and mimic-376a, which were related to cell survival, viability and proliferation. In the remaining sixteen functions there were eight, which were synergistically activated by both treatments which included organismal death, growth failure, lymphoid cancer and tumors, lymphohematopoietic neoplasia and cancer, lymphocytic neoplasm and incidence of tumors. (Figure 3.7, right side).

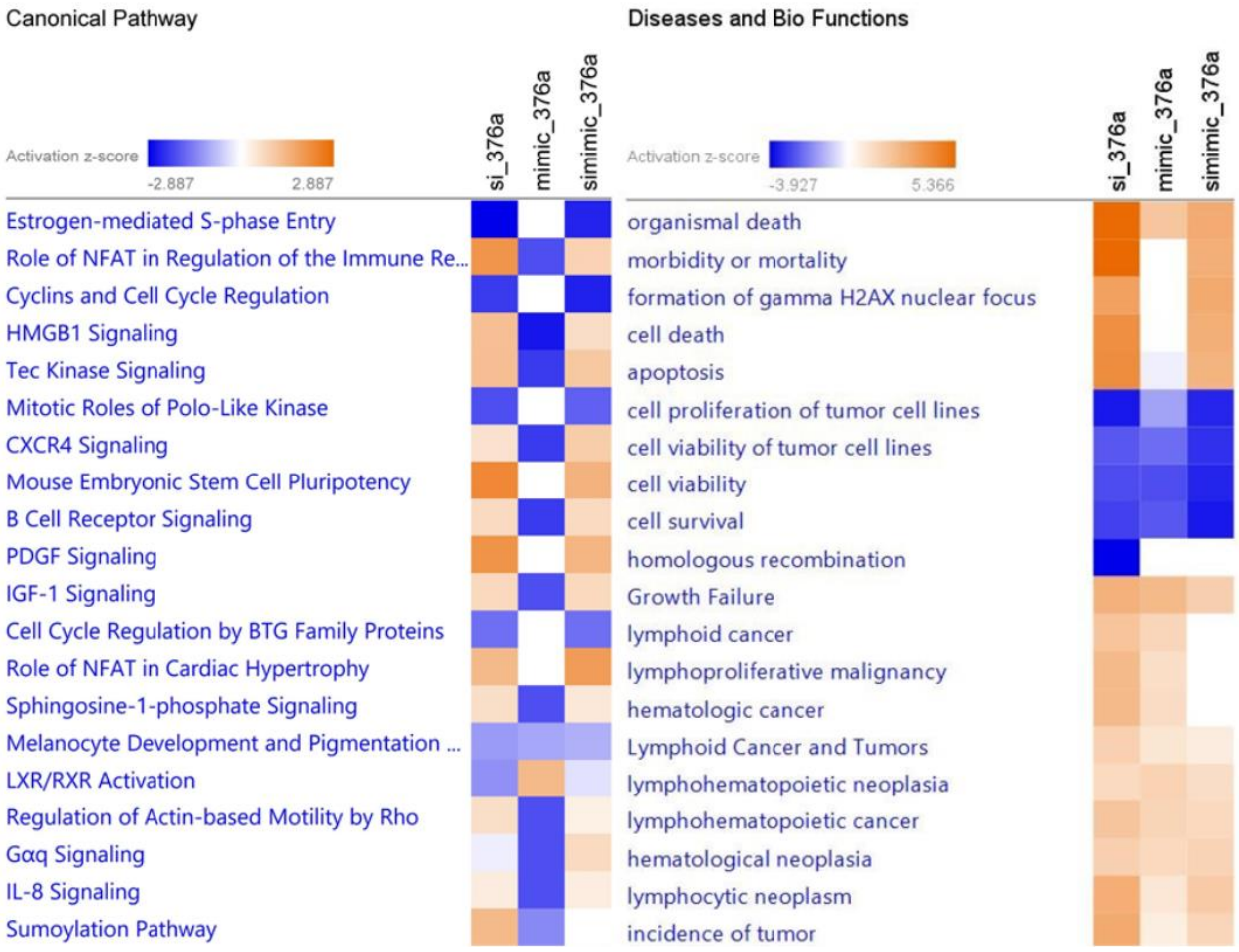

Figure 3.7: Top affected 'Canonical Pathways' (left) and 'Diseases and Bio Functions' (right) from the IPA core analyses of the miR-376a array data comparisons, orange color shows activation from the z-score and blue color shows inactivation on the pathway or function.

3.1.4 Target Predictions and Confirmations

For the predicted mRNA targets and the relevant genes affected by mimic and siRNA treatments, RT-qPCR experiments were conducted. STON2 and BMPR2 genes were selected from direct targets, which were decreased with si-CHRNA5 and mimic miR-376a treatments and further decreased when given in combination (Figure 3.8).

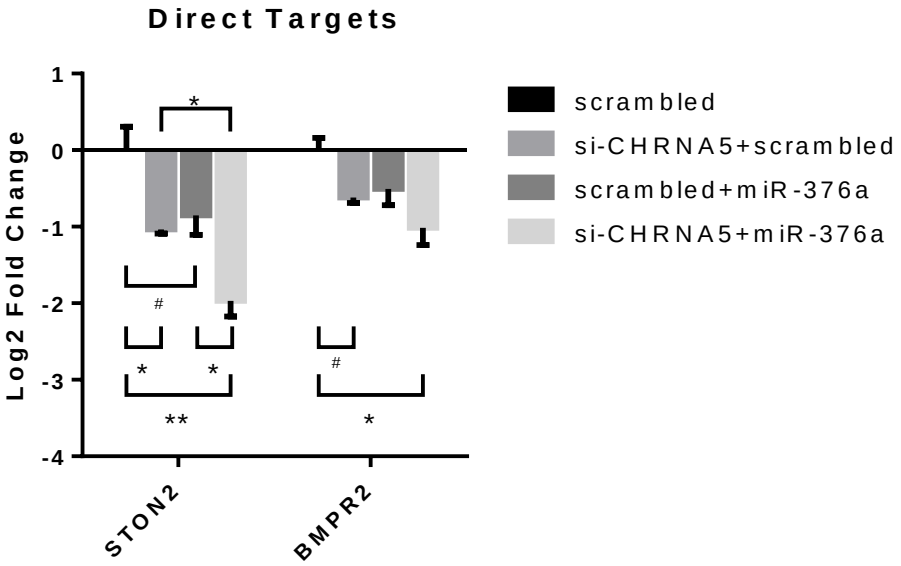

*Figure 3.8: RT-qPCR results of the direct targets of miR-376a, STON2 and BMPR2, on si-CHRNA5 and miR-376a mimic given samples. *: p-value ≤ 0.05 and **: p-value ≤ 0.01, #: p-value ≤ 0.1 from Tukey's multiple comparison test.*

Secondly, from p53 pathway; MDM2, FOS and CDKN1A (p21) genes were selected (Figure 3.9). On MDM2 I observed a decrease primarily from si-CHRNA5 treatment and a minimal effect from miR-376a mimic treatment (Figure 3.9, left). On the other hand, on FOS gene I observed a decrease mainly from the mimic treatment (Figure 3.9, middle). Lastly, in CDKN1A (also known as p21) I observed a drastic increase from si-CHRNA5 treatments, while mimic treatment led decrease minimally (Figure 3.9, right).

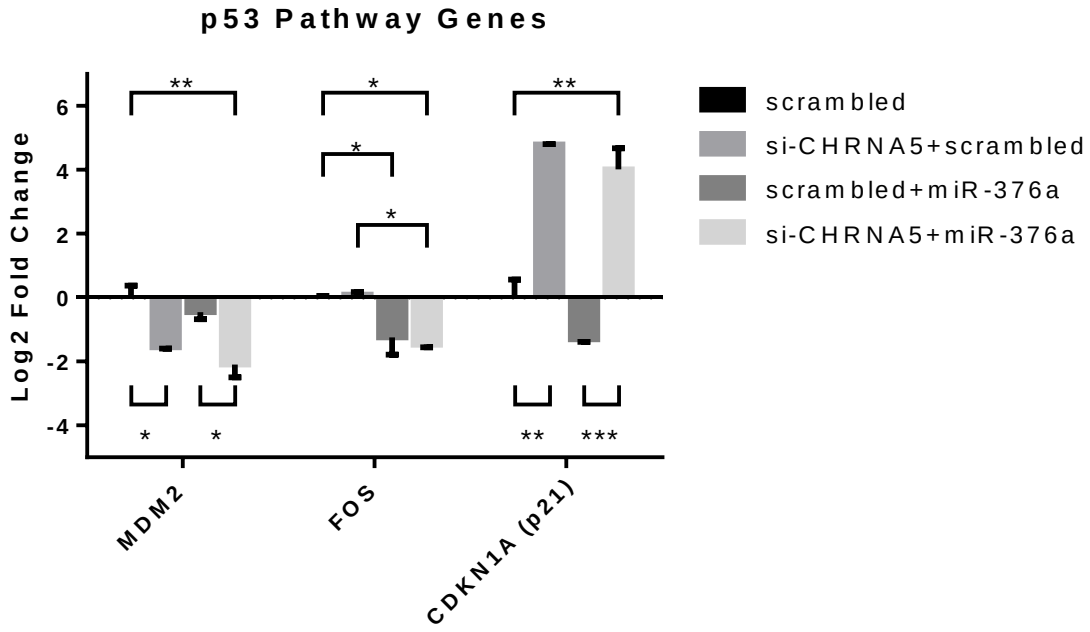

*Figure 3.9: RT-qPCR results of the p53 pathway genes , MDM2, FOS and CDKN1A (p21), on si-CHRNA5 and miR-376a mimic given samples. *: p-value ≤ 0.05, **: p-value ≤ 0.01, ****: p-value ≤ 0.001 from Tukey's multiple comparison test.*

On another note, to show effects on the cell cycle, I selected CDC6, WDHD1, BIRC5 and ANLN genes (Figure 3.10). From these, CDC6 and WDHD1 genes had a major decrease with si-CHRNA5 treatments and insignificant increase from mirR-376a mimics (Figure 3.10, left two groups). Then, on BIRC5 and ANLN genes I observed decrease with si-CHRNA5 and increase with miR-376 mimics and when given in combination, si-CHRNA5 effect was overcome (Figure 3.10, right two groups).

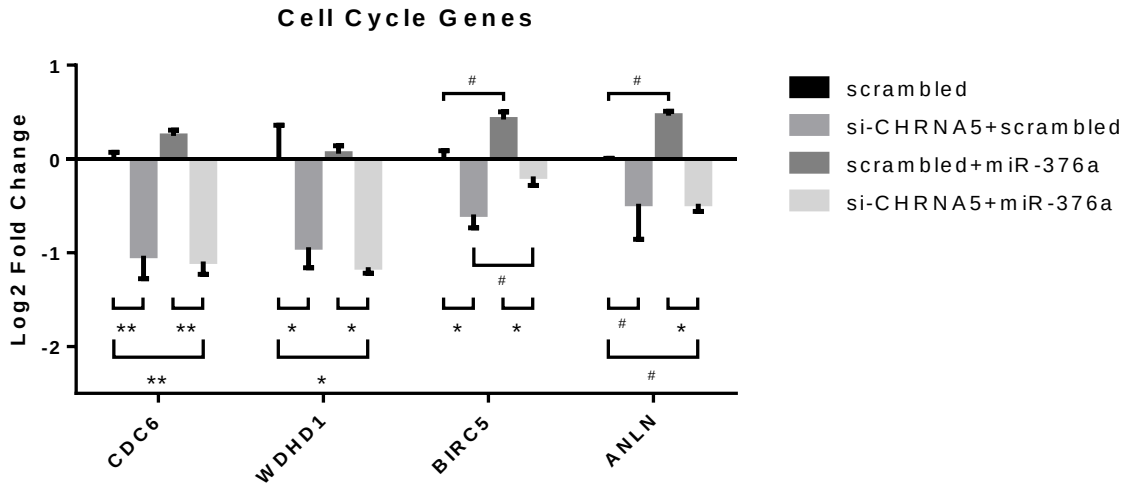

*Figure 3.10: RT-qPCR results of the cell cycle genes , CDC6, WDHD1, BIRC5 and ANLN, on si-CHRNA5 and miR-376a mimic given samples. *: p-value ≤ 0.05 and **: p-value ≤ 0.01 #: p-value ≤ 0.1 from Tukey's multiple comparison test.*

3.2 miR-376c

3.2.1 Preliminary *in silico* Analyses

Using online miRNet tool I generated a network for the miR-376c as in the Figure 3.11 and the enrichment test highlighted the genes relevant to cell cycle, apoptosis and cancer related pathways with green (sixteen out of eighty-four). Next, the predicted targets list taken from the mirDIP tool was used for statistical and functional classifications for biological processes using Enrichr and PantherDB online tools. In enrichment results; for KEGG, cancer related pathways and FOXO signaling were observed (Figure 3.12, purple). In Reactome however, development and neuron growth with axon guidance could be seen (Figure 3.12, red). On Panther results, Wnt signaling, ubiquitination and TGF-β signaling came out as significant pathways (Figure 3.12, green) and lastly in GO biological processes, transcription and differentiation related processes could be seen (Figure 3.12, blue). On the functional classifications for biological processes the results were similar to previous results obtained for miR-376a (Figure 3.4) and again prevailing

processes were about localization, adhesion, reproduction and development with only the addition of locomotion (*GO:0040011*) and growth (GO:0040007) as well as with small changes on the percentages (Figure 3.13).

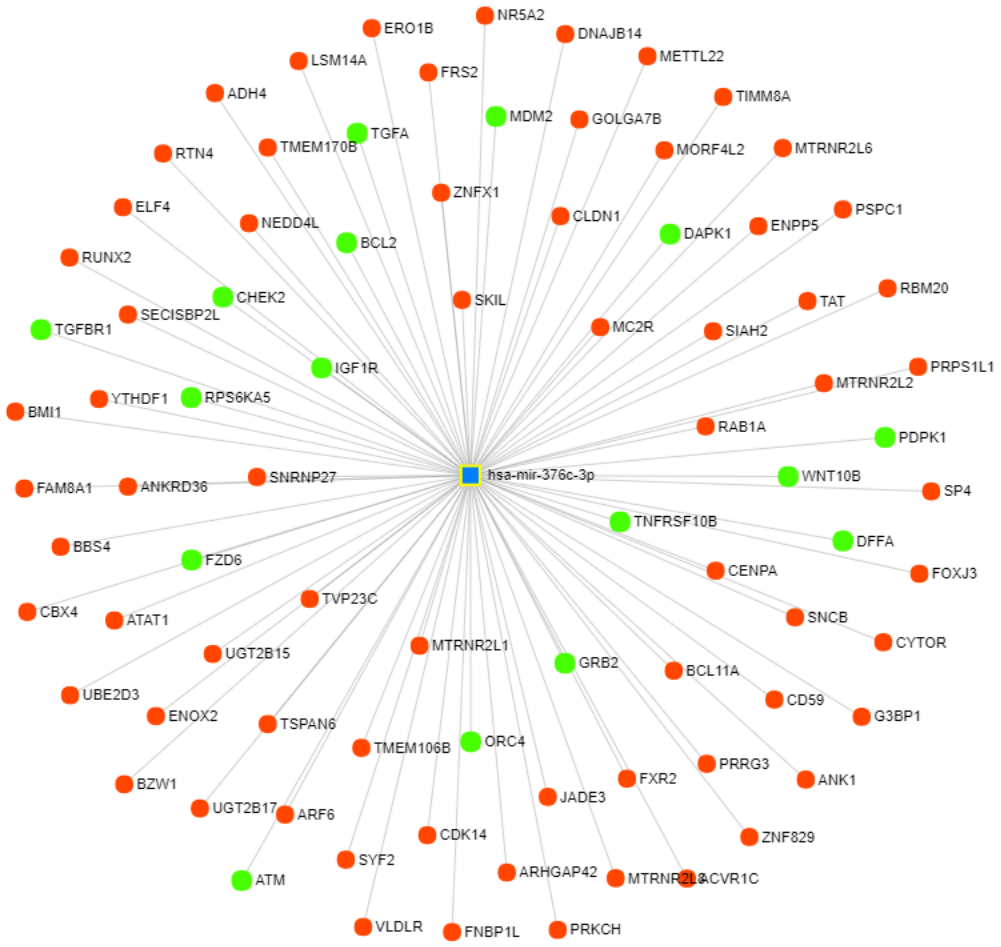

Figure 3.11: Target network of the miR-376c with miRNet tool where blue square shows miRNA and circles show gene targets, genes from cell cycle, apoptosis and cancer related pathways are labeled with green.

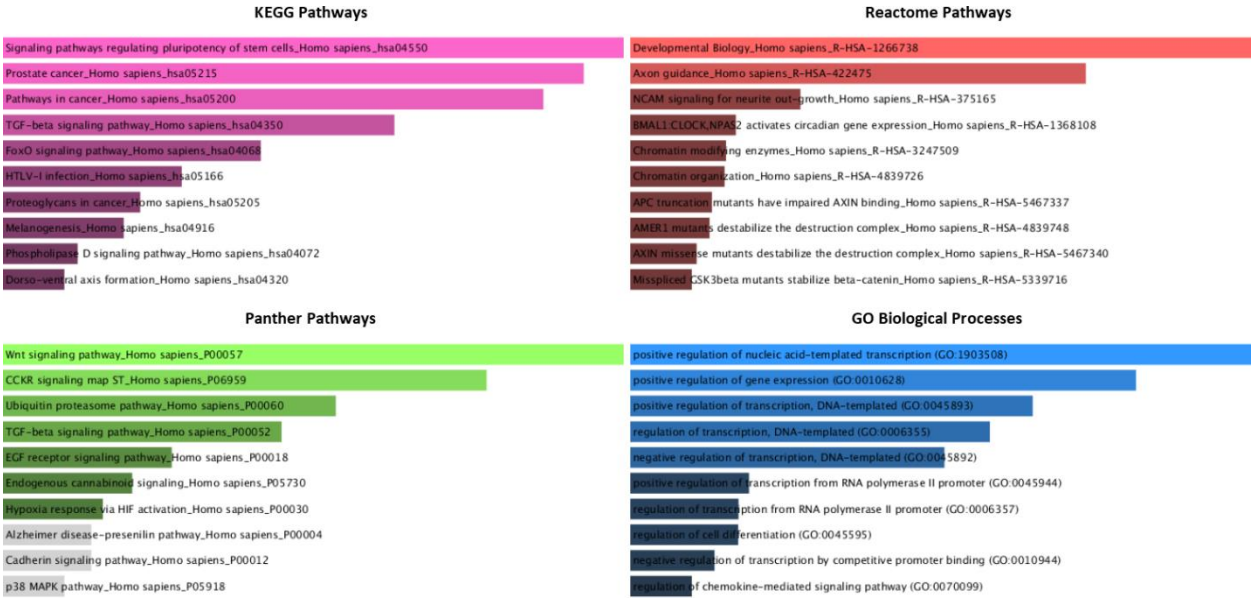

Figure 3.12: Results of the enrichments done on the online Enrichr tool for the miR-376c predicted targets from the mirDIP tool as bar graphs of combined scores of Z-scores ranks and p-values. Graphs were color coded as; purple for KEGG pathways, red for Reactome pathways, green for Panther Pathways and blue for GO Biological Processes.

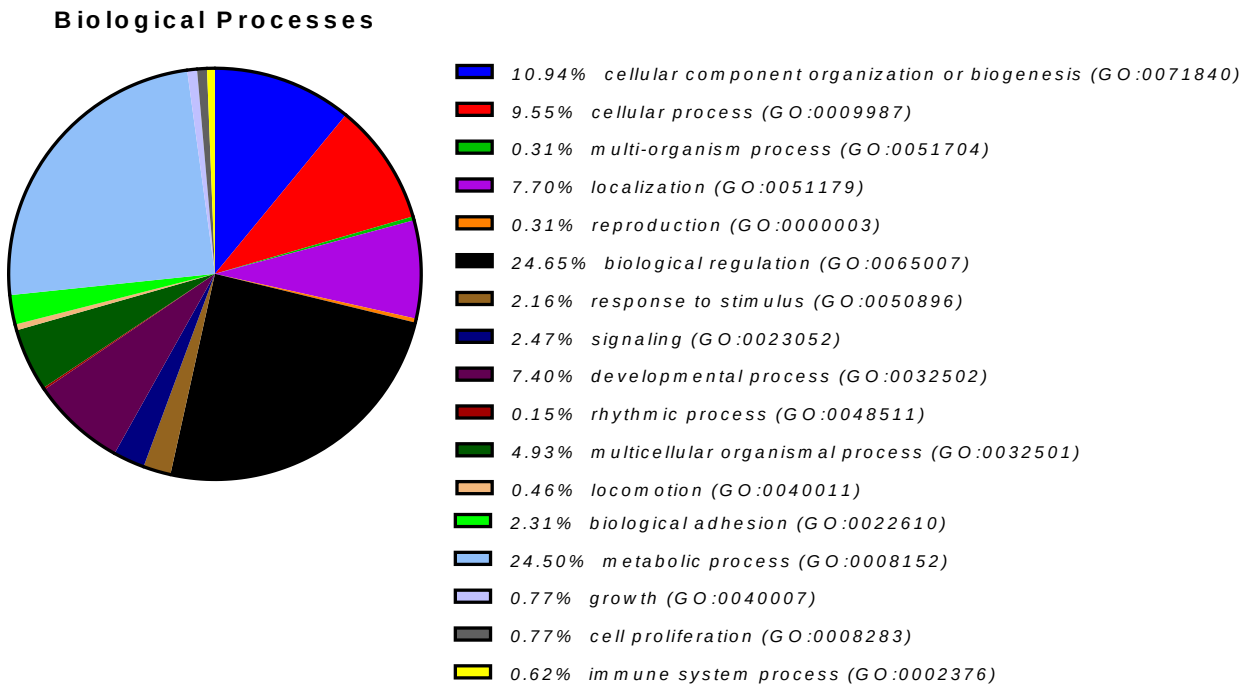

Figure 3.13: Functional classifications of miR-376c predicted targets from the mirDIP for the biological processes with the online PantherDB tool.

3.2.2 miRNA rescue and RT-qPCR Confirmations

I used miRNA mimics for the restoration of miR-376c expression in the presence or absence of si-CHRNA5 on the MCF7 cells. From the RT-qPCR experiments I observed a significant decrease in the CHRNA5 expression on si-CHRNA5 given samples as well as increased miR-376c expression on mimic given samples (Figure 3.14).

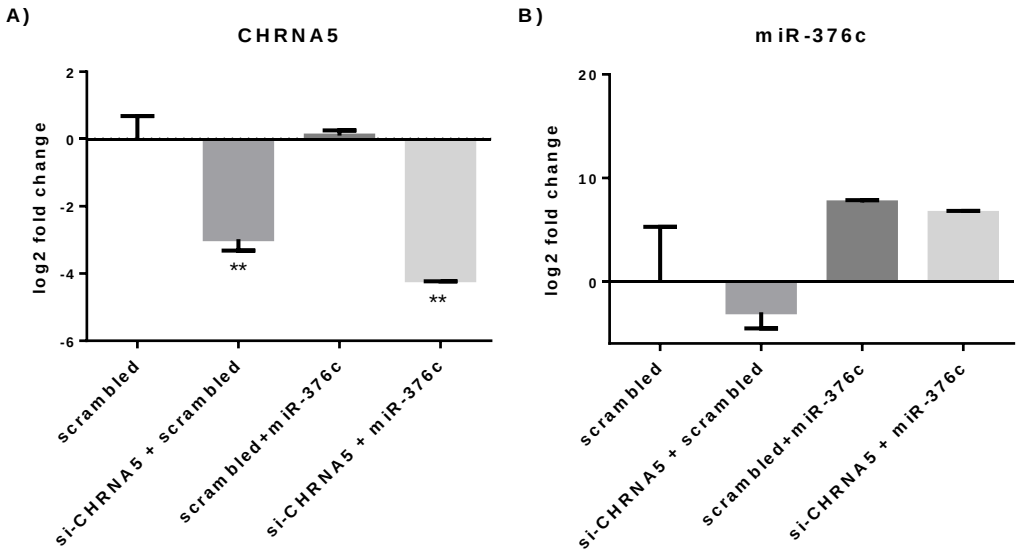

*Figure 3.14: RT-qPCR confirmations of the CHRNA5 downregulation with si-CHRNA5(A) and miR-376c rescue with miRNA mimic (B) **: p-value ≤ 0.01 when compared to scrambled control group.*

3.2.3 Target Predictions and Confirmations

Gene expression analyses were done on the selected genes of interest (for WDHW1, FOS, CDKN1A and CLDN genes) with the RT-qPCR for the miR-376c samples. and results can be seen in the Figure 3.15. I did RT-qPCR investigations of genes from each category we were interested. Which are; WDHD1 for cell cycle (Figure 3.15, A), FOS and CDKN1A (p21) for p53 pathway (Figure 3.15, B and C, respectively) and CLDN for cell cytoskeleton (Figure 3.15, D). In none of the qPCR studies conducted I couldn't see the significance in the expression changes coming from miR-376c and didn't investigate further.

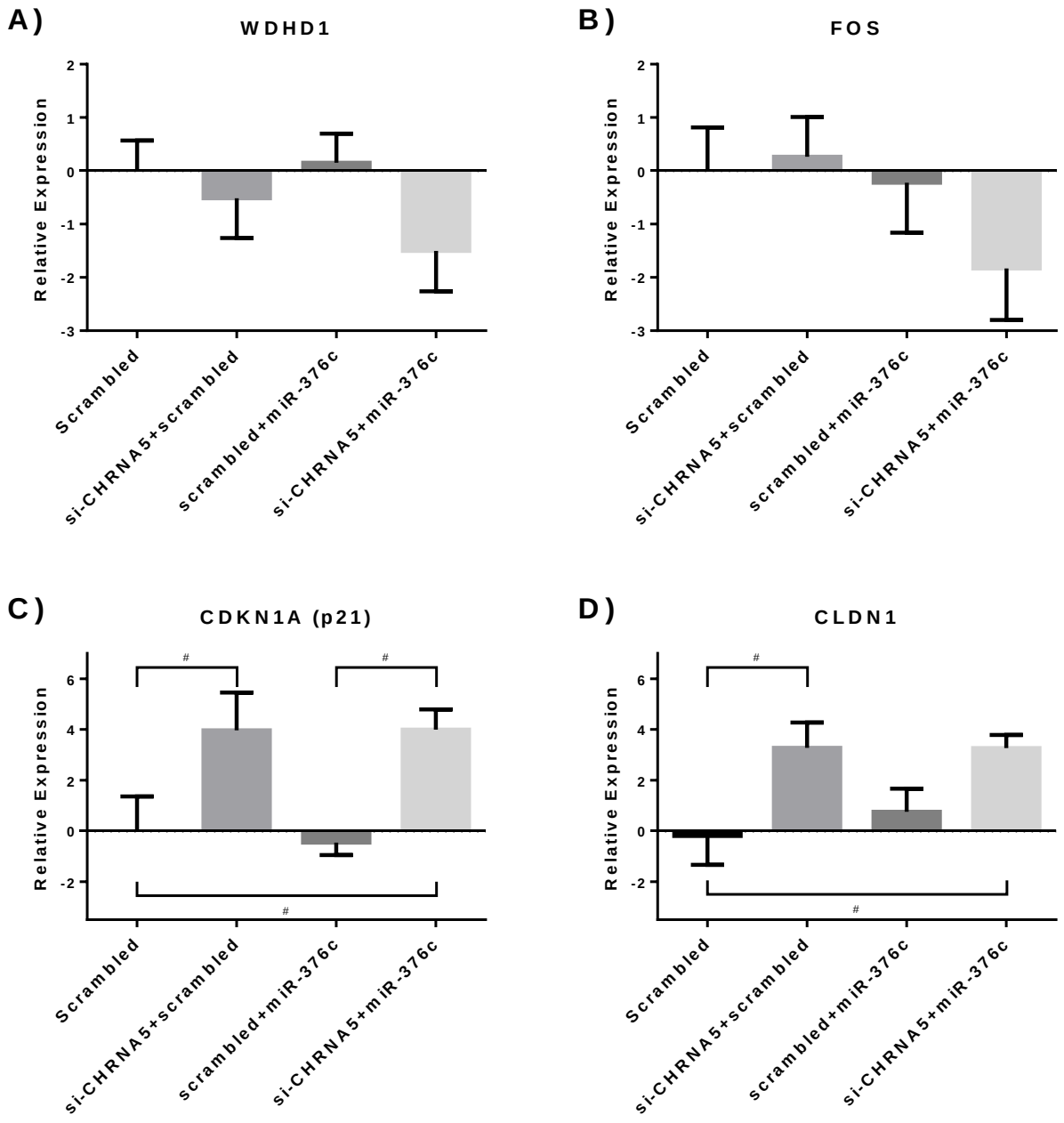

Figure 3.15: RT-qPCR results of the selected genes (A) WDHD1, (B) FOS, (C) CDKN1A (p21) and (D) CLDN on si-CHRNA5 and miR-376c mimic given samples. #: p-value ≤ 0.1 from Tukey's multiple comparison test.

3.3 Phalloidin Results

I also wanted to examine morphological effects of the miRNA mimics on combination with si-CHRNA5 on MCF7 cells, thus F-actin was stained using phalloidin molecules (Figure 3.16). Here I observed a phenotypical change on the cells which si-CHRNA5 was given. As the typical cubic shaped and densely packed MCF7 cells were transformed into more elongated shapes with less contacts in between. However, addition of both; miR-376a and miR-376c, mimics didn't cause much difference in the scramble groups and when in combination with si-CHRNA5, phenotypic change caused by siRNA was more apparent (Figure 3.16).

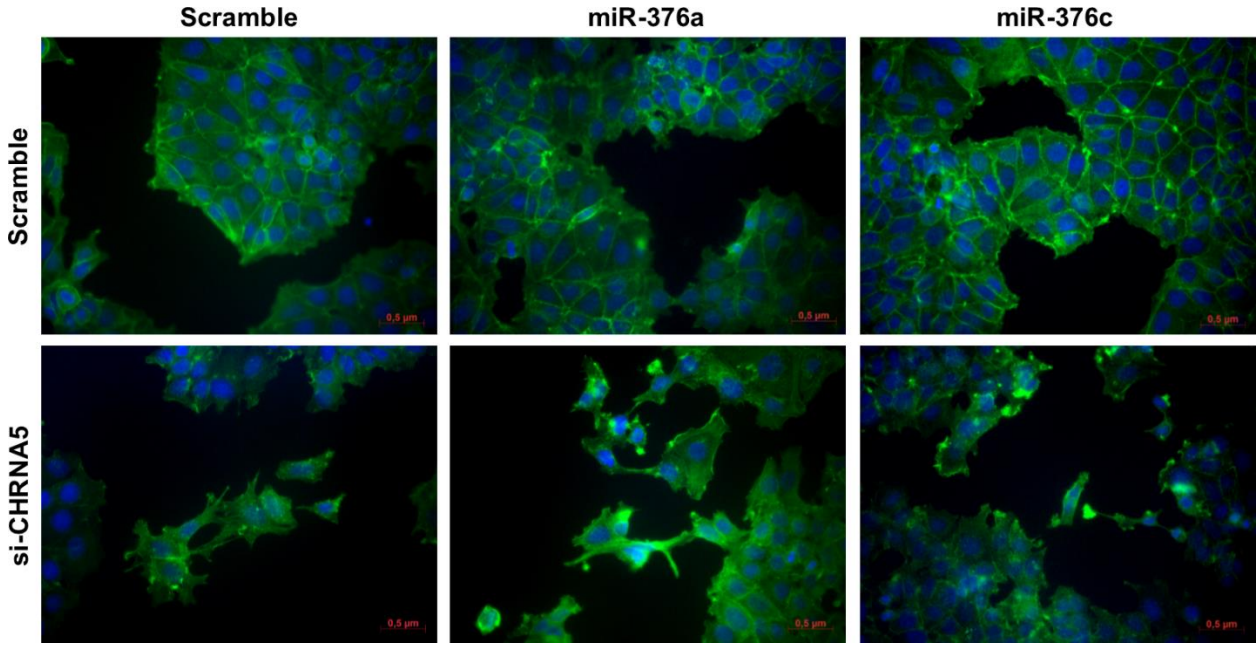

Figure 3.16: Phalloidin staining images of the miRNA mimic treated cells with or without si-CHRNA5, green shows actin filaments whereas blue shows DAPI staining of nuclei.

3.4 MTT Results

Lastly, I wanted to see the effects of the miRNA mimics, miR37a and miR37c, with or without si-CHRNA5 on the cell viability with MTT experiments (Figure 3.17). Results here indicated that both mimics can decrease cell viability when given alone, yet miR-376c was more effective than miR-376a (60% versus 78% respectively). Then with the addition of si-CHRNA5 we observed a significant decrease again on both cases; however, the groups were only significantly different from the control treatment (scrambled) but not from each other (Figure 3.17).

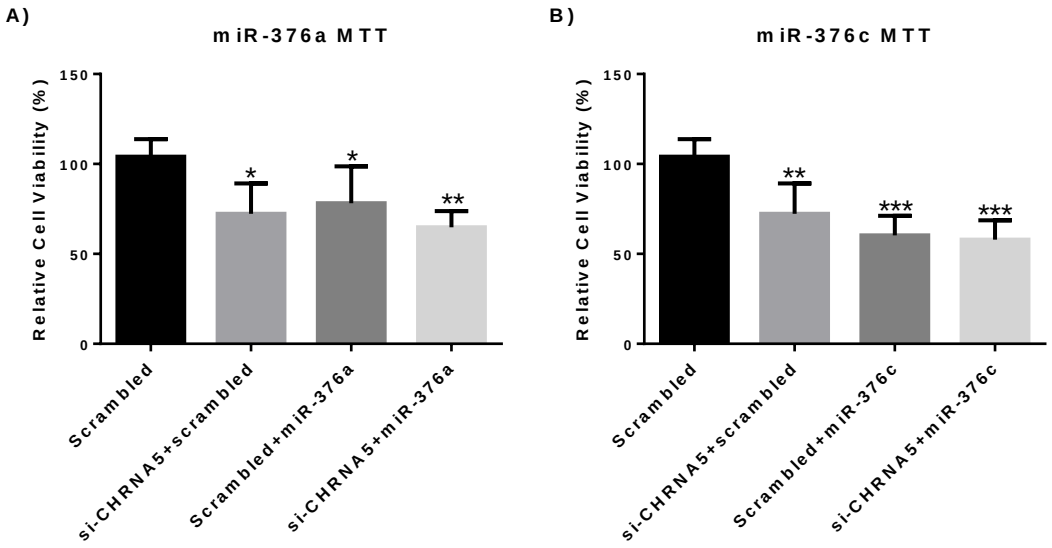

*Figure 3.17: MTT results showing the relative cell viability of the treatments with miR-376a (A) and miR-376c (B) mimics in the presence or absence of si-CHRNA5, *: p-value ≤ 0.05, **: p-value ≤ 0.01 and ****: p-value ≤ 0.0001, when compared to scrambled control group.*

3.5 Co-Culture Competition Experiments

For the study of cell competition, first, monoclonal GFP or BFP tagged cells were isolated from the polyclonal counterparts using serial dilutions method to get 100% labeled cell populations. Percentages of the tagged cells were measured by flow cytometry (Figure 3.18). The results showed that the cells used for the next experiments were all labeled

either by green or blue fluorescent proteins. In addition, I wanted to make sure the alternative transfection protocol (%0.003 HiPerfect transfection reagent) works as well, thus RNA obtained from samples treated with si-CHRNA5 and scramble was used for RT-qPCR for testing the expression changes in CHRNA5 (Figure 3.19), the results showed that the experiment was effective in silencing CHRNA5 levels at lower concentrations of HiPerfect reagent as well.

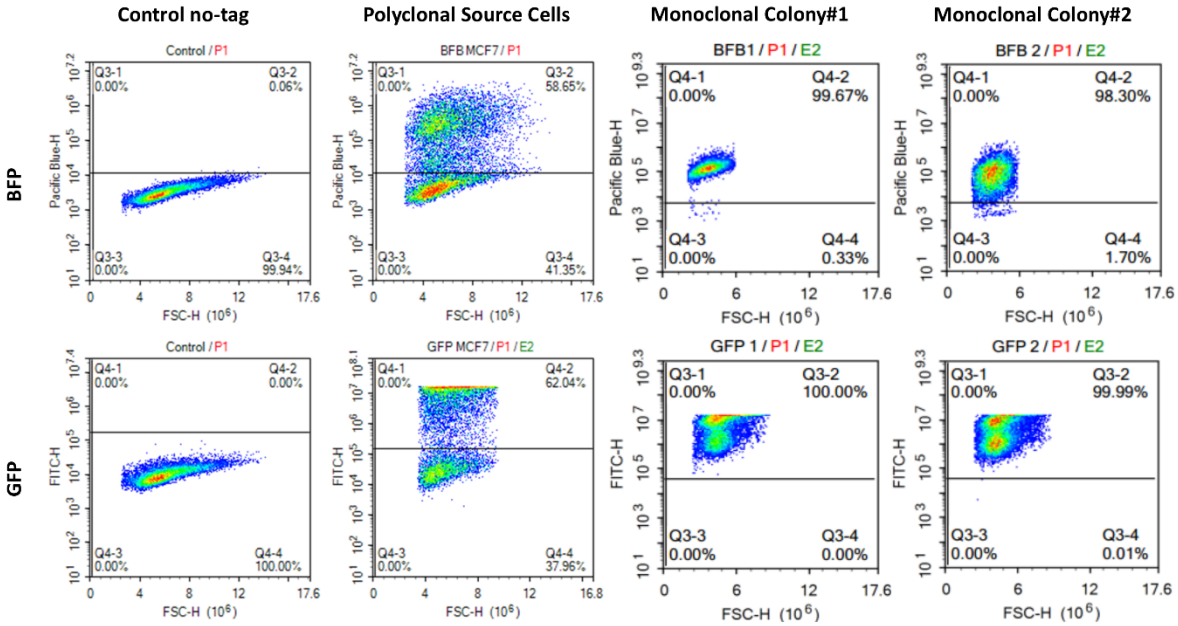

Figure 3.18: Single colony selection from the polyclonal cells; GFP (top row) and BFP (bottom row) counts from the untransfected control cells(first column), polyclonal cell populations (second column) and selected single colony populations(third and fourth columns).

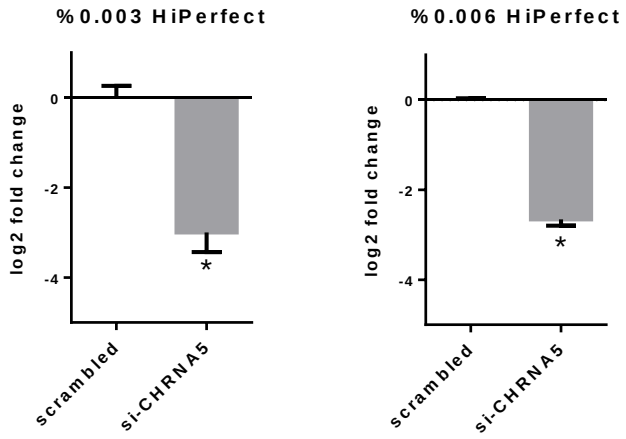

Figure 3.19: RT-qPCR results for CHRNA5 for the comparison of the different transfection trials.

To check effects of si-CHRNA5 and miRNA mimics listed in Table 3.1 in different combinations, competition experiments were done in three batches as shown in the Figure 3.20. Initially, for the competition of si-CHRNA5+miRNA mimics and miRNA mimic treated cells, first si-CHRNA5 and scramble transfections were made on GFP and BFP cells respectively, then on the second transfection phase all cells received the miRNA mimic molecules on the co-culture environment (Figure 3.20; 1st Experiment Column). Next in the second experiment, competition between the si-CHRNA5+miRNA mimics and si-CHRNA5 treated cells was checked. In which, GFP and BFP cells transfected with mimic or scramble molecules, respectively. Then on co-culture environment si-CHRNA5 versus scramble transfections are made (Figure 3.20; 2nd Experiment Column). Finally,

in third experiment, both procedures were repeated for miRNA mimics of miR-376c and miR-654 as explained before (Figure 3.20; 3rd Experiment Column).

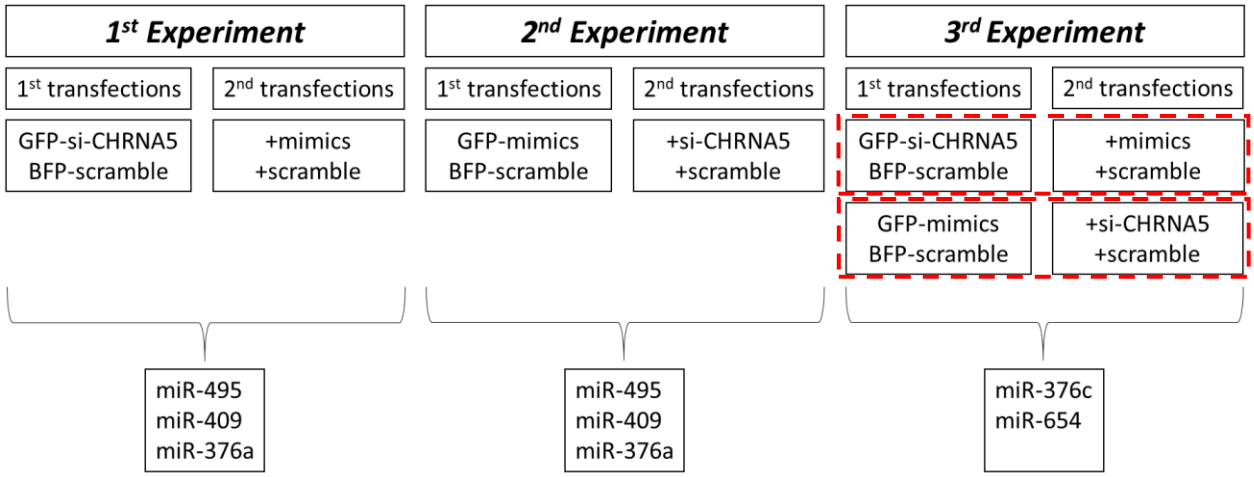

Figure 3.20: Diagram of experiment plans for tree different batches of competition assays.

On the first experiments' results when comparing the competition of si-CHRNA5 (green) and scramble (blue) cells I observed a decreased si-CHRNA5 treated cell percentage, 27.10±2.1%, against the scramble treated neighbors, 60.55±2.07%, in flow cytometry counts (Figure 3.21: '*Scramble'* image and graph). Also, with the addition of mimics for miR-495, miR-376a and miR-409, same trend could be seen as well as may be enhanced with GFP to BFP percentages of; 19.90±0.93% to 76.11±0.62%, 24.14±0.58% to 66.66±0.65% and 27.24±0.44% to 70.05±1.39%, respectively (Figure 3.21 labeled with corresponding miRNA names). However, an image quantification protocol is needed to analyze the relative proportions of the green and blue cells. All results can be seen in the Figure 3.21 as microscope images on the top panel and their corresponding flow count percentages on the bottom panel. In addition, to make sure GFP or BFP tags does not affect the experiment procedure, same experiment was performed again by swapping the GFP and BFP groups vice versa (Appendix Figure 1). Flow cytometry analyses provided quantitative differences between the groups (Figure 3.21(B)). Accordingly, 5 days of

exposure to siRNA5 alone or in the presence of mimics (2 days) were more effective than scramble (5 days) or mimic (2 days alone).

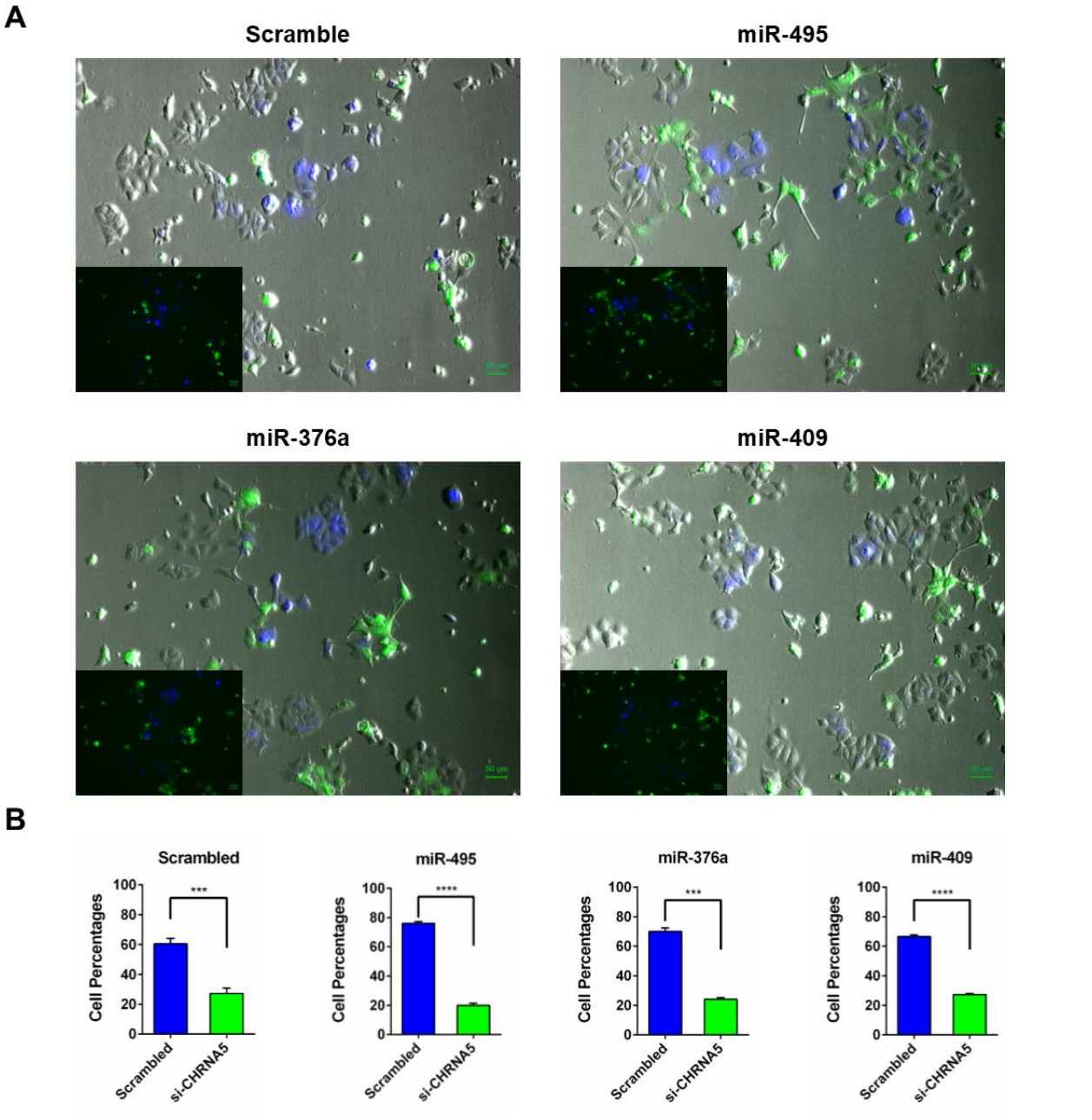

*Figure 3.21: Co-culture competition results of the first experiment for mimics of miR-495, miR-376a and miR-409: A) microscope images and B) respective cell percentages of green tagged si-CHRNA5 and blue tagged scramble cells on co-culture second transfections done with scramble or miRNA mimics as labeled above. ***: p-value < 0.001, ****: p-value < 0.0001*

On the second batch of experiments where I tried to examine the competition between miRNA mimics (green) and scramble (blue) treated cells I observed a decrease in the

mimic given cells against the scramble counterparts for all three miRNAs, miR-495, 26.96±0.78% (Figure 3.22; left panels), miR-376a, 32.76±0.42% (Figure 3.23; left panels) and miR-409, 32.49±0.65% (Figure 3.24; left panels) mimics with corresponding BFP percentages of 52.58±0.65%, 47.20±0.48% and 46.54±1.00%,respectively. However, when I introduced si-CHRNA5 on second transfections the difference between green and blue labeled cells for each miRNA group has decreased or even lost as in GFP to BFP percentages of; 35.34±0.42% to 44.51±0.95%, 42.72±0.72% to 37.60±0.93% and 41.06±0.35% to 38.29±0.81% for miR-495, miR-376a and miR-409 respectively (Figure 3.22, Figure 3.23 and Figure 3.24; right panels).

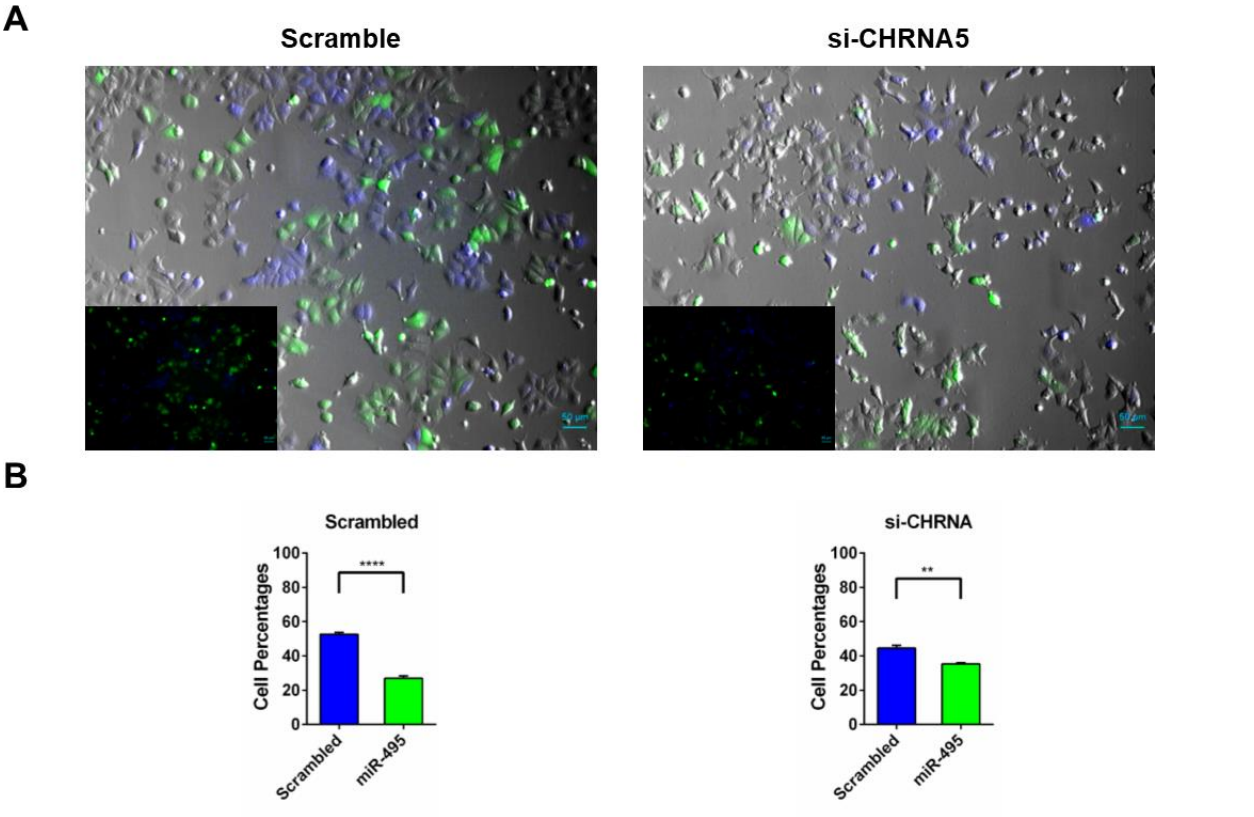

*Figure 3.22: Co-culture competition experiment results for the second batch for miR-495 with A) microscope images and B) their corresponding cell percentages of green tagged miR-495 mimic and blue tagged scramble treated cells in the absence (left) or presence (right) of si-CHRNA5. *: p-value < 0.05, **: p-value < 0.01*

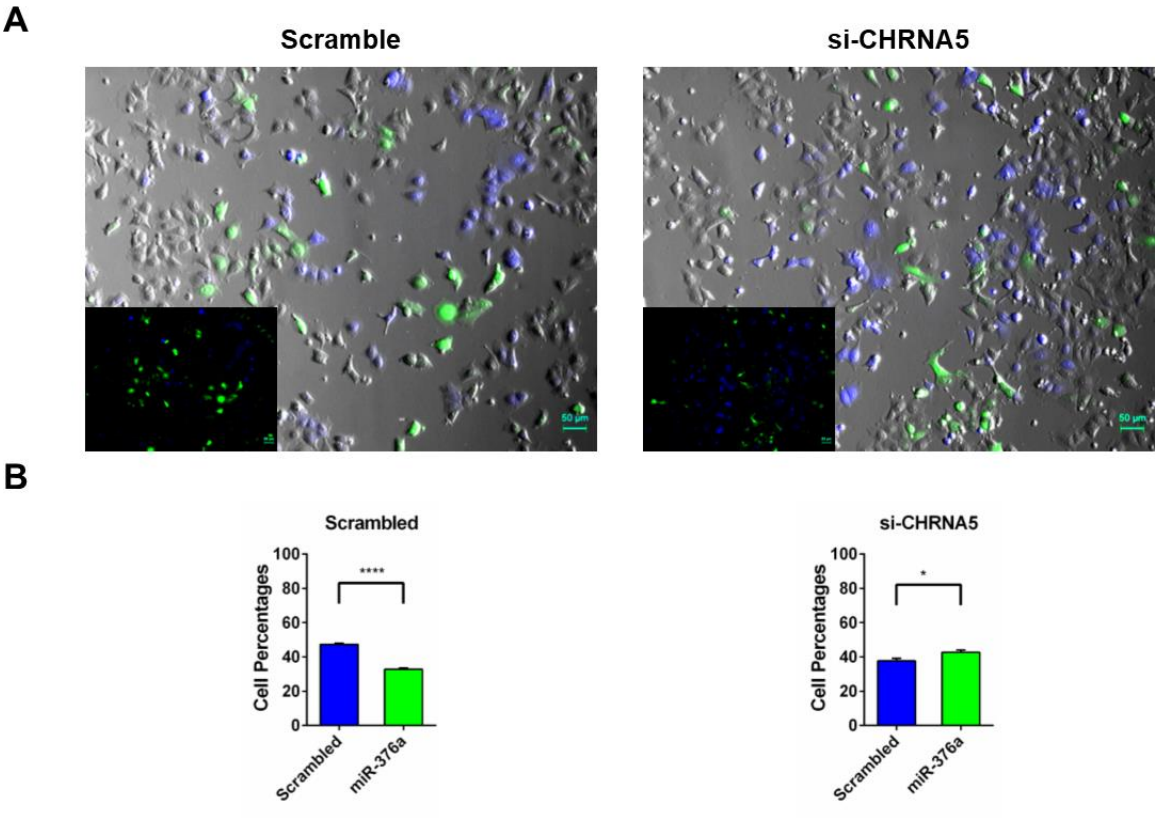

*Figure 3.23: Co-culture competition experiment results for the second batch for miR-376a with A) microscope images and B) their corresponding cell percentages of green tagged miR-376a mimic and blue tagged scramble treated cells in the absence (left) or presence (right) of si-CHRNA5. *: p-value < 0.05*

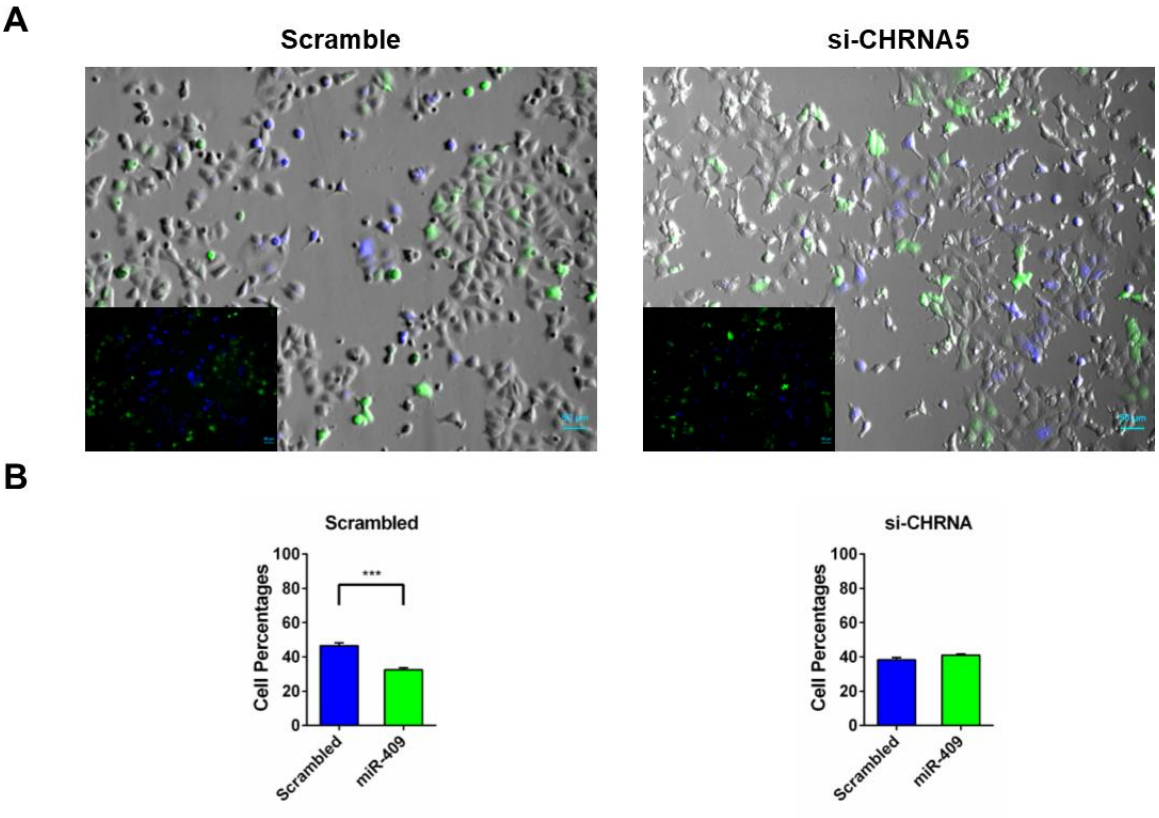

*Figure 3.24: Co-culture competition experiment results for the second batch for miR-409 with A) microscope images and B) their corresponding cell percentages of green tagged miR-409 mimic and blue tagged scramble treated cells in the absence (left) or presence (right) of si-CHRNA5. ***: p-value < 0.001*

Lastly, on the third and last experiment I repeated previous two experiments' procedures for the miR-376c and miR-654 mimics. At first part, I put si-CHRNA5 (green) and scramble (blue) given cells to co-culture environment and transfected with either scramble or mimics for miR-376c and miR-654 (Figure 3.25). Where I observed similar trend with first experiment (Figure 3.21), 31.60±0.47% green versus 54.28±2.43% blue cells. With the addition of miR-376c mimic difference becomes more significant, with green cell percentage of 25.45±1.58% and blue cell percentage of 65.20±0.34%. In the addition of miR-654 however, green cell percentage was 33.26±0.70% with blue cell percentage of 55.47±1.03% (Figure 3.25(B)).

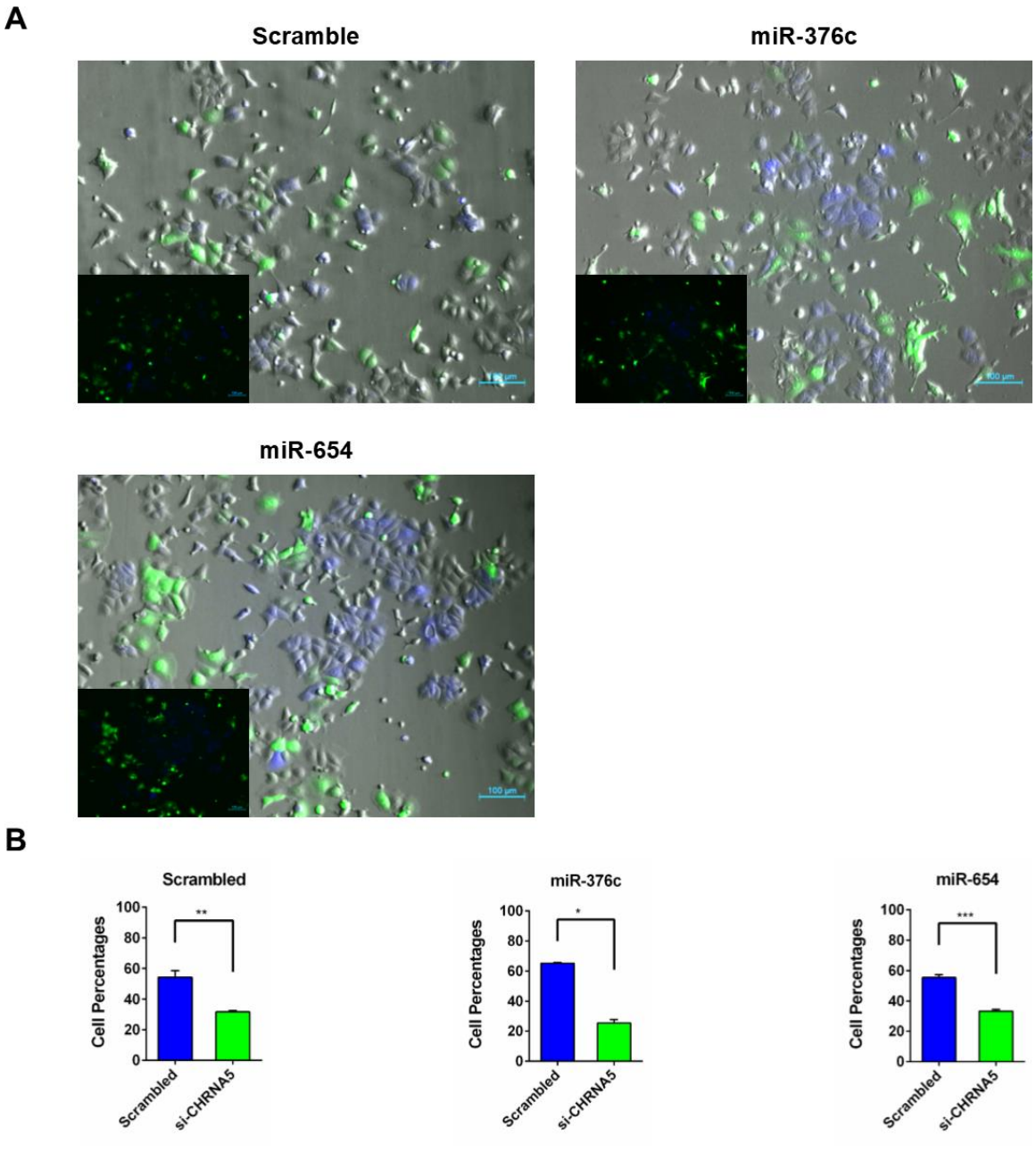

*Figure 3.25: Co-culture competition results of the third experiment part 1 for mimics of miR-376c and miR-654: A) microscope images and B) respective cell percentages of green tagged si-CHRNA5 and blue tagged scramble cells on co-culture second transfections done with scramble or miRNA mimics as labeled above. *: p-value < 0.05*

On the second part of third experiment, where I examined the competition of miRNA mimics (green) and scramble (blue) treated cells for miR-376c and miR-654, I observed a dissimilar result from previous second experiments' results (Figure 3.22, Figure 3.23 and Figure 3.24). As I observed increased mimic cell percentage, labeled green,

compared to scramble groups without si-CHRNA5 for both miR-376c and miR-654, 64.26±1.60% and 58.95±2.22% with blue percentages of 27.68±0.49% and 34.17±1.08%, respectively (Figure 3.26 and Figure 3.27 respectively; left panels). Then, with the addition of si-CHRNA5 to the co-culture environment I observed decreased difference between groups for both miRNA mimics, with green to blue percentages of; 51.13±2.49% to 34.78±3.16% and 45.70±4.21% to 39.77±3.60% for miR-376c and miR-654, respectively (Figure 3.26 and Figure 3.27; right panels).

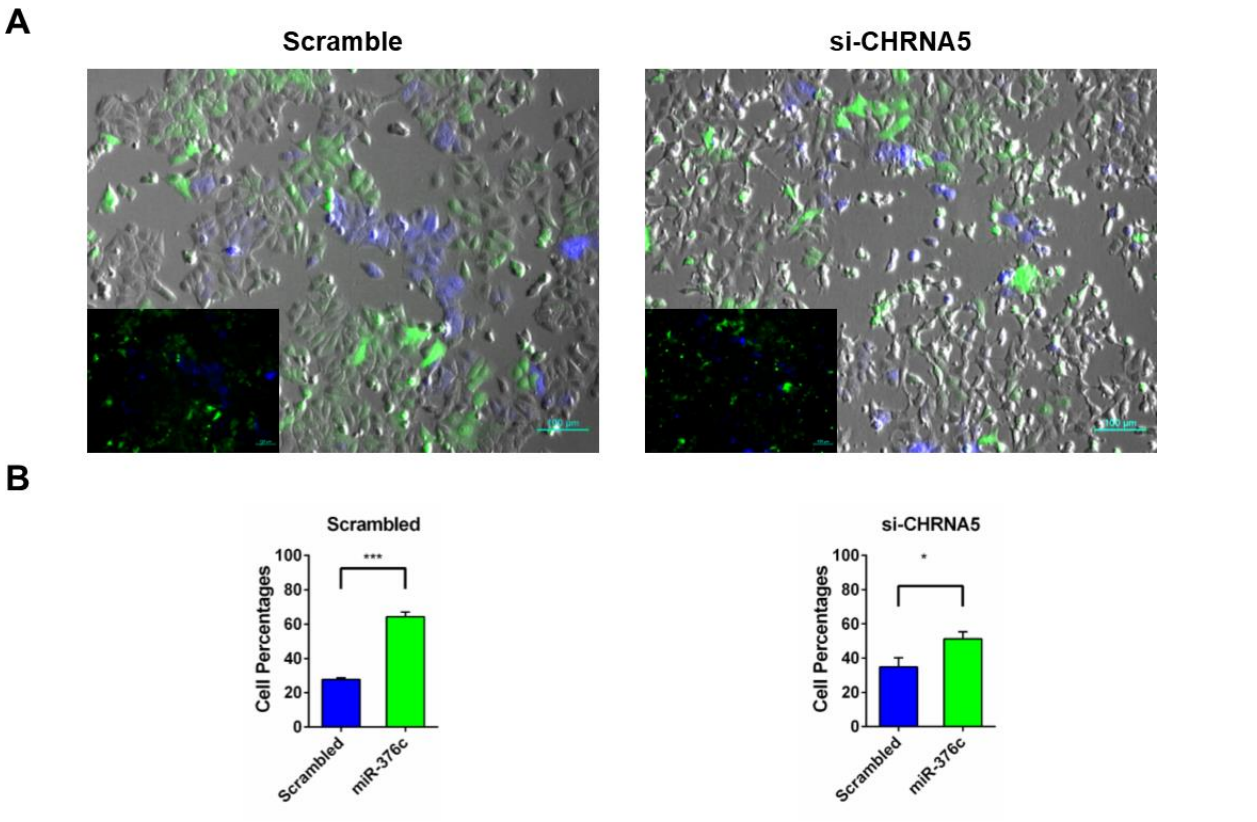

*Figure 3.26: Co-culture competition experiment results for the third experiment part 2 for miR-376c: A) microscope images and B) their corresponding cell percentages of green tagged miR-376c mimic and blue tagged scramble treated cells in the absence (left) or presence (right) of si-CHRNA5. *: p-value < 0.05, ***: p-value < 0.001*

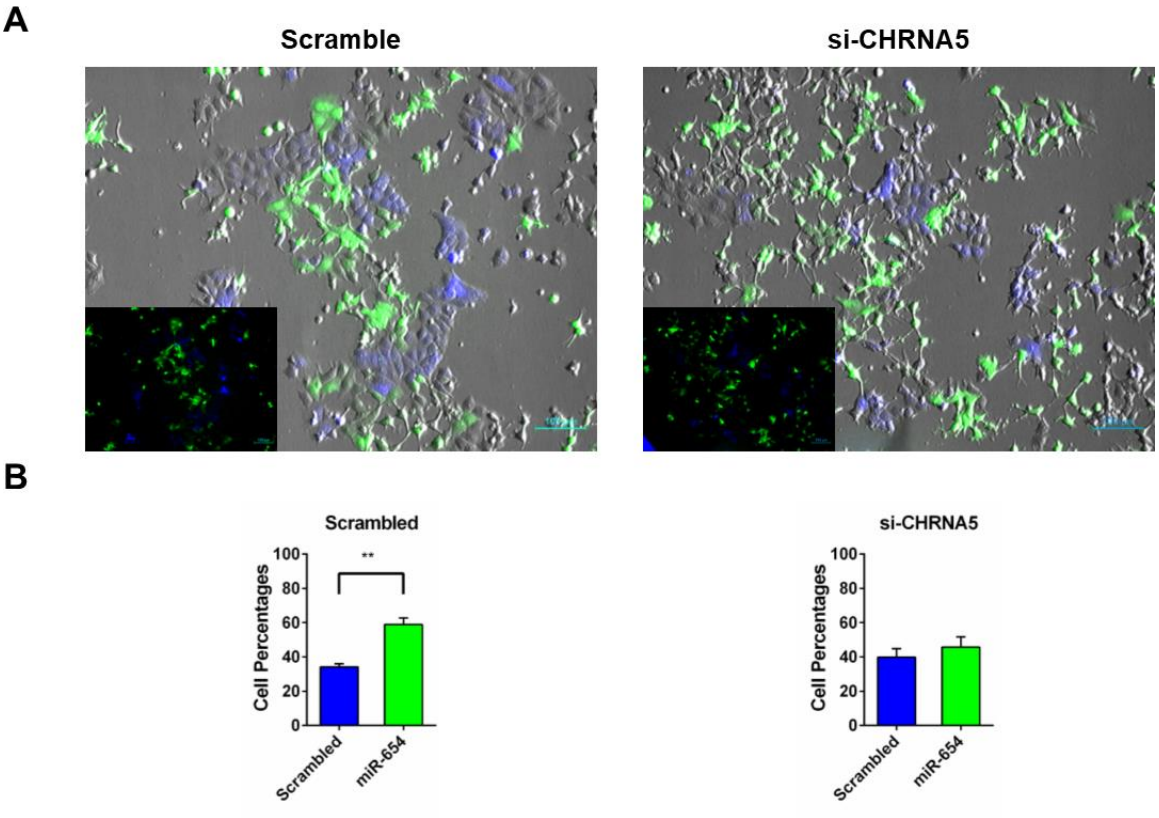

*Figure 3.27: Co-culture competition experiment results for the third experiment part 2 for miR-654: A) microscope images and B) their corresponding cell percentages of green tagged miR-654 mimic and blue tagged scramble treated cells in the absence (left) or presence (right) of si-CHRNA5. *: p-value < 0.05 ***: p-value < 0.001*

In the second part of the third experiment there was unexpected growth of the GFP labeled cells. Because of this the cell duplication times were studied by daily base counting of the cells. Where, BFP cells shown less growth rate than their GFP counterparts as well as control wild-type cells (Appendix Figure 2).

4 Discussion and Conclusions

Cholinergic receptor nicotinic alpha 5 (CHRNA5), is one of the subunits of nicotinic acetylcholine receptors, showing relevance to lung cancer and smoke addiction [26, 40]. In previous studies done by our group it was shown that depletion of CHRNA5 causes the cell cycle arrest, decrease in DNA damage response and increase in chemosensitivity through CHEK1 inhibition in the breast cancer cell line MCF7 [53]. In addition to the aforementioned effects, the studies investigating the relationship between nAChRs and miRNAs exist [222, 223], but to our current knowledge there was no study about relationship between CHRNA5 and miRNAs yet. Hence, a miRNA microarray was performed in our lab for the investigation of changes in miRNA profile with CHRNA5 siRNA treatment and some of most promising downregulated miRNAs were selected for further investigations in the present thesis (Figure1 and Table1) (Sahika Cingir, PhD Thesis, Bilkent University 2019).

In present master's study however, the main hypothesis was to enhance the antitumor effects of the si-CHRNA5 treatment on MCF7 cell line by restoration of the two downregulated miRNAs from miR-376 family, miR-376a and miR-376c, with miRNA mimics. For the investigation of this, various methods were followed and key findings can be listed as;

i. Two selected miRNAs from miR-376 family, miR-376a-3p and miR-376c-3p, which were found to be downregulated with si-CHRNA5 treatment in previous miRNA microarrays were validated with RT-qPCR. *In silico* analyses proved these miRNAs could be effective in the enhancement of antitumor effects of si-CHRNA5, thus I restored their expressions by using miRNA mimics. For studying

transcriptomic effects, microarray was performed for miR-376a-3p in combination with si-CHRNA5. Functional analyses with IPA pointed out miRNAs' relevance. In addition, several mRNA targets and affected genes expressions were validated with RT-qPCR to further support combinational effects of si-CHRNA5 and miRNA mimics for both miR-376a-3p and miR-376c-3p.

ii. Phalloidin staining and MTT assay were performed to investigate the functional effects, on phenotype and the cell viability, respectively of miRNA mimics in combination with si-CHRNA5 treatment. In which, I observed drastic changes in the cell phenotype with si-CHRNA5 treatment, as shown previously by Ermira Jahja (PhD Thesis, Bilkent University 2017) and on combined treatments I couldn't identify any significant changes. On the other hand, cell viabilities were decreased for both miRNAs and combined treatments.

iii. Lastly, I developed a co-culture experiment protocol for the observation of cell competition between two populations, using two different fluorescently labeled MCF7 cell lines. Then I applied this co-culture competition model for number of downregulated miRNAs with si-CHRNA5 treatment, where I tried different combinations and orders of treatments and observed changes in the cell percentages.

To sum up, I have identified the combinational effects of si-CHRNA5 together with the miRNA mimics of two members from miR-376 family. The addition of miRNA mimics to si-CHRNA5 model resembles the enhanced the antitumor effects.

4.1 CHRNA5 and miR-376 miRNAs as co-effectors

The importance of cholinergic signaling was shown in the breast cancer before in number of studies [36, 37, 42, 224]. Different nAChR compositions between MCF10A, normal epithelial cells, and MCF7 cell line were discovered, in which MFC7 expresses α4 and β4 subunits which are not present in the MCF10A cells [36]. As well as, co-expression of α9 subunit and estrogen receptor were shown in the breast tumor tissues by Lee and colleagues [42]. Additionally, a nAChR subunit, α7 causes the promotion of cancer stem cell population in the MCF7 cell line [224]. Lastly, role CHRNA5 plays in the breast cancer were revealed by our group recently, as the antitumor effects of CHRNA5 depletion [53]. On the other hand, miRNAs were investigated as important regulators in the breast cancer [225, 226]. The role of miR-143 was shown in the breast cancer cell growth and cell migration by a study [227]. Whereas, expression miR-200c was related with inhibition at tumor cell proliferation and colony formation [228]. Because of these reasons; roles of miRNAs on si-CHRNA5 treated cells were to be further discovered (Sahika Cingir, PhD Thesis, Bilkent University 2019).

Using miRNA expression technologies in addition to nucleic acid modulators was a used strategy in the literature before [229, 230]. For example, in a study done on ovarian cancer cells, combination of miR-126-3p mimics and PLXNB2 siRNA was shown to be more effective in decreasing the cell viability, when compared to either treatment alone [229]. On the other hand, in another study involving renal cell carcinoma cell lines, the combinational role of overexpression of both miR-532 and AQP9 in decreasing cell invasion was revealed [230]. In this regard, we also thought the antitumor effects of the si-CHRNA5 treatment could also be enhanced by using miRNAs.

Two miRNAs from miR-376 family, miR-376a and miR-376c were discovered to be downregulated by si-CHRNA5 treatment in a microarray study (Sahika Cingir, PhD Thesis, Bilkent University 2019) which was validated in present study (Figure 3.1). Review of the literature (references give in the introduction part) and in silico results (Figure 3.2-Figure 3.4 for miR-376a and Figure 3.11-Figure 3.13 for miR-376c) proven these two miRNAs might be effective targets for enhancing the effects of si-CHRNA5 and I did the rescue of these miRNAs with miRNA mimics in presence/absence of CHRNA5 (Figure 3.5 and Figure 3.14).

Further investigations in these two miRNA rescue models pointed out that siRNA effect was more potent than the effects of either miRNA. Whole transcriptome analysis showed the range of differential expression in si-CHRNA5 treatment was greater than the miR-376a treatment alone (Figure 3.6). However, between si-CHRNA5 and miR-376a transcriptomic profiles there was a mild but inverse correlation (Figure 3.6). Effects of this mild antagonism can be seen in the pathway comparisons in IPA core analysis results (Figure 3.7). From these reciprocally affected pathways; NFAT, HMGB1, CXCR4, IGF1 and sphingosine-1-phosphate signaling pathways were all activated by si-CHRNA5 and inhibited by miR-376a mimic treatments. When these pathways are investigated; firstly; role of NFAT signaling was shown in the invasive human ductal carcinomas as promoting carcinoma invasion [231]. Secondly, HMGB1 was proven to be overexpressed in number of tumor types as well as accelerates tumor growth [232]. On the other hand, CXCR4 activation and signaling was associated with tumor metastasis [233]. Whereas, sphingosine-1-phosphate signaling might have roles in metastasis and is related with clinical outcomes of the breast cancer patients [234]. Lastly, IGF1 is an important growth

factor for growth, survival and suppression apoptosis [235]. Which has roles in tumorigenesis and drug resistance in number of cancer types [236]. As a whole, changes in activities of these pathways might clarify the enhanced antitumor effects caused by miR-376a. Apart from that, changes in the expression of selected genes were again more prominent in the si-CHRNA5 given cells when compared with the miRNA mimic counterparts, except for FOS which was only modulated by miRNA mimic (Figure 3.8, Figure 3.9, Figure 3.10, Figure 3.15). Same pattern was proven in the phalloidin staining results as well, groups with si-CHRNA5 treatment showed the disrupted cell phenotypes (Ermira Jahja, PhD Thesis, Bilkent University 2017). However, in the groups of miRNA mimics alone or addition of miRNA mimics to siRNA there was no notable difference (Figure 3.16). Opposingly, in MTT results, there was significant decrease in the miRNA treatment groups for both, miR-376a and miR-376c samples (Figure 3.17, Figure 3.1); the mechanism they affect the cell viability remains to be undiscovered though. Overall, miRNA effects were not prominently observable on the MCF7 cells transcriptome. However, miRNAs can also regulate their targets by repressing the translational activity without causing mRNA degradation [237]. Because of this, the effects of the miRNAs we are using might be on the proteomics levels on the cells instead of mRNA transcriptome. There were different trends for each group of genes in RT-qPCR results. Firstly, in direct targets, STON2 and BMPR2 genes, both were decreased with si-CHRNA5 and miR-376a mimic treatments alone, as well as in combination group (Figure 3.8). In STON2 gene expression I observed a significant synergistic effect. Which was shown in the epithelial ovarian cancer patients as correlated with shorter survival and poor prognosis [238] before. As well as in thyroid carcinoma cells STON2 gene was shown to be directly

regulated by miR-199b-5p. Decreased expression of miR-199b-5p caused an increase in STON2 levels which induced growth, migration and invasion [239]. BMPR2 on the other hand, was only shown in one cancer study; in which BMPR2 deletion extended survival rate of Pten-null prostate cancer mouse models [240]. Altogether, these findings might indicate miR-376a could show antitumor effects through these two genes.

Secondly in p53 pathway genes (Figure 3.9), decrease of MDM2, which is a known proto-oncogene and negative regulator of TP53 gene [241], was enhanced with miR-376a addition to si-CHRNA5 treatment. Whereas, FOS gene was only modulated by mimic treatment and decreased. FOS is another known oncogene [242, 243] and was shown to be regulated by TP53 before [244]. Lastly, from p53 pathway expression of CDKN1A was increased in si-CHRNA5 treatment [53], but miR-376a treatment decreased the expression. CDKN1A is a downstream protein of p53 pathway and represses cell cycle [245]. As a whole, these findings might indicate to the effects of miR-376a on proliferation inhibition. However, antagonistic effects of si-CHRNA5 and miR-376a on CDKN1A points out there might be another mechanism regulating the expression of CDKN1A expression. When genes on the cell cycle group was checked however, miR-376a acted either antagonistically or didn't had effect in four genes studied; CDC6, WDHD1, BIRC5 and ANLN (Figure 3.10). Relation of these four genes with cell proliferation and tumorigenesis were shown in the literature before [246-249]. Expression changes in these genes were more pronounced in microarray data than results in the RT-qPCR studies.

When RT-qPCR results for miR-376c samples were considered; in any of the genes studied; WDHD1, FOS, CDKN1A and CLDN1, there was no significant change with miR-376c treatments. In addition to cell cycle and p53 pathway genes; expression of CLDN1

gene, a tight junction protein [250], for cytoskeletal effects was also studied. Because any gene studied showed significant expression changes, the miR-376c effect on genes weren't pursued any further.

4.2 Co-culture Competition Model for the Observation of Combination Treatments

After transfection procedure, to obtain cells with same background, single colony selection is a common method used in the literature [215]. For this purpose, serial dilution method was used, which can be counted as a limiting dilution method [219]. As a result, all cells used in the following experiments certainly carried the fluorescent tags (Figure 3.18). For this purpose, fluorescence-activated cell sorting (FACS) could also be used, however that would compromise the sterility of the cells for further experiments. Thus, limiting dilution method was used for single colony selection instead of sorting with FACS. In addition, transfection protocol was revised for using less transfection reagent (0.003%), which proved to be effective as well as previously used protocol (0.006%) (Figure 3.19).
While conducting co-culture competition experiment the main purpose was to change the cell dynamics between differentially treated cells. Depending on the percentages of treatment and control cell populations the relationship between si-CHRNA5 and miRNA mimic treatments could be determined as synergism or antagonism. If there was no observable difference between differentially labeled control and treatment cells in the culture, the conclusion would indicate no significant effect in between. If there was a decrease in the treatment cell population, that would point towards a synergistic effect; or increase in the treatment cell group would indicate an antagonistic effect. Similar methods were utilized by different research groups before [215, 217, 218]. For example,

researchers used a co-culture method for drug screening [217] and in another study, gene knock-outs by shRNAs and interference by siRNAs were used to reveal essential genes for cancer cells [218].

When co-culture competition results in the present thesis is considered on the other hand, the conclusions reached using MTT and in the thesis of Sahika Cingir-Koker (2019) could also be further supported. These were, miRNAs that were used could be effective in enhancing the antitumor effects of si-CHRNA5 treatment; and effects of si-CHRNA5 was stronger than the miRNA mimic treatments. Firstly, in Figure 3.21 and Figure 3.25 the addition of miRNA mimics further decreased the cell percentages against scramble + mimic treatment groups, which would indicate enhanced si-CHRNA5 effect. The trend shown in the first experiment was also observed on the trial experiment in which GFP and BFP tags were switched vice versa (Appendix Figure 1). Secondly, in reverse treatment experiments (Figure 3.22, Figure 3.23, Figure 3.24, Figure 3.26 and Figure 3.27), the addition of si-CHRNA5 to the environment decreased or nullified the differences in between miRNA mimic and scramble treated cell groups. This might indicate, anti-proliferative effects of si-CHRNA5 treatment was greater than the miRNA mimics in which it caused the decrease in both groups not in just treatment group. When cell percentages in the third batch of experiments were considered (Figure 3.25, Figure 3.26 and Figure 3.27), the population of GFP cells were more pronounced than the previous experiments. This might be due to an error during seeding of the cells to co-culture environment or GFP cell population might give rise to more competitive sub-clone *de novo*, as showed in a previous paper [177]. Later on, when the growth rates of these GFP and BFP clones were checked in a duplication time experiment; the growth rates of BFP cells were less than

their GFP tagged or wild-type counterparts (Appendix Figure 2), which would mean, during the single colony selections or in later passaging steps a BFP cell clone with less growth potential might have been selected. Therefore, growth rates of the cells should be checked prior to the experiment procedure.

Lastly, regarding the acquisition of results; during this study two methods were used, fluorescent imaging and flow readings. Between these two, the acquisition of cell percentages by flow cytometry allows to get more informative results, whereas by fluorescent imaging the effects on the cell phenotype can be seen as well as changes in cell numbers. However, when images are taken one should be unbiased and for this purpose automated imaging systems would be more beneficial, as used in the literature before [218]. In addition, an image quantification protocol is needed to analyze the relative proportions of the green and blue cells.

4.3 Conclusions and Future Perspectives

In conclusion, in this master's study, the roles of two miRNAs from miR-376 family in the CHRNA5 depleted MCF7 cell line model was investigated; using RT-qPCR, microarray (miR-376a) and pathway analyses, viability assays and phalloidin staining. Where certain synergistic and antagonistic effects between si-CHRNA5 and miRNA mimic treatments were observed and confirmed by the RT-qPCR. Main finding of the study was miR-376a enhanced antitumor effects of the si-CHRNA5 treatment. However, there was a mild negative correlation between transcriptomic profiles of si-CHRNA5 and miR-376a treatments. This might indicate certain genes that lead to resistance in antiproliferative effects of CHRNA5 depletion could have been reversed by miRNA mimic, resulting in enhanced antitumor effects. In addition, a method, that is using two different fluorescently

labeled cells, for investigation of combinational treatments and their effects on cell competition was developed. This procedure then applied for the multiple miRNAs, including miR-376a family, in combination with CHRNA5 depletion in MCF7 cell line model. Where it further supported the enhancement in the antitumoral effect of the si-CHRNA5 treatment.

In addition to this study, effects of miR-376 family miRNAs and si-CHRNA5 treatment could be further pursued by following studies:

- The mechanism in which miR-376a and miR-376c affects the tumor cells in the presence or absence of the CHRNA5 should be further investigated.
- STON2 which had shown to have a synergistic pattern here should be checked in protein level as well as with luciferase assays.
- The synergistic and antagonistic effects shown here should be further studied mechanistically.
- The effects of the miRNA mimics on the drug resistance can be studied as well; whether they could enhance the increase in chemosensitivity acquired by CHRNA5 depletion or not.
- All miRNAs used in the study belongs to a chromosomal cluster located at the 14q32.31; this region should be further studied in regards to epigenetic differences or expression in the presence or absence of the CHRNA5.

On the other hand, co-culture competition method devised and used in this master's study can be also enhanced further by:

- The expression of CHRNA5 can be knocked-down stably by using shRNA vectors including GFP and competition with control cells can be observed in number of

passages. In addition, miRNA mimics can be used in this setting to observe how cell competition dynamics are affected.

- An automated imaging system coupled with an image quantification module could increase the potential of the co-culture competition experiments further, as number of the molecules investigated could increase exponentially.
- Instead of a double treatment method as used here, both molecules can be given as a combination pre-treatment to the cells then seeded on to the co-culture environment and acquisition of results in different time points could allow to investigate changes in the cell competition.

References

1. Lodish, H.F. and J.E. Darnell, *Molecular cell biology*. 2008, W.H. Freeman and Company: New York, N.Y. p. 1107-1108.
2. Ferlay, J., et al. *Global Cancer Observatory: Cancer Today*. 2018 [cited 2018 20/12]; Available from: https://gco.iarc.fr/today.
3. Caffarel, M.M., et al., *Molecular Biology of Breast Cancer*, in *eLS*. 2016, John Wiley & Sons, Ltd (Ed.).
4. Stingl, J. and C. Caldas, *Molecular heterogeneity of breast carcinomas and the cancer stem cell hypothesis.* Nat Rev Cancer, 2007. **7**(10): p. 791-9.
5. Weigelt, B., et al., *Refinement of breast cancer classification by molecular characterization of histological special types.* J Pathol, 2008. **216**(2): p. 141-50.
6. Malhotra, G.K., et al., *Histological, molecular and functional subtypes of breast cancers.* Cancer Biol Ther, 2010. **10**(10): p. 955-60.
7. Perou, C.M., et al., *Molecular portraits of human breast tumours.* Nature, 2000. **406**(6797): p. 747-52.
8. Cooper, C.S., *Applications of microarray technology in breast cancer research.* Breast Cancer Res, 2001. **3**(3): p. 158-75.
9. Neve, R.M., et al., *A collection of breast cancer cell lines for the study of functionally distinct cancer subtypes.* Cancer Cell, 2006. **10**(6): p. 515-27.
10. Soule, H.D., et al., *A human cell line from a pleural effusion derived from a breast carcinoma.* J Natl Cancer Inst, 1973. **51**(5): p. 1409-16.
11. Stewart, T.A., K.T. Yapa, and G.R. Monteith, *Altered calcium signaling in cancer cells.* Biochim Biophys Acta, 2015. **1848**(10 Pt B): p. 2502-11.
12. Leanza, L., et al., *Pharmacological targeting of ion channels for cancer therapy: In vivo evidences.* Biochim Biophys Acta, 2016. **1863**(6 Pt B): p. 1385-97.
13. Monteith, G.R., N. Prevarskaya, and S.J. Roberts-Thomson, *The calcium-cancer signalling nexus.* Nat Rev Cancer, 2017. **17**(6): p. 367-380.
14. Varga, K., et al., *Expression of calcium pumps is differentially regulated by histone deacetylase inhibitors and estrogen receptor alpha in breast cancer cells.* BMC Cancer, 2018. **18**(1): p. 1029.
15. McAndrew, D., et al., *ORAI1-mediated calcium influx in lactation and in breast cancer.* Mol Cancer Ther, 2011. **10**(3): p. 448-60.
16. Chen, Y.F., et al., *Calcium store sensor stromal-interaction molecule 1-dependent signaling plays an important role in cervical cancer growth, migration, and angiogenesis.* Proc Natl Acad Sci U S A, 2011. **108**(37): p. 15225-30.
17. Zhu, H., et al., *Elevated Orai1 expression mediates tumor-promoting intracellular Ca2+ oscillations in human esophageal squamous cell carcinoma.* Oncotarget, 2014. **5**(11): p. 3455-71.
18. Motiani, R.K., et al., *STIM1 and Orai1 mediate CRAC channel activity and are essential for human glioblastoma invasion.* Pflugers Arch, 2013. **465**(9): p. 1249-60.
19. Umemura, M., et al., *Store-operated Ca2+ entry (SOCE) regulates melanoma proliferation and cell migration.* PLoS One, 2014. **9**(2): p. e89292.
20. Grando, S.A., *Connections of nicotine to cancer.* Nat Rev Cancer, 2014. **14**(6): p. 419-29.

21. Improgo, M.R., et al., *ASCL1 regulates the expression of the CHRNA5/A3/B4 lung cancer susceptibility locus.* Mol Cancer Res, 2010. **8**(2): p. 194-203.
22. Schuller, H.M., *A new twist to neurotransmitter receptors and cancer.* network, 2017. **26**: p. 30.
23. Sun, H.J., Y.F. Jia, and X.L. Ma, *Alpha5 Nicotinic Acetylcholine Receptor Contributes to Nicotine-Induced Lung Cancer Development and Progression.* Front Pharmacol, 2017. **8**: p. 573.
24. Improgo, M.R., et al., *Nicotinic acetylcholine receptors mediate lung cancer growth.* Front Physiol, 2013. **4**: p. 251.
25. Improgo, M.R., et al., *The nicotinic acetylcholine receptor CHRNA5/A3/B4 gene cluster: dual role in nicotine addiction and lung cancer.* Prog Neurobiol, 2010. **92**(2): p. 212-26.
26. Improgo, M.R., et al., *From smoking to lung cancer: the CHRNA5/A3/B4 connection.* Oncogene, 2010. **29**(35): p. 4874-84.
27. Maus, A.D., et al., *Human and rodent bronchial epithelial cells express functional nicotinic acetylcholine receptors.* Mol Pharmacol, 1998. **54**(5): p. 779-88.
28. Wang, Y., et al., *Human bronchial epithelial and endothelial cells express alpha7 nicotinic acetylcholine receptors.* Mol Pharmacol, 2001. **60**(6): p. 1201-9.
29. Nguyen, V.T., et al., *Choline acetyltransferase, acetylcholinesterase, and nicotinic acetylcholine receptors of human gingival and esophageal epithelia.* J Dent Res, 2000. **79**(4): p. 939-49.
30. Arredondo, J., et al., *Receptor-mediated tobacco toxicity: regulation of gene expression through alpha3beta2 nicotinic receptor in oral epithelial cells.* Am J Pathol, 2005. **166**(2): p. 597-613.
31. Macklin, K.D., et al., *Human vascular endothelial cells express functional nicotinic acetylcholine receptors.* J Pharmacol Exp Ther, 1998. **287**(1): p. 435-9.
32. Kawashima, K. and T. Fujii, *The lymphocytic cholinergic system and its contribution to the regulation of immune activity.* Life Sci, 2003. **74**(6): p. 675-96.
33. Battaglioli, E., et al., *Expression and transcriptional regulation of the human alpha3 neuronal nicotinic receptor subunit in T lymphocyte cell lines.* J Neurochem, 1998. **71**(3): p. 1261-70.
34. Grando, S.A., et al., *A nicotinic acetylcholine receptor regulating cell adhesion and motility is expressed in human keratinocytes.* J Invest Dermatol, 1995. **105**(6): p. 774-81.
35. Grando, S.A., et al., *Activation of keratinocyte nicotinic cholinergic receptors stimulates calcium influx and enhances cell differentiation.* J Invest Dermatol, 1996. **107**(3): p. 412-8.
36. Kalantari-Dehaghi, M., et al., *The nicotinic acetylcholine receptor-mediated reciprocal effects of the tobacco nitrosamine NNK and SLURP-1 on human mammary epithelial cells.* Int Immunopharmacol, 2015. **29**(1): p. 99-104.
37. Lee, C.H., et al., *Overexpression and activation of the alpha9-nicotinic receptor during tumorigenesis in human breast epithelial cells.* J Natl Cancer Inst, 2010. **102**(17): p. 1322-35.
38. Calleja-Macias, I.E., M. Kalantari, and H.U. Bernard, *Cholinergic signaling through nicotinic acetylcholine receptors stimulates the proliferation of cervical*

cancer cells: an explanation for the molecular role of tobacco smoking in cervical carcinogenesis? Int J Cancer, 2009. **124**(5): p. 1090-6.
39. Ye, Y.N., et al., *The modulating role of nuclear factor-kappaB in the action of alpha7-nicotinic acetylcholine receptor and cross-talk between 5-lipoxygenase and cyclooxygenase-2 in colon cancer growth induced by 4-(N-methyl-N-nitrosamino)-1-(3-pyridyl)-1-butanone.* J Pharmacol Exp Ther, 2004. **311**(1): p. 123-30.
40. Lam, D.C., et al., *Expression of nicotinic acetylcholine receptor subunit genes in non-small-cell lung cancer reveals differences between smokers and nonsmokers.* Cancer Res, 2007. **67**(10): p. 4638-47.
41. Song, P., et al., *Acetylcholine is synthesized by and acts as an autocrine growth factor for small cell lung carcinoma.* Cancer Res, 2003. **63**(1): p. 214-21.
42. Lee, C.H., et al., *Crosstalk between nicotine and estrogen-induced estrogen receptor activation induces alpha9-nicotinic acetylcholine receptor expression in human breast cancer cells.* Breast Cancer Res Treat, 2011. **129**(2): p. 331-45.
43. Chernyavsky, A.I., et al., *Structure and function of the nicotinic arm of acetylcholine regulatory axis in human leukemic T cells.* Int J Immunopathol Pharmacol, 2009. **22**(2): p. 461-72.
44. Trombino, S., et al., *Alpha7-nicotinic acetylcholine receptors affect growth regulation of human mesothelioma cells: role of mitogen-activated protein kinase pathway.* Cancer Res, 2004. **64**(1): p. 135-45.
45. Siegel, H.N. and R.J. Lukas, *Nicotinic agonists regulate alpha-bungarotoxin binding sites of TE671 human medulloblastoma cells.* J Neurochem, 1988. **50**(4): p. 1272-8.
46. Lukas, R.J., *Expression of ganglia-type nicotinic acetylcholine receptors and nicotinic ligand binding sites by cells of the IMR-32 human neuroblastoma clonal line.* J Pharmacol Exp Ther, 1993. **265**(1): p. 294-302.
47. Han, W., et al., *Relationship of common variants in CHRNA5 with early-onset schizophrenia and executive function.* Schizophr Res, 2019. **206**: p. 407-412.
48. Coverstone, E.D., et al., *A novel genetic marker of decreased inflammation and improved survival after acute myocardial infarction.* Basic Res Cardiol, 2018. **113**(5): p. 38.
49. Perez-Morales, R., et al., *CHRNA3 rs1051730 and CHRNA5 rs16969968 polymorphisms are associated with heavy smoking, lung cancer, and chronic obstructive pulmonary disease in a mexican population.* Ann Hum Genet, 2018. **82**(6): p. 415-424.
50. Schote, A.B., et al., *Sex, ADHD symptoms, and CHRNA5 genotype influence reaction time but not response inhibition.* J Neurosci Res, 2019. **97**(2): p. 215-224.
51. Kuryatov, A., W. Berrettini, and J. Lindstrom, *Acetylcholine receptor (AChR) alpha5 subunit variant associated with risk for nicotine dependence and lung cancer reduces (alpha4beta2)(2)alpha5 AChR function.* Mol Pharmacol, 2011. **79**(1): p. 119-25.
52. Wu, H., et al., *Is susceptibility locus for lung cancer in the 15q25 nicotinic acetylcholine receptor gene cluster CHRNA5-A3-B4 associated with risk of gastric cancer?* Med Oncol, 2013. **30**(2): p. 576.

53. Cingir Koker, S., et al., *Cholinergic Receptor Nicotinic Alpha 5 (CHRNA5) RNAi is associated with cell cycle inhibition, apoptosis, DNA damage response and drug sensitivity in breast cancer.* PLoS One, 2018. **13**(12): p. e0208982.
54. Bartel, D.P., *MicroRNAs: target recognition and regulatory functions.* Cell, 2009. **136**(2): p. 215-33.
55. Fabian, M.R., N. Sonenberg, and W. Filipowicz, *Regulation of mRNA translation and stability by microRNAs.* Annu Rev Biochem, 2010. **79**: p. 351-79.
56. Zhu, W., et al., *Dissection of protein interactomics highlights microRNA synergy.* PLoS One, 2013. **8**(5): p. e63342.
57. Fu, J., et al., *miR-30a suppresses breast cancer cell proliferation and migration by targeting Eya2.* Biochem Biophys Res Commun, 2014. **445**(2): p. 314-9.
58. Feng, R. and L. Dong, *Inhibitory effect of miR-184 on the potential of proliferation and invasion in human glioma and breast cancer cells in vitro.* Int J Clin Exp Pathol, 2015. **8**(8): p. 9376-82.
59. Pacurari, M., et al., *The microRNA-200 family targets multiple non-small cell lung cancer prognostic markers in H1299 cells and BEAS-2B cells.* Int J Oncol, 2013. **43**(2): p. 548-60.
60. Wang, H., et al., *Negative regulation of Hif1a expression and TH17 differentiation by the hypoxia-regulated microRNA miR-210.* Nat Immunol, 2014. **15**(4): p. 393-401.
61. Adlakha, Y.K. and N. Saini, *miR-128 exerts pro-apoptotic effect in a p53 transcription-dependent and -independent manner via PUMA-Bak axis.* Cell Death Dis, 2013. **4**: p. e542.
62. Chen, D., et al., *miR-100 induces epithelial-mesenchymal transition but suppresses tumorigenesis, migration and invasion.* PLoS Genet, 2014. **10**(2): p. e1004177.
63. Liang, Z., et al., *Regulation of miR-19 to breast cancer chemoresistance through targeting PTEN.* Pharm Res, 2011. **28**(12): p. 3091-100.
64. Rodriguez-Gonzalez, F.G., et al., *MicroRNA-30c expression level is an independent predictor of clinical benefit of endocrine therapy in advanced estrogen receptor positive breast cancer.* Breast Cancer Res Treat, 2011. **127**(1): p. 43-51.
65. Li, D., et al., *Antagonism of microRNA-99a promotes cell invasion and down-regulates E-cadherin expression in pancreatic cancer cells by regulating mammalian target of rapamycin.* Acta Histochem, 2014. **116**(5): p. 723-9.
66. Bhaskaran, M. and M. Mohan, *MicroRNAs: history, biogenesis, and their evolving role in animal development and disease.* Vet Pathol, 2014. **51**(4): p. 759-74.
67. Ikeda, S., et al., *Altered microRNA expression in human heart disease.* Physiol Genomics, 2007. **31**(3): p. 367-73.
68. Care, A., et al., *MicroRNA-133 controls cardiac hypertrophy.* Nat Med, 2007. **13**(5): p. 613-8.
69. Yang, B., et al., *The muscle-specific microRNA miR-1 regulates cardiac arrhythmogenic potential by targeting GJA1 and KCNJ2.* Nat Med, 2007. **13**(4): p. 486-91.
70. Thum, T., D. Catalucci, and J. Bauersachs, *MicroRNAs: novel regulators in cardiac development and disease.* Cardiovasc Res, 2008. **79**(4): p. 562-70.

71. Dai, Y., et al., *Microarray analysis of microRNA expression in peripheral blood cells of systemic lupus erythematosus patients.* Lupus, 2007. **16**(12): p. 939-46.
72. Chang, S., et al., *Small regulatory RNAs in neurodevelopmental disorders.* Hum Mol Genet, 2009. **18**(R1): p. R18-26.
73. Cogswell, J.P., et al., *Identification of miRNA changes in Alzheimer's disease brain and CSF yields putative biomarkers and insights into disease pathways.* J Alzheimers Dis, 2008. **14**(1): p. 27-41.
74. Harris, T.A., et al., *MicroRNA-126 regulates endothelial expression of vascular cell adhesion molecule 1.* Proc Natl Acad Sci U S A, 2008. **105**(5): p. 1516-21.
75. Zhang, B., et al., *microRNAs as oncogenes and tumor suppressors.* Dev Biol, 2007. **302**(1): p. 1-12.
76. Ciafre, S.A., et al., *Extensive modulation of a set of microRNAs in primary glioblastoma.* Biochem Biophys Res Commun, 2005. **334**(4): p. 1351-8.
77. Calin, G.A., et al., *MicroRNA profiling reveals distinct signatures in B cell chronic lymphocytic leukemias.* Proc Natl Acad Sci U S A, 2004. **101**(32): p. 11755-60.
78. Cimmino, A., et al., *miR-15 and miR-16 induce apoptosis by targeting BCL2.* Proc Natl Acad Sci U S A, 2005. **102**(39): p. 13944-9.
79. Michael, M.Z., et al., *Reduced accumulation of specific microRNAs in colorectal neoplasia.* Mol Cancer Res, 2003. **1**(12): p. 882-91.
80. Murakami, Y., et al., *Comprehensive analysis of microRNA expression patterns in hepatocellular carcinoma and non-tumorous tissues.* Oncogene, 2006. **25**(17): p. 2537-45.
81. Takamizawa, J., et al., *Reduced expression of the let-7 microRNAs in human lung cancers in association with shortened postoperative survival.* Cancer Res, 2004. **64**(11): p. 3753-6.
82. Johnson, S.M., et al., *RAS is regulated by the let-7 microRNA family.* Cell, 2005. **120**(5): p. 635-47.
83. Hayashita, Y., et al., *A polycistronic microRNA cluster, miR-17-92, is overexpressed in human lung cancers and enhances cell proliferation.* Cancer Res, 2005. **65**(21): p. 9628-32.
84. O'Donnell, K.A., et al., *c-Myc-regulated microRNAs modulate E2F1 expression.* Nature, 2005. **435**(7043): p. 839-43.
85. Eis, P.S., et al., *Accumulation of miR-155 and BIC RNA in human B cell lymphomas.* Proc Natl Acad Sci U S A, 2005. **102**(10): p. 3627-32.
86. Metzler, M., et al., *High expression of precursor microRNA-155/BIC RNA in children with Burkitt lymphoma.* Genes Chromosomes Cancer, 2004. **39**(2): p. 167-9.
87. He, L., et al., *A microRNA polycistron as a potential human oncogene.* Nature, 2005. **435**(7043): p. 828-33.
88. Iorio, M.V., et al., *MicroRNA gene expression deregulation in human breast cancer.* Cancer Res, 2005. **65**(16): p. 7065-70.
89. Camps, C., et al., *hsa-miR-210 Is induced by hypoxia and is an independent prognostic factor in breast cancer.* Clin Cancer Res, 2008. **14**(5): p. 1340-8.
90. Jansen, M.P., et al., *High miR-26a and low CDC2 levels associate with decreased EZH2 expression and with favorable outcome on tamoxifen in metastatic breast cancer.* Breast Cancer Res Treat, 2012. **133**(3): p. 937-47.

91. Tavazoie, S.F., et al., *Endogenous human microRNAs that suppress breast cancer metastasis.* Nature, 2008. **451**(7175): p. 147-52.
92. Gasparini, P., et al., *microRNA expression profiling identifies a four microRNA signature as a novel diagnostic and prognostic biomarker in triple negative breast cancers.* Oncotarget, 2014. **5**(5): p. 1174-84.
93. Mulrane, L., et al., *microRNAs: a new class of breast cancer biomarkers.* Expert Rev Mol Diagn, 2014. **14**(3): p. 347-63.
94. Fu, L., et al., *Serum expression levels of microRNA-382-3p, -598-3p, -1246 and -184 in breast cancer patients.* Oncol Lett, 2016. **12**(1): p. 269-274.
95. Blenkiron, C., et al., *MicroRNA expression profiling of human breast cancer identifies new markers of tumor subtype.* Genome Biol, 2007. **8**(10): p. R214.
96. Riaz, M., et al., *miRNA expression profiling of 51 human breast cancer cell lines reveals subtype and driver mutation-specific miRNAs.* Breast Cancer Res, 2013. **15**(2): p. R33.
97. Rupaimoole, R. and F.J. Slack, *MicroRNA therapeutics: towards a new era for the management of cancer and other diseases.* Nat Rev Drug Discov, 2017. **16**(3): p. 203-222.
98. Cheng, C.J., et al., *MicroRNA silencing for cancer therapy targeted to the tumour microenvironment.* Nature, 2015. **518**(7537): p. 107-10.
99. Nishimura, M., et al., *Therapeutic synergy between microRNA and siRNA in ovarian cancer treatment.* Cancer Discov, 2013. **3**(11): p. 1302-15.
100. Pan, B.L., et al., *Decreased microRNA-182-5p helps alendronate promote osteoblast proliferation and differentiation in osteoporosis via the Rap1/MAPK pathway.* Biosci Rep, 2018. **38**(6).
101. Kozomara, A. and S. Griffiths-Jones, *miRBase: integrating microRNA annotation and deep-sequencing data.* Nucleic Acids Res, 2011. **39**(Database issue): p. D152-7.
102. Griffiths-Jones, S., et al., *miRBase: microRNA sequences, targets and gene nomenclature.* Nucleic Acids Res, 2006. **34**(Database issue): p. D140-4.
103. Ambros, V., et al., *A uniform system for microRNA annotation.* RNA, 2003. **9**(3): p. 277-9.
104. Tekirdag, K.A., et al., *MIR376 family and cancer.* Histol Histopathol, 2016. **31**(8): p. 841-55.
105. Xie, B., et al., *miRCancer: a microRNA-cancer association database constructed by text mining on literature.* Bioinformatics, 2013. **29**(5): p. 638-44.
106. Zhang, L., et al., *miR-376a inhibits breast cancer cell progression by targeting neuropilin-1 NR.* Onco Targets Ther, 2018. **11**: p. 5293-5302.
107. Haapa-Paananen, S., et al., *Functional profiling of precursor MicroRNAs identifies MicroRNAs essential for glioma proliferation.* PLoS One, 2013. **8**(4): p. e60930.
108. Zheng, Y., et al., *miR-376a suppresses proliferation and induces apoptosis in hepatocellular carcinoma.* FEBS Lett, 2012. **586**(16): p. 2396-403.
109. Wang, Y., et al., *MiR-376a suppresses the proliferation and invasion of non-small-cell lung cancer by targeting c-Myc.* Cell Biol Int, 2018. **42**(1): p. 25-33.
110. Yang, L., et al., *MiR-376a promotion of proliferation and metastases in ovarian cancer: Potential role as a biomarker.* Life Sci, 2017. **173**: p. 62-67.

111. Yabushita, S., et al., *Circulating microRNAs in serum of human K-ras oncogene transgenic rats with pancreatic ductal adenocarcinomas.* Pancreas, 2012. **41**(7): p. 1013-8.
112. Deng, Y., Y. Xiong, and Y. Liu, *miR-376c inhibits cervical cancer cell proliferation and invasion by targeting BMI1.* Int J Exp Pathol, 2016. **97**(3): p. 257-65.
113. Tu, L., et al., *hsa-miR-376c-3p Regulates Gastric Tumor Growth Both In Vitro and In Vivo.* Biomed Res Int, 2016. **2016**: p. 9604257.
114. Jiang, W., et al., *MicroRNA-376c suppresses non-small-cell lung cancer cell growth and invasion by targeting LRH-1-mediated Wnt signaling pathway.* Biochem Biophys Res Commun, 2016. **473**(4): p. 980-986.
115. Duan, Z., et al., *MicroRNA-199a-3p is downregulated in human osteosarcoma and regulates cell proliferation and migration.* Mol Cancer Ther, 2011. **10**(8): p. 1337-45.
116. Jin, Y., et al., *MicroRNA-376c inhibits cell proliferation and invasion in osteosarcoma by targeting to transforming growth factor-alpha.* DNA Cell Biol, 2013. **32**(6): p. 302-9.
117. Wang, K., et al., *MiR-376c-3p regulates the proliferation, invasion, migration, cell cycle and apoptosis of human oral squamous cancer cells by suppressing HOXB7.* Biomed Pharmacother, 2017. **91**: p. 517-525.
118. Zehavi, L., et al., *Silencing of a large microRNA cluster on human chromosome 14q32 in melanoma: biological effects of mir-376a and mir-376c on insulin growth factor 1 receptor.* Mol Cancer, 2012. **11**: p. 44.
119. Yoshitaka, T., et al., *Analysis of microRNAs expressions in chondrosarcoma.* J Orthop Res, 2013. **31**(12): p. 1992-8.
120. Wang, L., et al., *Downregulated miR-495 [Corrected] Inhibits the G1-S Phase Transition by Targeting Bmi-1 in Breast Cancer.* Medicine (Baltimore), 2015. **94**(21): p. e718.
121. Chen, Y., et al., *Demethylation of miR-495 inhibits cell proliferation, migration and promotes apoptosis by targeting STAT-3 in breast cancer.* Oncol Rep, 2017. **37**(6): p. 3581-3589.
122. Guan, Y.X., et al., *Lnc RNA SNHG20 participated in proliferation, invasion, and migration of breast cancer cells via miR-495.* J Cell Biochem, 2018. **119**(10): p. 7971-7981.
123. Wang, H., et al., *MicroRNA-495 Inhibits Gastric Cancer Cell Migration and Invasion Possibly via Targeting High Mobility Group AT-Hook 2 (HMGA2).* Med Sci Monit, 2017. **23**: p. 640-648.
124. Eun, J.W., et al., *MicroRNA-495-3p functions as a tumor suppressor by regulating multiple epigenetic modifiers in gastric carcinogenesis.* J Pathol, 2018. **244**(1): p. 107-119.
125. Ahmadi, A., et al., *miR-199a-5p and miR-495 target GRP78 within UPR pathway of lung cancer.* Gene, 2017. **620**: p. 15-22.
126. Chen, S.M., et al., *MicroRNA-495 inhibits proliferation of glioblastoma multiforme cells by downregulating cyclin-dependent kinase 6.* World J Surg Oncol, 2013. **11**: p. 87.
127. Nie, S., et al., *miR-495 mediates metabolic shift in glioma cells via targeting Glut1.* J Craniofac Surg, 2015. **26**(2): p. e155-8.

128. Zhang, B., et al., *Hsa-miR-495 acts as a tumor suppressor gene in glioma via the negative regulation of MYB.* Mol Med Rep, 2016. **14**(1): p. 977-82.
129. Zhang, G., et al., *miR-409-3p suppresses breast cancer cell growth and invasion by targeting Akt1.* Biochem Biophys Res Commun, 2016. **469**(2): p. 189-95.
130. Wan, L., et al., *MicroRNA-409-3p functions as a tumor suppressor in human lung adenocarcinoma by targeting c-Met.* Cell Physiol Biochem, 2014. **34**(4): p. 1273-90.
131. Xu, X., et al., *MicroRNA-409-3p inhibits migration and invasion of bladder cancer cells via targeting c-Met.* Mol Cells, 2013. **36**(1): p. 62-8.
132. Geraldo, M.V., H.I. Nakaya, and E.T. Kimura, *Down-regulation of 14q32-encoded miRNAs and tumor suppressor role for miR-654-3p in papillary thyroid cancer.* Oncotarget, 2017. **8**(6): p. 9597-9607.
133. Di Lisio, L., et al., *Mantle cell lymphoma: transcriptional regulation by microRNAs.* Leukemia, 2010. **24**(7): p. 1335-42.
134. Kent, W.J., et al., *The human genome browser at UCSC.* Genome Res, 2002. **12**(6): p. 996-1006.
135. Formosa, A., et al., *MicroRNAs, miR-154, miR-299-5p, miR-376a, miR-376c, miR-377, miR-381, miR-487b, miR-485-3p, miR-495 and miR-654-3p, mapped to the 14q32.31 locus, regulate proliferation, apoptosis, migration and invasion in metastatic prostate cancer cells.* Oncogene, 2014. **33**(44): p. 5173-82.
136. Lehner, B., et al., *Epigenetic silencing of genes and microRNAs within the imprinted Dlk1-Dio3 region at human chromosome 14.32 in giant cell tumor of bone.* BMC Cancer, 2014. **14**: p. 495.
137. Haller, F., et al., *Localization- and mutation-dependent microRNA (miRNA) expression signatures in gastrointestinal stromal tumours (GISTs), with a cluster of co-expressed miRNAs located at 14q32.31.* J Pathol, 2010. **220**(1): p. 71-86.
138. Gonzalez-Vallinas, M., et al., *Epigenetically Regulated Chromosome 14q32 miRNA Cluster Induces Metastasis and Predicts Poor Prognosis in Lung Adenocarcinoma Patients.* Mol Cancer Res, 2018. **16**(3): p. 390-402.
139. Peterson, S.M., et al., *Common features of microRNA target prediction tools.* Front Genet, 2014. **5**: p. 23.
140. Enright, A.J., et al., *MicroRNA targets in Drosophila.* Genome Biol, 2003. **5**(1): p. R1.
141. John, B., et al., *Human MicroRNA targets.* PLoS Biol, 2004. **2**(11): p. e363.
142. Betel, D., et al., *Comprehensive modeling of microRNA targets predicts functional non-conserved and non-canonical sites.* Genome Biol, 2010. **11**(8): p. R90.
143. Lewis, B.P., C.B. Burge, and D.P. Bartel, *Conserved seed pairing, often flanked by adenosines, indicates that thousands of human genes are microRNA targets.* Cell, 2005. **120**(1): p. 15-20.
144. Reczko, M., et al., *Functional microRNA targets in protein coding sequences.* Bioinformatics, 2012. **28**(6): p. 771-6.
145. Paraskevopoulou, M.D., et al., *DIANA-microT web server v5.0: service integration into miRNA functional analysis workflows.* Nucleic Acids Res, 2013. **41**(Web Server issue): p. W169-73.

146. Wong, N. and X. Wang, *miRDB: an online resource for microRNA target prediction and functional annotations.* Nucleic Acids Res, 2015. **43**(Database issue): p. D146-52.
147. Fan, Y., et al., *miRNet - dissecting miRNA-target interactions and functional associations through network-based visual analysis.* Nucleic Acids Res, 2016. **44**(W1): p. W135-41.
148. Fan, Y. and J. Xia, *miRNet-Functional Analysis and Visual Exploration of miRNA-Target Interactions in a Network Context.* Methods Mol Biol, 2018. **1819**: p. 215-233.
149. Shirdel, E.A., et al., *NAViGaTing the micronome--using multiple microRNA prediction databases to identify signalling pathway-associated microRNAs.* PLoS One, 2011. **6**(2): p. e17429.
150. Tokar, T., et al., *mirDIP 4.1-integrative database of human microRNA target predictions.* Nucleic Acids Res, 2018. **46**(D1): p. D360-D370.
151. Schena, M., et al., *Quantitative monitoring of gene expression patterns with a complementary DNA microarray.* Science, 1995. **270**(5235): p. 467-70.
152. Heller, M.J., *DNA microarray technology: devices, systems, and applications.* Annu Rev Biomed Eng, 2002. **4**: p. 129-53.
153. Dalma-Weiszhausz, D.D., et al., *The affymetrix GeneChip platform: an overview.* Methods Enzymol, 2006. **410**: p. 3-28.
154. Dell'Aversana, C., C. Giorgio, and L. Altucci, *MicroRNA Expression Profiling Using Agilent One-Color Microarray.* Methods Mol Biol, 2017. **1509**: p. 169-183.
155. Jayaswal, V., et al., *Identification of microRNA-mRNA modules using microarray data.* BMC Genomics, 2011. **12**: p. 138.
156. Hua, L., L. Li, and P. Zhou, *Identifying breast cancer subtype related miRNAs from two constructed miRNAs interaction networks in silico method.* Biomed Res Int, 2013. **2013**: p. 798912.
157. Hua, L., et al., *Prioritizing breast cancer subtype related miRNAs using miRNA-mRNA dysregulated relationships extracted from their dual expression profiling.* J Theor Biol, 2013. **331**: p. 1-11.
158. Cho, J.H., et al., *Systems biology of interstitial lung diseases: integration of mRNA and microRNA expression changes.* BMC Med Genomics, 2011. **4**: p. 8.
159. Peng, X., et al., *Computational identification of hepatitis C virus associated microRNA-mRNA regulatory modules in human livers.* BMC Genomics, 2009. **10**: p. 373.
160. Fountzilas, E., et al., *A microRNA activity map of human mesenchymal tumors: connections to oncogenic pathways; an integrative transcriptomic study.* BMC Genomics, 2012. **13**: p. 332.
161. Bustin, S. and T. Nolan, *Talking the talk, but not walking the walk: RT-qPCR as a paradigm for the lack of reproducibility in molecular research.* Eur J Clin Invest, 2017. **47**(10): p. 756-774.
162. Tan, G.W. and L.P. Tan, *High-Throughput RT-qPCR for the Analysis of Circulating MicroRNAs.* Methods Mol Biol, 2017. **1580**: p. 7-19.
163. Carnielli, C.M., F.V. Winck, and A.F. Paes Leme, *Functional annotation and biological interpretation of proteomics data.* Biochim Biophys Acta, 2015. **1854**(1): p. 46-54.

164. Ashburner, M., et al., *Gene ontology: tool for the unification of biology. The Gene Ontology Consortium.* Nat Genet, 2000. **25**(1): p. 25-9.
165. Kanehisa, M. and S. Goto, *KEGG: kyoto encyclopedia of genes and genomes.* Nucleic Acids Res, 2000. **28**(1): p. 27-30.
166. Fabregat, A., et al., *The Reactome Pathway Knowledgebase.* Nucleic Acids Res, 2018. **46**(D1): p. D649-D655.
167. Liberzon, A., et al., *The Molecular Signatures Database (MSigDB) hallmark gene set collection.* Cell Syst, 2015. **1**(6): p. 417-425.
168. Culhane, A.C., et al., *GeneSigDB--a curated database of gene expression signatures.* Nucleic Acids Res, 2010. **38**(Database issue): p. D716-25.
169. Consortium, E.P., *An integrated encyclopedia of DNA elements in the human genome.* Nature, 2012. **489**(7414): p. 57-74.
170. Mi, H., et al., *Large-scale gene function analysis with the PANTHER classification system.* Nat Protoc, 2013. **8**(8): p. 1551-66.
171. Mi, H., et al., *PANTHER version 11: expanded annotation data from Gene Ontology and Reactome pathways, and data analysis tool enhancements.* Nucleic Acids Res, 2017. **45**(D1): p. D183-D189.
172. Chen, E.Y., et al., *Enrichr: interactive and collaborative HTML5 gene list enrichment analysis tool.* BMC Bioinformatics, 2013. **14**: p. 128.
173. Kuleshov, M.V., et al., *Enrichr: a comprehensive gene set enrichment analysis web server 2016 update.* Nucleic Acids Res, 2016. **44**(W1): p. W90-7.
174. Kramer, A., et al., *Causal analysis approaches in Ingenuity Pathway Analysis.* Bioinformatics, 2014. **30**(4): p. 523-30.
175. Simpson, P., *Parameters of cell competition in the compartments of the wing disc of Drosophila.* Dev Biol, 1979. **69**(1): p. 182-93.
176. Simpson, P. and G. Morata, *Differential mitotic rates and patterns of growth in compartments in the Drosophila wing.* Dev Biol, 1981. **85**(2): p. 299-308.
177. Penzo-Mendez, A.I., et al., *Spontaneous Cell Competition in Immortalized Mammalian Cell Lines.* PLoS One, 2015. **10**(7): p. e0132437.
178. Oliver, E.R., et al., *Ribosomal protein L24 defect in belly spot and tail (Bst), a mouse Minute.* Development, 2004. **131**(16): p. 3907-20.
179. Merino, M.M., R. Levayer, and E. Moreno, *Survival of the Fittest: Essential Roles of Cell Competition in Development, Aging, and Cancer.* Trends Cell Biol, 2016. **26**(10): p. 776-788.
180. Kajita, M. and Y. Fujita, *EDAC: Epithelial defence against cancer-cell competition between normal and transformed epithelial cells in mammals.* J Biochem, 2015. **158**(1): p. 15-23.
181. Abrams, J.M., *Competition and compensation: coupled to death in development and cancer.* Cell, 2002. **110**(4): p. 403-6.
182. de la Cova, C., et al., *Drosophila myc regulates organ size by inducing cell competition.* Cell, 2004. **117**(1): p. 107-16.
183. Johnston, L.A., *Socializing with MYC: cell competition in development and as a model for premalignant cancer.* Cold Spring Harb Perspect Med, 2014. **4**(4): p. a014274.
184. Moreno, E. and K. Basler, *dMyc transforms cells into super-competitors.* Cell, 2004. **117**(1): p. 117-29.

185. Moreno, E., K. Basler, and G. Morata, *Cells compete for decapentaplegic survival factor to prevent apoptosis in Drosophila wing development.* Nature, 2002. **416**(6882): p. 755-9.
186. Rodrigues, A.B., et al., *Activated STAT regulates growth and induces competitive interactions independently of Myc, Yorkie, Wingless and ribosome biogenesis.* Development, 2012. **139**(21): p. 4051-61.
187. Vincent, J.P., et al., *Steep differences in wingless signaling trigger Myc-independent competitive cell interactions.* Dev Cell, 2011. **21**(2): p. 366-74.
188. Landsberg, K.P., et al., *Increased cell bond tension governs cell sorting at the Drosophila anteroposterior compartment boundary.* Curr Biol, 2009. **19**(22): p. 1950-5.
189. Goers, L., P. Freemont, and K.M. Polizzi, *Co-culture systems and technologies: taking synthetic biology to the next level.* J R Soc Interface, 2014. **11**(96).
190. Paschos, N.K., et al., *Advances in tissue engineering through stem cell-based co-culture.* J Tissue Eng Regen Med, 2015. **9**(5): p. 488-503.
191. Cottet, S., et al., *Microaerophilic conditions permit to mimic in vitro events occurring during in vivo Helicobacter pylori infection and to identify Rho/Ras-associated proteins in cellular signaling.* J Biol Chem, 2002. **277**(37): p. 33978-86.
192. Wu, M.H., S.B. Huang, and G.B. Lee, *Microfluidic cell culture systems for drug research.* Lab Chip, 2010. **10**(8): p. 939-56.
193. Hesselman, M.C., et al., *A multi-platform flow device for microbial (co-) cultivation and microscopic analysis.* PLoS One, 2012. **7**(5): p. e36982.
194. Kawada, H., et al., *Rapid ex vivo expansion of human umbilical cord hematopoietic progenitors using a novel culture system.* Exp Hematol, 1999. **27**(5): p. 904-15.
195. Bian, L., et al., *Coculture of human mesenchymal stem cells and articular chondrocytes reduces hypertrophy and enhances functional properties of engineered cartilage.* Tissue Eng Part A, 2011. **17**(7-8): p. 1137-45.
196. Bacchus, W., et al., *Synthetic two-way communication between mammalian cells.* Nat Biotechnol, 2012. **30**(10): p. 991-6.
197. Moraes, C., et al., *Organs-on-a-chip: a focus on compartmentalized microdevices.* Ann Biomed Eng, 2012. **40**(6): p. 1211-27.
198. Kim, J.B., *Three-dimensional tissue culture models in cancer biology.* Semin Cancer Biol, 2005. **15**(5): p. 365-77.
199. Zhou, J., et al., *The repair of large segmental bone defects in the rabbit with vascularized tissue engineered bone.* Biomaterials, 2010. **31**(6): p. 1171-9.
200. Kim, S., et al., *In vivo bone formation from human embryonic stem cell-derived osteogenic cells in poly(d,l-lactic-co-glycolic acid)/hydroxyapatite composite scaffolds.* Biomaterials, 2008. **29**(8): p. 1043-53.
201. Mummery, C., et al., *Differentiation of human embryonic stem cells to cardiomyocytes: role of coculture with visceral endoderm-like cells.* Circulation, 2003. **107**(21): p. 2733-40.
202. Matsuura, K., et al., *Fabrication of mouse embryonic stem cell-derived layered cardiac cell sheets using a bioreactor culture system.* PLoS One, 2012. **7**(12): p. e52176.

203. Laugwitz, K.L., et al., *Postnatal isl1+ cardioblasts enter fully differentiated cardiomyocyte lineages.* Nature, 2005. **433**(7026): p. 647-53.
204. Griffith, C.K., et al., *Diffusion limits of an in vitro thick prevascularized tissue.* Tissue Eng, 2005. **11**(1-2): p. 257-66.
205. Caspi, O., et al., *Tissue engineering of vascularized cardiac muscle from human embryonic stem cells.* Circ Res, 2007. **100**(2): p. 263-72.
206. Mondrinos, M.J., et al., *Engineering three-dimensional pulmonary tissue constructs.* Tissue Eng, 2006. **12**(4): p. 717-28.
207. Poulsom, R., et al., *Bone marrow contributes to renal parenchymal turnover and regeneration.* J Pathol, 2001. **195**(2): p. 229-35.
208. Moore, R.N., et al., *Enhanced differentiation of embryonic stem cells using co-cultivation with hepatocytes.* Biotechnol Bioeng, 2008. **101**(6): p. 1332-43.
209. Sanchez-Ramos, J., et al., *Adult bone marrow stromal cells differentiate into neural cells in vitro.* Exp Neurol, 2000. **164**(2): p. 247-56.
210. Stine, M.J., et al., *Integration of genotypic and phenotypic screening reveals molecular mediators of melanoma-stromal interaction.* Cancer Res, 2011. **71**(7): p. 2433-44.
211. Ghiabi, P., et al., *Endothelial cells provide a notch-dependent pro-tumoral niche for enhancing breast cancer survival, stemness and pro-metastatic properties.* PLoS One, 2014. **9**(11): p. e112424.
212. Domogauer, J.D., S.M. de Toledo, and E.I. Azzam, *A Mimic of the Tumor Microenvironment: A Simple Method for Generating Enriched Cell Populations and Investigating Intercellular Communication.* J Vis Exp, 2016(115).
213. Buchanan, C.F., et al., *Cross-talk between endothelial and breast cancer cells regulates reciprocal expression of angiogenic factors in vitro.* J Cell Biochem, 2012. **113**(4): p. 1142-51.
214. Chiew, G.G.Y., et al., *Bioengineered three-dimensional co-culture of cancer cells and endothelial cells: A model system for dual analysis of tumor growth and angiogenesis.* Biotechnol Bioeng, 2017. **114**(8): p. 1865-1877.
215. Eekels, J.J., et al., *A competitive cell growth assay for the detection of subtle effects of gene transduction on cell proliferation.* Gene Ther, 2012. **19**(11): p. 1058-64.
216. Merlo, L.M., et al., *An in vitro co-culture model of esophageal cells identifies ascorbic acid as a modulator of cell competition.* BMC Cancer, 2011. **11**: p. 461.
217. Rao, T.D., N. Rosales, and D.R. Spriggs, *Dual-fluorescence isogenic high-content screening for MUC16/CA125 selective agents.* Mol Cancer Ther, 2011. **10**(10): p. 1939-48.
218. Vizeacoumar, F.J., et al., *A negative genetic interaction map in isogenic cancer cell lines reveals cancer cell vulnerabilities.* Mol Syst Biol, 2013. **9**: p. 696.
219. Longo, P.A., et al., *Single cell cloning of a stable mammalian cell line.* Methods Enzymol, 2014. **536**: p. 165-72.
220. Gautier, L., et al., *affy--analysis of Affymetrix GeneChip data at the probe level.* Bioinformatics, 2004. **20**(3): p. 307-15.
221. Brettschneider, J., et al., *Quality assessment for short oligonucleotide microarray data.* Technometrics, 2008. **50**(3): p. 241-264.

222. Rauthan, M., et al., *MicroRNA Regulation of nAChR Expression and Nicotine-Dependent Behavior in C. elegans.* Cell Rep, 2017. **21**(6): p. 1434-1441.
223. Ebrahimpour, A., et al., *Nicotine Modulates Growth Factors and MicroRNA to Promote Inflammatory and Fibrotic Processes.* J Pharmacol Exp Ther, 2019. **368**(2): p. 169-178.
224. Hirata, N., Y. Sekino, and Y. Kanda, *Nicotine increases cancer stem cell population in MCF-7 cells.* Biochem Biophys Res Commun, 2010. **403**(1): p. 138-43.
225. Hamam, R., et al., *Circulating microRNAs in breast cancer: novel diagnostic and prognostic biomarkers.* Cell Death Dis, 2017. **8**(9): p. e3045.
226. Mandujano-Tinoco, E.A., et al., *New emerging roles of microRNAs in breast cancer.* Breast Cancer Res Treat, 2018. **171**(2): p. 247-259.
227. Tavanafar, F., et al., *Restoration of miR-143 expression could inhibit migration and growth of MDA-MB-468 cells through down-regulating the expression of invasion-related factors.* Biomed Pharmacother, 2017. **91**: p. 920-924.
228. Jones, R., et al., *Re-expression of miR-200c suppresses proliferation, colony formation and in vivo tumor growth of murine claudin-low mammary tumor cells.* Oncotarget, 2017. **8**(14): p. 23727-23749.
229. Xiang, G. and Y. Cheng, *MiR-126-3p inhibits ovarian cancer proliferation and invasion via targeting PLXNB2.* Reprod Biol, 2018. **18**(3): p. 218-224.
230. Yamada, Y., et al., *Role of pre-miR-532 (miR-532-5p and miR-532-3p) in regulation of gene expression and molecular pathogenesis in renal cell carcinoma.* Am J Clin Exp Urol, 2019. **7**(1): p. 11-30.
231. Jauliac, S., et al., *The role of NFAT transcription factors in integrin-mediated carcinoma invasion.* Nat Cell Biol, 2002. **4**(7): p. 540-4.
232. Lotze, M.T. and R.A. DeMarco, *Dealing with death: HMGB1 as a novel target for cancer therapy.* Curr Opin Investig Drugs, 2003. **4**(12): p. 1405-9.
233. Sun, X., et al., *CXCL12 / CXCR4 / CXCR7 chemokine axis and cancer progression.* Cancer Metastasis Rev, 2010. **29**(4): p. 709-22.
234. Tsuchida, J., et al., *Clinical Impact of Sphingosine-1-Phosphate in Breast Cancer.* Mediators Inflamm, 2017. **2017**: p. 2076239.
235. Brahmkhatri, V.P., C. Prasanna, and H.S. Atreya, *Insulin-like growth factor system in cancer: novel targeted therapies.* Biomed Res Int, 2015. **2015**: p. 538019.
236. Denduluri, S.K., et al., *Insulin-like growth factor (IGF) signaling in tumorigenesis and the development of cancer drug resistance.* Genes Dis, 2015. **2**(1): p. 13-25.
237. Huang, T.C., S.M. Pinto, and A. Pandey, *Proteomics for understanding miRNA biology.* Proteomics, 2013. **13**(3-4): p. 558-67.
238. Sun, X., et al., *Stonin 2 Overexpression is Correlated with Unfavorable Prognosis and Tumor Invasion in Epithelial Ovarian Cancer.* Int J Mol Sci, 2017. **18**(8).
239. Ren, L., et al., *miR-199b-5p-Stonin 2 axis regulates metastases and epithelial-to-mesenchymal transition of papillary thyroid carcinoma.* IUBMB Life, 2019. **71**(1): p. 28-40.
240. Lu, X., et al., *Opposing roles of TGFbeta and BMP signaling in prostate cancer development.* Genes Dev, 2017. **31**(23-24): p. 2337-2342.

241. Patel, K.R. and H.D. Patel, *p53: An Attractive Therapeutic Target for Cancer.* Curr Med Chem, 2019.
242. Muhammad, N., et al., *Involvement of c-Fos in the Promotion of Cancer Stem-like Cell Properties in Head and Neck Squamous Cell Carcinoma.* Clin Cancer Res, 2017. **23**(12): p. 3120-3128.
243. Krishna, A., et al., *Differential Expression of c-fos Proto-Oncogene in Normal Oral Mucosa versus Squamous Cell Carcinoma.* Asian Pac J Cancer Prev, 2018. **19**(3): p. 867-874.
244. Elkeles, A., et al., *The c-fos proto-oncogene is a target for transactivation by the p53 tumor suppressor.* Mol Cell Biol, 1999. **19**(4): p. 2594-600.
245. Li, H. and B. Zheng, *Overexpression of the Ubiquitin-Specific Peptidase 9 X-Linked (USP9X) Gene is Associated with Upregulation of Cyclin D1 (CCND1) and Downregulation of Cyclin-Dependent Inhibitor Kinase 1A (CDKN1A) in Breast Cancer Tissue and Cell Lines.* Med Sci Monit, 2019. **25**: p. 4207-4216.
246. Jiang, W., et al., *Downregulation of Cdc6 inhibits tumorigenesis of osteosarcoma in vivo and in vitro.* Biomed Pharmacother, 2019. **115**: p. 108949.
247. Liu, B., et al., *MicroRNA-494-dependent WDHDI inhibition suppresses epithelial-mesenchymal transition, tumor growth and metastasis in cholangiocarcinoma.* Dig Liver Dis, 2019. **51**(3): p. 397-411.
248. Zhang, H., et al., *MALAT1 accelerates the development and progression of renal cell carcinoma by decreasing the expression of miR-203 and promoting the expression of BIRC5.* Cell Prolif, 2019: p. e12640.
249. Xu, J., et al., *Overexpression of ANLN in lung adenocarcinoma is associated with metastasis.* Thorac Cancer, 2019.
250. Hoevel, T., et al., *Expression and targeting of the tight junction protein CLDN1 in CLDN1-negative human breast tumor cells.* J Cell Physiol, 2002. **191**(1): p. 60-8.

Appendix

Appendix A: Co-culture competition results of the first experiment; for switched treatments on GFP and BFP labeled cells.

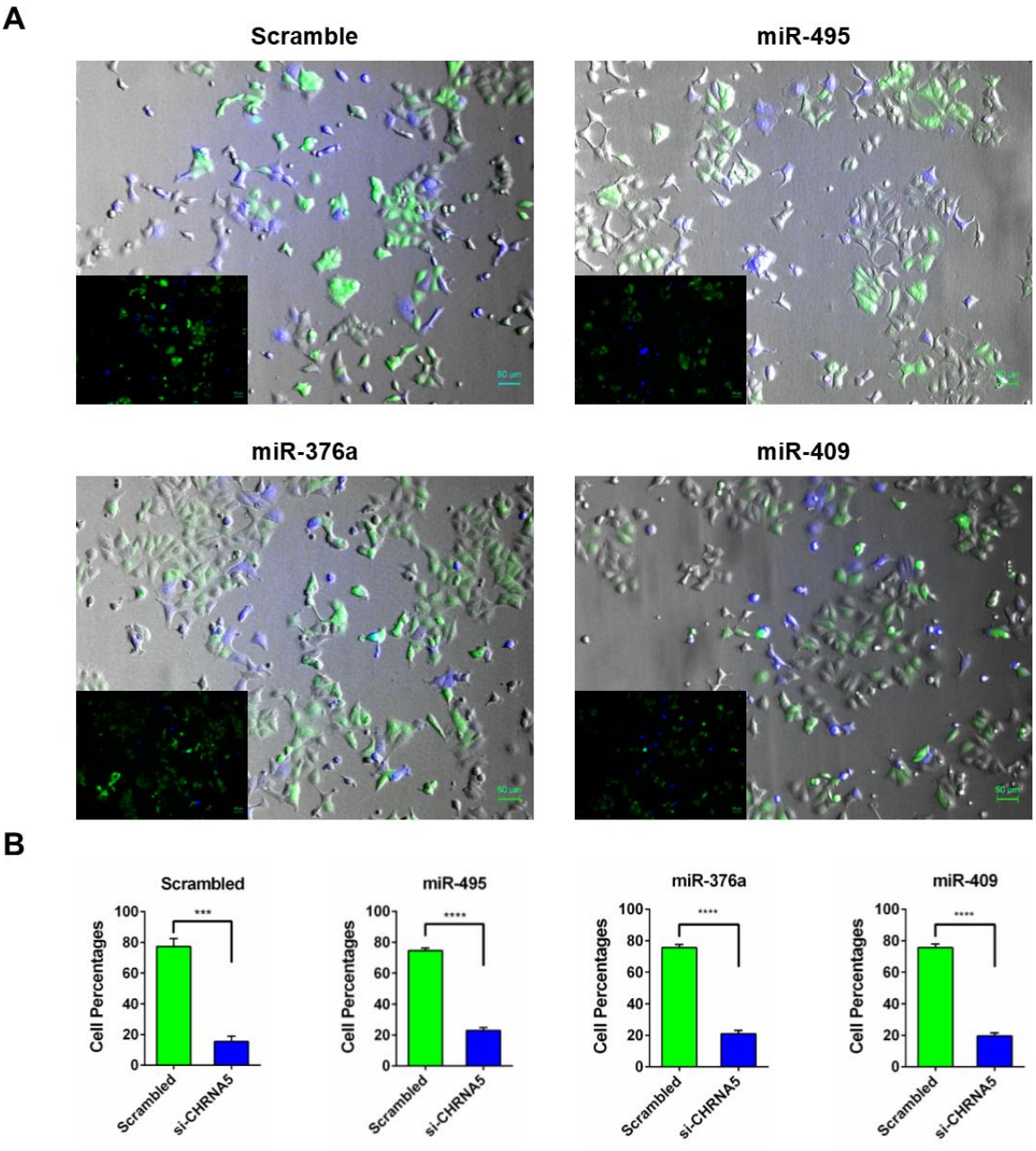

*Appendix Figure 1: Co-culture competition results of the first experiment for mimics of miR-495, miR-376a and miR-409: A) microscope images and B) respective cell percentages of blue tagged si-CHRNA5 and green tagged scramble cells on co-culture second transfections done with scramble or miRNA mimics as labeled above. ***: p-value < 0.001, ****: p-value < 0.0001*

Appendix B: Cell duplication experiment results of GFP and BFP labeled cells in comparison with wild-type MCF7 cells.

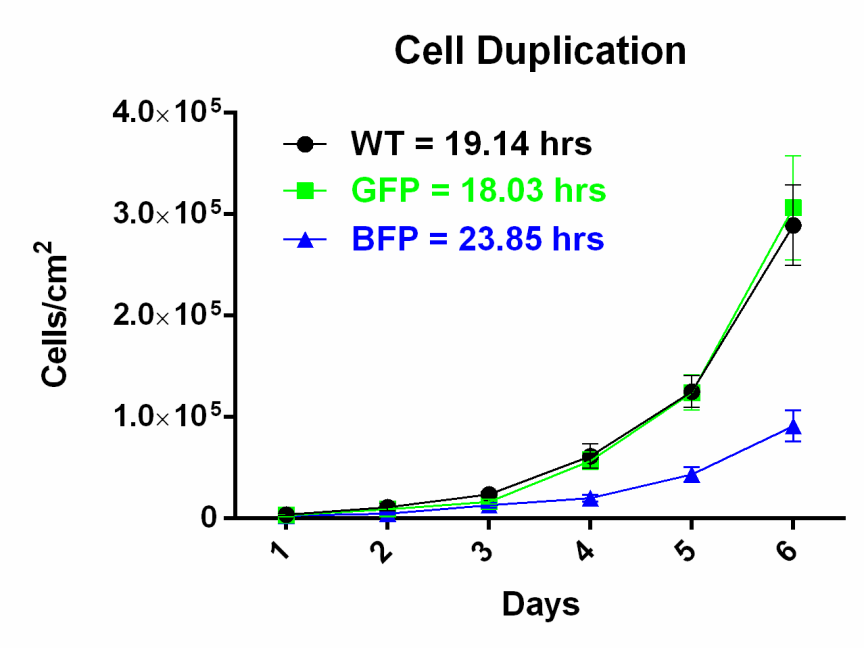

Appendix Figure 2: Cell doubling graphs of the GFP and BFP labeled cells and comparison with wild-type MCF7 cells with their calculated duplications times. Equal number of cells were seeded into 6 different wells and during following 6 days cells were collected and counted with hemocytometer. Doubling times were calculated by subtracting the initial number of cells from final number of cells and taking 6-day period of time as time reference.